Universidade de Brasília

Instituto de Ciências Biológicas

Programa de Pós-Graduação em Biologia Animal

Obtenção de matriz extracelular descelularizada de córtex ovariano bovino e sua caracterização

Cecibel María León Félix

Tese de doutorado

Brasília-DF

2023

Universidade de Brasília

Instituto de Ciências Biológicas

Programa de Pós-Graduação em Biologia Animal

Obtenção de matriz extracelular descelularizada de córtex ovariano bovino e sua caracterização

Cecibel María León Félix

Orientadora: Profª. Drª. Carolina Madeira Lucci

Tese apresentada ao Programa de Pós-Graduação em Biologia Animal da Universidade de Brasília como parte dos requisitos necessários para a obtenção do título de Doutor em Biologia Animal.

Tese de doutorado

Brasília-DF

2023

Dedico esta tese a Brasília pela oportunidade de crescimento pessoal e profissional.

AGRADECIMENTO

Gostaria de agradecer a todas as pessoas que tornaram este trabalho possível. Especialmente à minha orientadora, Dra. Carolina Madeira Lucci, pela oportunidade e confiança concedidas para desenvolver o doutorado. Além de me guiar no desenvolvimento deste trabalho, também sou grata pela amizade compartilhada durante o processo. Agradeço também à minha coorientadora, Dra. Christiani Andrade Amorim, pela oportunidade de realizar o intercâmbio de estudo e pelo valioso ensino oferecido durante essa experiência. E, não menos importante, agradeço à Dra. Andrea Q. Maranhão pelo ensino na área da biologia molecular. Todos vocês foram fundamentais para o sucesso desta jornada e sou muito grata por toda ajuda e apoio recebidos.

Agradeço ao meu pai, Dante José León Rosales, à minha mãe, Alicia Elvira Félix Romero (*in memoriam*), e aos meus irmãos, Lizbet Leon Felix, Dante David Leon Felix e Josué Leon Felix, pelo suporte durante todo o processo. Além disso, sou grata aos meus amigos Carlos Emilio Molano Paternina, Diana Veronica Suárez Naranjo, Jesus Manuel Perez Clara, José Miguel Quintero Ferrer, Jorge Luis Triana Riveros, Ledymar Foncault Moreno, Marco António Rodruiguez Martinez, Paul Aguilar Sánchez e Renato Felix da Silva pelo apoio dado durante todo o desenvolvimento da pesquisa e pela minha experiência no Brasil.

Agradecemos a EMBRAPA-CENARGEN pela doação dos ovários bovinos, em especial Nayara Ribeiro Kussano e Ligiane de Oliveira Leme. Agradecemos também ao Laboratório de Microscopia e Microanálise da Universidade de Brasília pela utilização do microscópio eletrônico de varredura, em especial a Ingrid Gracielle M. da Silva. Por fim, expressamos nossa gratidão à Unidade de Transplante de Rim e Pancreático do Hospital Saint-Luc da UCLouvain pela doação dos ovários humanos utilizados neste estudo, dos quais foram obtidas as células estromais.

Agradeço ao apoio da bolsa da Coordenação de Aperfeiçoamento de Pessoal de Nível Superior - Brasil (CAPES) (Código Financeiro 001).

SUMÁRIO

LISTA DE FIGURAS

LISTA DE TABELAS

LISTA DE ABREVIAÇÕES

AA - Antibióticos e antimicóticos

ACN - Acetonitrila

APD - Determinação avançada de pico

ART - Tecnologias de reprodução assistida

CO2 - Dióxido de carbono

DAB - 3,3'-diaminobenzidina

DAPI - 4',6'-diamino-2-fenil-indol

Decell group – Grupo descelularizado

dMEC – Matriz extracelular descelularizada

DMEM - Meio de Eagle modificado de Dulbecco

DNA - Ácido desoxirribonucleico

DNase I – Desoxirribonuclease I

DPBS - Solução salina tamponada com fosfato de Dulbecco

DTT - 1,4-Ditiotreitol

EDTA – Ácido etilenodiamino tetra-acético

EMILIN-1 - Elastina microfibrila interfacer-1

FDR - Taxa de descoberta falsa

GAGs - Glicosaminoglicanos

HEPES – Ácido sulfônico N-2-hidroxietilpiperazina-N-2-etano

HI FBS – Soro fetal bovino inativado pelo calor

LC-MS/MS - Cromatografia líquida - espectrometria de massa em tandem

MEC - Matriz extracelular

MM = Padrão de tamanho molecular TrackItTM 1kb Ladder

NaCl – Cloreto de sódio

NaF - Fluoreto de sódio

NaOH - Hidróxido de sódio

OAT - Ovário artificial transplantável

ORA – Análise de super-representação

pb – Par de bases

PMSF – Fluoreto de fenilmetilsulfonila

PSM - correspondências de espectro de peptídeo

RNase – Ribonuclease

SD - Desvio padrão

SDC - Desoxicolato de sódio

SEM - Microscopia eletrônica de varredura

SLES - Lauril éter sulfato de sódio

TMT - Marcação de massa em tandem

RESUMO

A descelularização da matriz extracelular (MEC) de tecido ovariano está sendo investigada como uma possibilidade de desenvolvimento de um ovário artificial transplantável (OAT), uma alternativa que surge para preservar a fertilidade em mulheres diagnosticadas com câncer, que poderiam se tornar inférteis devido à quimioterapia e/ou radioterapia. Os métodos existentes de obtenção de MEC descelularizada (dMEC) do tecido ovariano não foram otimizados e só alcançaram sucesso em camundongos. Os objetivos do presente estudo foram (1) obter uma dMEC de tecido ovariano de bovino usando a menor concentração de docedil sulfato de dódio (SDS) e o menor tempo de incubação que garantam a descelularização; e (2) analisar a proteômica da MEC antes e depois da descelularização. Para a obtenção da dMEC de córtex ovariano bovino, foram testadas as concentrações de SDS e NaOH de 1% e 0,2M, 0,5% e 0,1M, 0,1% e 0,02M, e 0,05% e 0,01%, com tempos de incubação de 24h, 12h e 6h. O tecido obtido de cada tratamento foi analisado por histologia, eletroforese e quantificação do DNA para verificar a descelularização. A análise histológica confirmou a descelularização, e a coloração com tricrômico de Mallory mostrou a conservação das fibras de colágeno em todas as amostras após cada tratamento. Além disso, a menor concentração de SDS que não mostrou DNA remanescente na análise de eletroforese foi de 0,1%, quando incubado por 24h e 12h. A quantificação do DNA resultou em < 0.2 ng DNA/mg de tecido ovariano utilizando estes protocolos. Ademais, a viabilidade celular mostrou que a dMEC (obtida por 0,1% de SDS e 0,02M NaOH por 12h) não era tóxico para as células ovarianas humanas durante o cultivo *in vitro* por até 72h. Por meio de análise proteômica foram identificadas 155 proteínas do *matrisome* MEC nativa do córtex ovariano bovino, e 145 na dMEC. Após a descelularização, apenas 10 proteínas do *matrisome* foram perdidas, e nenhuma delas pertencia à categoria de processos biológicos reprodutivos. Também, demonstramos que o colágeno tipo VI alfa 3 e *heparan sulfate proteoglycan 2* foram os componentes mais abundantes da MEC ovariana bovina. As análises bioinformáticas mostraram que as proteínas, tanto da MEC nativa como da dMEC, apresentam funções que se enquadram em 12 processos biológicos, 19 componentes celulares e 13 funções moleculares. Os resultados obtidos neste trabalho podem contribuir para a compreensão das funções desempenhadas pelas proteínas da MEC ovariana nos processos de ovogênese, foliculogênese e esteroidogênese. Além disso, as proteínas identificadas da MEC podem servir como base de novos materiais para um OAT.

Palavras-chave: ovário, SDS, descelularização, *matrisome*, proteômica**.**

ABSTRACT

Decellularization of the ovarian tissue extracellular matrix (ECM) is being investigated as a potential approach for developing a transplantable artificial ovary (TAO). This alternative aims to preserve fertility in women diagnosed with cancer, who could become infertile due to chemotherapy and/or radiotherapy. Existing methods to obtain decellularized ECM (dECM) from ovarian tissue are arbitrary and have only been successful in mice. The objectives of this study were: (1) to obtain dECM from bovine ovarian tissue using minimum concentration of SDS and incubation period that ensures decellularization; and (2) to analyze the ECM before and after decellularization through proteomics. To obtain dECM from bovine ovarian cortex, SDS and NaOH concentrations of 1% and 0.2M, 0.5% and 0.1M, 0.1% and 0.02M, and 0.05% and 0.01% were tested, with incubation times of 24h, 12h, and 6h. The tissue from each treatment was analyzed through histology, electrophoresis, and DNA quantification to confirm decellularization. Histological analysis confirmed decellularization, and Mallory's trichrome staining showed the preservation of collagen and elastin fibers in all samples after each treatment. Moreover, the lowest concentration of SDS that showed no remaining DNA in electrophoresis analysis was 0.1%, when incubated for 24h and 12h. DNA quantification resulted in < 0.2 ng DNA/mg of ovarian tissue using these protocols. Additionally, cell viability showed that the dECM (obtained using 0.1% SDS and 0.02M NaOH for 12h) was not toxic to human ovarian cells during *in vitro* culture for up to 72h. Through proteomic analysis, 155 proteins from the native matrisome of bovine ovarian cortex were identified, along with 145 in the dECM. After decellularization, only 10 matrisome proteins were lost, none of which belonged to the category of reproductive biological processes. Bioinformatics analyses revealed that both native and dECM proteins have functions related to 12 biological processes, 19 cellular components, and 13 molecular functions. Additionally, collagen type VI alpha 3 and heparan sulfate proteoglycan 2 were identified as the most abundant components of bovine ovarian ECM. The results obtained in this study may contribute to the understanding of the functions carried out by ovarian ECM proteins in the processes of oogenesis, folliculogenesis, and steroidogenesis. Furthermore, the proteins identified within the ECM may serve as a foundation for the development of new materials for an TAO.

Keywords: ovary, SDS, decellularization, matrisome, proteomic.

I. INTRODUÇÃO

Pacientes mulheres com diagnóstico de câncer recebem tratamento de quimioterapia e/ou radioterapia para preservar sua saúde, mas no processo de tratamento as pacientes podem ficar inférteis (Maltaris *et al*., 2007). Por isso, a reprodução assistida apresenta diferentes alternativas para conservar a fertilidade nestas pacientes como, por exemplo, a criopreservação de embrião, criopreservação de oócitos imaturos ou maduros e a criopreservação e transplante de tecido ovariano (Donnez *et al.*, 2013). Apesar disso, nem todas essas alternativas de preservação da fertilidade podem ser aplicadas em todas as pacientes, como é o caso das pacientes pré-púberes ou das pacientes sem parceiro determinado. Uma das alternativas para estes tipos de pacientes é a criopreservação de tecido ovariano para futuro autotransplante (Donnez e Dolmans, 2017). Essa técnica já resultou no nascimento de mais de 200 bebês humanos (Dolmans *et al*., 2020). Porém, em alguns casos, esta alternativa tem o risco de reintroduzir células do câncer na paciente (Sonmezer e Oktay, 2010; Donnez e Dolmans, 2017), especialmente quando o tipo de câncer apresenta moderada ou alta probabilidade de metástase no ovário, como leucemia, neuroblastoma, câncer de ovário, hemangiossarcoma, entre outros (Donnez *et al*., 2013). Por essas razões mencionadas, propõe-se a técnica de ovário artificial transplantável (OAT) como possível alternativa para preservar a fertilidade nestas pacientes (Amorim e Shikanov, 2016).

O OAT tem como objetivo obter folículos antrais a partir de folículos pré-antrais isolados do tecido ovariano; para isso, é necessário fornecer uma matriz extracelular (MEC) que, além de fornecer suporte físico, interaja dinamicamente com os folículos isolados. Dessa forma, os folículos pré-antrais isolados poderiam se desenvolver totalmente e a paciente teria a oportunidade de ter filhos biológicos. Os folículos, por estarem circundados por uma lâmina basal, que separa seletivamente as moléculas que entraram em contato com as células da granulosa e o oócito e exclui os capilares e as células vermelhas do folículo (Rodgers *et al*., 2003; Irving-Rodgers e Rodgers, 2006), asseguram que, no autotransplante dos folículos pré-antrais isolados de uma paciente com câncer, as células malignas não sejam reimplantadas (Shaw *et al*., 1996). Diversas pesquisas têm sido feitas com o intuito de oferecer uma MEC, como suporte físico, para folículos isolados. Para isso, diferentes materiais foram testados, por exemplo, colágeno (Telfer *et al*., 1990), coágulo de plasma (Gosden, 1990; Carroll e Gosten, 1993; Dolmans *et al*., 2007; Dolmans *et al*., 2008), fibrina (Smith *et al*., 2014; Rajabzadeh *et al.*, 2015; Chiti *et al*., 2016), alginato (Vanacker *et al*., 2014) e combinações de fibrina-alginato, fibrina-

colágeno (Kniazeva *et al*., 2015) e fibrina-ácido hialurônico (Paulini *et al*., 2016). No entanto, nenhum deles foi capaz de desenvolver todas as funções da MEC natural do ovário (Berkholtz *et al*., 2006; Woodruff e Shea, 2007). Devido a isso, surgiu na comunidade cientifica a ideia de utilizar a MEC nativa do ovário mediante a aplicação do método de descelularização.

A descelularização é uma técnica que consiste em retirar as células e manter a MEC sem gerar alteração na sua composição e morfologia. Esta técnica foi aplicada pela primeira vez em tecido ovariano bovino e humano com resultados animadores por Laronda *et al*. (2015). A partir de então, outros estudos foram realizados neste sentido (Liu *et al*., 2017; Alshaikh *et al*., 2019; Eivazkhani *et al*., 2019; Pors *et al*., 2019; Pennarossa *et al*., 2020), obtendo-se o desenvolvimento completo dos folículos pré-antrais e nascimento de camundongos (Buckenmeyer *et al*., 2020). Não obstante, diferentes agentes químicos foram usados nos protocolos de descelularização, como, por exemplo, Triton X (Liu *et al*., 2017), lauril éter sulfato de sódio (Hassanpour *et al*., 2018), desoxicolato de sódio (Alshaikh *et al*., 2019), hidróxido de sódio (Eivazkhani *et al*., 2019), EDTA (Buckenmeyer *et al*., 2020), desoxicolate (Pennarossa *et al*., 2020) e hidróxido de amônio (Nikniaz *et al*., 2021), destacando-se o agente químico dodecil sulfato de sódio (SDS) (Laronda *et al*., 2015; Liu *et al*., 2017; Alshaikh *et al*., 2019, 2020; Eivazkhani *et al*., 2019; Pors *et al*., 2019; Pennarossa *et al*., 2020; Nikniaz *et al*., 2021). Ainda assim, foi descrito que o SDS pode desnaturar as proteínas da MEC do tecido durante o processo de descelularização (Faulk *et al*., 2014) e sua remoção completa é difícil, deixando resíduos na MEC resultante (Zvarova *et al*., 2016, White *et al*., 2017, Kraft *et al*., 2020), o que poderia ser prejudicial para o processo de recelularização e no momento do transplante. Além disso, os protocolos de descelularização com SDS em ovário utilizam concentrações que não foram otimizadas (variam de 1% a 0,1%), variações no tempo de incubação (3 horas a dias) e associações com mais agentes químicos e biológicos (DNase I e/ou RNase). Partindo dessas problemáticas, a ideia deste projeto de pesquisa era obter uma MEC descelularizada com menor concentração de SDS e com menor tempo de incubação capaz de remover o material nuclear do tecido, mas mantendo as características físicas e as funções celulares da MEC nativa. Além disso, decidimos aplicar a análise proteômica na MEC nativa e na MEC descelularizada do tecido ovariano bovino para elucidar a composição molecular e as funções da MEC na fisiologica reprodutiva.

II. REFERENCIAL TEÓRICO

1. Ovário

O ovário é a gônada feminina que produz hormônios esteroides sexuais e gametas femininos. Além disso, é um tecido formado, da parte externa para a parte interna, por um epitélio germinal, uma túnica albugínea, uma região cortical e uma região medular. O epitélio germinal é formado por uma camada de células epiteliais cuboides, enquanto a túnica albugínea é formada por tecido conectivo denso. A região cortical é formada por tecido conjuntivo denso, células estromais como células fusiformes, células intersticiais e células endócrinas, folículos ovarianos e corpos lúteos; e a região medular por tecido conjuntivo frouxo, *rete ovari*, que é composta por células hilares, como células cuboides e colunares, vasos sanguíneos, vasos linfáticos, nervos e musculo liso (Mescher, 2016; Bacha e Bacha, 2017; Kinnear *et al*., 2020). Também, o ovário pode ser dividido em parênquima e estroma. O parênquima é composto por folículos ovarianos, enquanto o estroma é composto por células do sistema imunológico, vasos sanguíneos, vasos linfáticos, nervos, epitélio germinal, túnica albugínea, *rete ovari* intraovárica, células mãe ovarianas, células hilares, células fusiformes, células intersticiais, células endócrinas e a matriz extracelular (MEC) ovariana (Kinnear *et al*., 2020). No presente trabalho serão descritos os folículos ovarianos e a MEC ovariana no decorrer do texto.

1.1. Folículos ovarianos

Os folículos ovarianos são considerados as unidades fundamentais do ovário e estão compostos, de dentro para fora, por um oócito primário, uma ou mais camadas de células epiteliais, denominadas células da granulosa, e uma lâmina basal. Eles se encontram em diferentes etapas de desenvolvimento no ovário; por isso, são classificados morfologicamente em folículos primordiais, folículos primários, folículos secundários e folículos antrais (Figura 1). Os folículos primordiais têm uma camada de células da granulosa achatadas ao redor do oócito primário e uma lâmina basal. Os folículos primários têm um oócito primário, uma zona pelúcida, uma camada de células da granulosas cuboides e uma lâmina basal. Os folículos secundários possuem um oócito primário, uma zona pelúcida, mais de uma camada de células da granulosa cuboide, uma lâmina basal e uma camada de células da teca. Os folículos antrais têm um oócito primário, uma zona pelúcida, células da granulosa (as células da granulosas murais e as células do *cumulus oophorus)*, um antro que contém o líquido folicular, uma lâmina basal e várias camadas de células da teca interna e externa (Hafez e Hafez, 2004; Mescher, 2016;

Koeppen e Stanton, 2018). Nota-se que, independentemente da etapa de desenvolvimento de qualquer folículo ovariano, o oócito sempre aparece protegido pela lâmina basal.

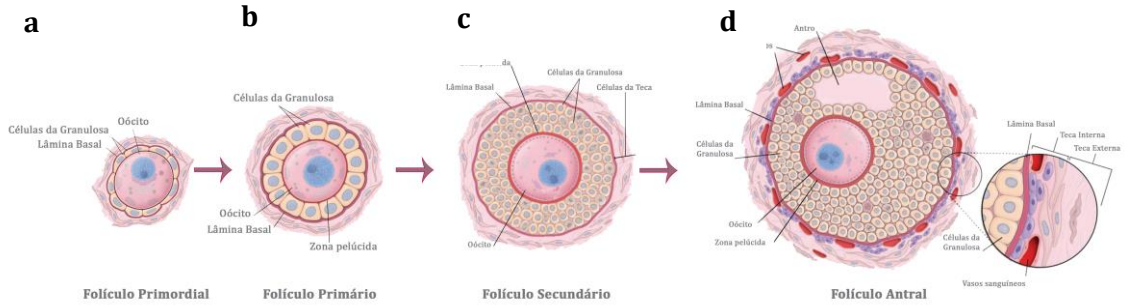

Figura 1. Imagem dos folículos ovarianos (Adaptado de Pawlina & Ross, 2016). (a) O folículo primordial é constituído por um oócito primário circundado por uma monocamada de células da granulosa achatadas e uma lâmina basal. (b) O folículo primário é composto por um oócito primário, início de formação da zona pelúcida, uma camada de células da granulosa cuboides e uma lâmina basal. (c) O folículo secundário possui um oócito primário, uma zona pelúcida, mais de uma camada de células da granulosa cuboides, uma lâmina basal e uma camada de células da teca. (d) O folículo antral é caracterizado por um oócito primário, uma zona pelúcida, várias camadas de células da granulosa, uma cavidade antral, uma lâmina basal e várias camadas de células da teca interna e externa.

A lâmina basal é formada por moléculas de colágeno tipo IV e por laminina (Zhao e Luck, 1995; Irving-Rodgers e Rodgers, 2006), e circunda as células da granulosa, que, por sua vez, envolvem ao oócito. Por isso, a lâmina basal limita o contato de células e de moléculas com as células da granulosa e o oócito, influenciando o desenvolvimento e especialização das células epiteliais do folículo (Rodgers *et al*., 2003; Irving-Rodgers e Rodgers, 2006). Portanto, a lâmina basal impede a entrada de células ou microrganismos no interior do folículo ovariano, evitando a transmissão de doenças como o câncer, quando se trabalha com folículos isolados. Por isso, quando um folículo ovariano isolado é inserido em uma MEC ovariana descelularizada e transplantado para a paciente, ele não representa nenhum risco na transmissão de doença no momento da recuperação de fertilidade dessa paciente.

1.2. Matriz extracelular ovariana

A MEC é uma estrutura tridimensional formada por polissacarídeos, fatores de crescimento, citocinas e proteínas, estas últimas podem ser estruturais e funcionais (Badylak, 2002). A função mais conhecida da MEC é o suporte físico que proporciona ao tecido; não obstante, a MEC interage de forma dinâmica com as células do tecido (Badylak, 2002). Por essa razão, a MEC também desenvolve funções complexas que regulam, por exemplo, a forma e a função da célula, a regeneração ou cicatrização do tecido (Badylak, 2002; Alberts *et al*., 2017) e a difusão de nutrientes e oxigênio para as células (Nelson e Cox, 2014). Com respeito à MEC, especificamente do ovário, se vem investigando há pouco tempo sua composição, assim como a função de cada componente e a interação entre eles. Por isso, só há trabalhos de MEC em ovário de mulher e de porca. No caso das mulheres, a MEC do córtex do tecido ovariano (após isolamento dos folículos ovarianos) apresenta 16 subtipos de colágenos, 27 glicoproteínas, 8 proteoglicanos, 16 proteínas vinculadas da MEC, 22 proteínas reguladoras da MEC e 9 fatores secretores da MEC (Ouni *et al*., 2022). E no caso das porcas, a MEC do tecido ovariano descelularizado apresenta 11 subtipos de colágenos, 36 glicoproteínas, 8 proteoglicanos, 11 proteínas vinculadas da MEC e 16 proteínas reguladoras da MEC e 5 fatores secretores da MEC, de um total de 440 proteínas desse tecido (Henning *et al.*, 2019). Não obstante, foram identificadas 5723 proteínas no ovário de macacas-rhesus (*Macaca mulatta*), mas não foram descritas especificamente quantas eram da MEC (He *et al*., 2014). Dessa forma, podemos concluir que a MEC do ovário é composta principalmente por colágeno, glicosaminoglicanos, glicoproteínas e proteoglicanos (Figura 2), os quais serão descritos de forma geral no continuar do texto.

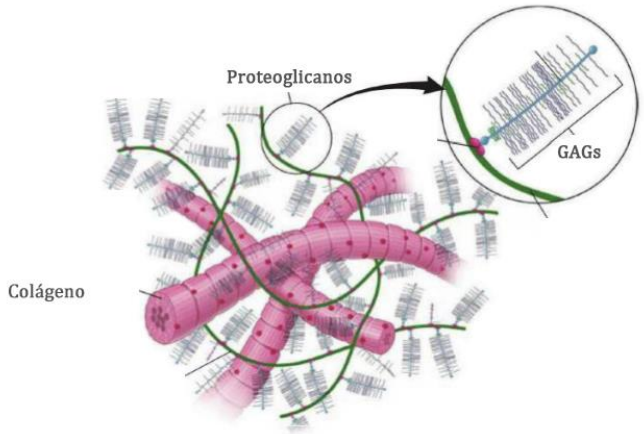

Figura 2. Imagem dos principais componentes da matriz extracelular ovariana (Adaptado de Pawlina & Ross, 2016). A matriz extracelular é formada por fibras de colágeno, proteoglicanos e glicosaminoglicanos (GAGs).

- **Colágeno**

O colágeno é um dos componentes que está em maior porcentagem no ovário, assim como em outros tipos de tecidos. Ele é uma proteína filamentosa formada por três cadeias polipeptídicas entrelaçadas em forma helicoidal (De Robertis e Hib, 2004), proporcionando resistência e elasticidade à MEC, além de suporte para a migração das células (De Robertis e Hib, 2004; Hynes e Naba, 2012). O ovário apresenta diferentes tipos de colágeno, como, colágeno tipo I, II, III, IV, VI, VIII, XII, XIV e/ou XVIII (Ouni *et al*., 2018; Henning *et al.*, 2019). No caso da mulher, o colágeno tipo VI encontra-se em maior concentração no córtex do tecido ovárico e distribuído em todo o interstício da MEC ovariana; enquanto o colágeno tipo IV está principalmente na membrana basal do folículo ovariano (Ouni *et al*., 2018). A porcentagem de colágeno na MEC ovariana aumenta progressivamente do período pré-púbere à menopausa, atingindo o pico na idade reprodutiva da mulher. Além disso, as fibras de colágeno mais finas acham-se em maior porcentagem no período pré-púbere, e as fibras mais grossas na idade reprodutiva (Ouni *et al*., 2022). No caso da porca, o colágeno tipo I encontra-se numa porcentagem mais elevada no córtex do que na medula, e o colágeno tipo IV localiza-se nas células da granulosa dos folículos ovarianos. Além disso, a cadeia alfa 1 do colágeno tipo II e a cadeia alfa 2 do colágeno tipo V foram encontrados no ovário da porca (Henning *et al.*, 2019).

- **Glicosaminoglicanos**

Os glicosaminoglicanos (GAGs) são outros componentes importantes da MEC ovariana. Eles são heteropolissacarídeos compostos por unidades dissacarídeos repetitivos e específicos, em que um dos dois monossacarídeos possui um grupo amino (N-acetilglicosamina ou N-acetilgalactosamina) e um ácido urônico (ácido D-glicurônico ou ácido L-idurônico) (De Robertis e Hib, 2004; Nelson e Cox, 2014). Vários GAGs contêm grupo sulfato esterificado; a combinação do grupo sulfato com o grupo carbóxilo dos resíduos de ácido urônico resulta em uma carga negativa que atrai moléculas de Na^+, e as quais, por sua vez, atraem moléculas de água, produzindo turgência da MEC (De Robertis e Hib, 2004). Os GAGs são fundamentais para as ligações das células com citocinas e com fatores de crescimento (Badylak, 2002). No caso na MEC do ovário da mulher, os GAGs estão distribuídos em toda a região cortical (Ouni *et al*., 2018). Neste caso, a porcentagem de GAGs aumenta significativamente de período pré-púbere à idade reprodutiva, além de que, a porcentagem de GAGs é semelhante entre a idade reprodutiva e a menopausa (Ouni *et al*., 2020).

- **Glicoproteínas**

As glicoproteínas são moléculas que contêm uma ou algumas cadeias oligossacarídicas ligadas de modo covalente a uma proteína (Nelson e Coxe, 2014). Na MEC do córtex do ovário da mulher, encontram-se as seguintes glicoproteínas: fibrilina-1, tenascina-XB, elastina microfibrila interfacer-1 (EMILIN-1), cadeia alfa, beta ou gama de fibrinogênio e laminina (Ouni *et al*., 2018). A elastina representa aproximadamente 5% da MEC do tecido ovariano da mulher e aumenta em porcentagem do período pré-púbere à idade reprodutiva, mas diminui na menopausa (Ouni *et al*., 2020). Enquanto a fibrilina-1 encontra-se em porcentagem similar na idade pré-púbere e reprodutiva; no entanto, na menopausa, reduz-se quase à metade (Ouni *et al*., 2020). E a EMILIN-1 está espalhada heterogeneamente pela MEC do tecido ovariano da mulher, e sua porcentagem aumenta ligeiramente do período pré-púbere à idade reprodutiva e diminui na menopausa (Ouni *et al*., 2020). Na porca, a EMILIN-1 encontra-se numa porcentagem mais elevada no córtex do que na medula (Henning *et al.*, 2019). As três glicoproteínas mencionadas anteriormente (elastina, fibrilina-1 e EMILIN-1) desenvolvem funções de elasticidade na MEC do ovário (Ouni *et al*., 2018; Ouni *et al*., 2020).

- **Proteoglicanos**

Os proteoglicanos são macromoléculas formadas por uma ou mais cadeias de glicosaminoglicanos sulfatados ligados de modo covalente a um núcleo de proteína extracelular (Nelson e Cox, 2014; Albert *et al*., 2017). Na MEC do tecido ovariano da mulher, encontra-se, por exemplo, osteoglicina, lumican e proteoglicanas de heparan sulfato-2 (Ouni *et al*., 2018).

2. Ovário Artificial Transplantável

O ovário artificial transplantável (OAT) é uma técnica de reprodução assistida em desenvolvimento. Esta técnica pretende criar um meio extracelular similar ao do ovário natural para que folículos isolados possam ser introduzidos nele e sejam capazes de se desenvolver completamente. Desta forma, ambos os componentes do ovário, folículos ovarianos e MEC ovariana, interagem entre si e permitem o desenvolvimento das funções do ovário (como foi descrito anteriormente).

Na ideia de fornecer uma MEC para o OAT, materiais não sintéticos, como colágeno, fibrina, coágulo de plasma e alginato, e sintéticos, como polietilenoglicol, foram testados como matriz para o desenvolvimento de um OAT. Embora alguns dos resultados da

literatura apresentados abaixo sejam animadores, esses tipos de materiais ainda apresentam limitações, tais como: 1) a sobrevivência folicular relativamente baixa (< 50 %) após o transplante (Dolmans *et al*., 2008; Vanacker *et al*., 2014; Rajabzadeh *et al*., 2015; Paulini *et al*, 2016), 2) a não identificação de todos os componentes, especificamente no caso do coágulo de plasma, que pode possuir componentes que influenciam negativamente no desenvolvimento folicular, e 3) a degradação rápida de outros materiais após o transplante, como no caso do alginato e da fibrina (Vanacker *et al*., 2011; Smith *et al*., 2014).

O primeiro material testado como matriz foi o colágeno, e nele foram colocados folículos pré-antrais isolados de camundongo. Essa estrutura foi alotransplantada ortotopicamente em camundongo, propiciando o desenvolvimento dos folículos pré-antrais a folículos pré-ovulatórios, mas sem ovulação. Após a recuperação dos oócitos dos folículos de maior tamanho do enxerto, eles foram fertilizados *in vitro* e geraram quatro blastocistos (Telfer *et al*., 1990).

Outro material testado como matriz foi o coágulo de plasma. Neste material foi possível o desenvolvimento completo dos folículos ovarianos e a obtenção de ninhadas de camundongos. Por um lado, Gosden (1990) obteve vinte e sete nascimentos e, por outro lado, Carroll e Gosden (1993) obtiveram doze nascimentos. Tudo isto aconteceu quando folículos primordiais isolados frescos e criopreservados de camundongos foram inseridos no coágulo de plasma, e o conjunto foi alotransplantado ortotopicamente em camundongo (Gosden, 1990; Carroll e Gosden, 1993). Apesar dos bons resultados com coágulo de plasma em camundongos, em humanos, só foi possível a obtenção de folículos secundários e folículos antrais, a partir de folículos pré-antrais humanos inseridos no coágulo de plasma e xenotrasplantado ortotopicamente no camundongo (Dolmans et *al*., 2007; Dolmans *et al*., 2008). No entanto, o problema de trabalhar com o coágulo de plasma é o fato dos componentes proteicos, como fatores de crescimento e/ou leucócitos, variarem de um indivíduo para outro (Gobbi e Vitale., 2012; Anitua *et al*.,2013), tornando difícil otimizar a concentração ideal destes componentes na matriz para OAT.

Além do coágulo de plasma, a fibrina foi outro material que permitiu nascimentos de oito camundongos. Isto foi possível quando folículos primordiais e primários foram inseridos na mistura de fibrina-fator de crescimento endotelial vascular, e esta estrutura alotransplantada ortotopicamente em camundongos (Kniazeva *et al*., 2015). Além disso, Smith *et al*. (2014) e Chiti *et al*. (2016) também investigaram a fibrina como matriz para OAT. Nesse material não sintético, foram inseridos folículos pré-antrais e células do

estroma do ovário, obtendo-se folículos antrais e corpos lúteos, além da produção de hormônios sexuais após o alotransplante no camundongo (Smith *et al*., 2014; Chiti *et al*., 2016). Apesar dos bons resultados com a fibrina, foi relatado que essa matriz se degradou em menos de 30 dias após o transplante (Smith *et al*., 2014), sendo isto uma limitação para o desenvolvimento folicular de outras espécies.

O mais recente material não sintético testado como matriz para um OAT foi o alginato, onde foi possível obter folículos antrais de camundongos. Isso aconteceu quando folículos pré-antrais e células do ovário, ambos de camundongos, foram inseridos na matriz de alginato e autotransplantado heterotopicamente (Vanacker *et al*., 2014). Por um lado, foi testada a mistura de fibrina-alginato e fibrina-colágeno como matriz, obtendo-se o desenvolvimento folicular dos folículos primordiais e primários de camundongos (Kniazeva *et al*., 2015). Por outro lado, foi testada a mistura fibrina-ácido hialurônico como matriz, evidenciando a sobrevivência dos folículos pré-antrais e das células do estroma do ovário, ambos provenientes de tecido ovariano criopreservado humano e após o xenotransplante heterotópico para camundongos (Paulini *et al*, 2016).

O único material sintético testado como matriz com a ideia de desenvolver um OAT foi o polietilenoglicol. Nesse material, foi possível o desenvolvimento folicular completo e a diminuição dos níveis de FSH após 30 e 60 dias do alotransplante ortotópico de folículos pré-antrais de camundongo (Kim *et al*., 2016).

Em resumo, resultados animadores como o desenvolvimento folicular completo, produção hormonal, obtenção de embriões e de nascimentos foram alcançados em camundongos quando se utilizaram materiais não sintéticos e sintéticos como matriz para um OAT. Entretanto, não foi possível desenvolver uma matriz que desempenhe todas essas funções em outras espécies. Isso pode ser devido à constituição da MEC ovariana natural, que é formada por diferentes componentes, e até o presente momento, as matrizes testadas possuíam apenas um ou dois dos componentes da MEC ovariana natural. Desta forma, com objetivo de desenvolver um OAT, levantou-se a ideia de manter intacta a MEC do ovário mediante a técnica de descelularização da MEC ovariana com agentes químicos, enzimático e/ou físicos; o qual será discutida nos tópicos abaixo.

2.1. Descelularização da MEC do ovário

A técnica de descelularização consiste em remover as células e o material genético do tecido, conservando no processo a MEC nativa (Gilbert *et al*., 2006). Um tecido é considerado descelularizado quando tem as seguintes características: 1) <50 ng de DNA por mg de peso seco de MEC, 2) <200 par de bases (pb) de tamanho de fragmento de DNA, e 3) ausência de material nuclear no tecido quando este é corado com Hematoxilina-Eosina ou 4',6'-diamino-2-fenil-indol (DAPI) (Crapo *et al*., 2011). Além disso, a MEC nativa descelularizada conserva seus componentes acelulares e propriedades, possibilitando que esta estrutura, em contato com novas células, seja capaz de formar novamente o mesmo tipo de tecido que foi descelularizado e com as mesmas funções; além de não gerar uma reação imunológica no receptor após o transplante (Hrebikova *et al*., 2015). Com este objetivo, estão sendo utilizados agentes físicos (temperatura, sonicação, entre outras), químicos (SDS, Triton X-100, entre outros) e/ou biológicos (DNase I e/ou RNase) para descelularizar diferentes tipos de tecidos como, por exemplo, fígado, coração, pulmão, pâncreas, intestino, rim, bexiga, osso, cartilagem e placenta (Crapo *et al*., 2011; Guruswamy e Vermette, 2018). Especificamente no caso do tecido ovariano a técnica de descelularização está sendo realizada principalmente por agentes químicos.

A descelularização química é realizada mediante a aplicação de agentes químicos, tendo como exemplo, agentes alcalinos ou ácidos, soluções hipertônicas ou hipotônicas, detergentes não iônicos e/ou iônicos, e álcoois (Hoshiba *et al*., 2010; Hrebikova *et al*., 2015). Esses agentes modificam as ligações intercelulares e extracelulares, isto por sua vez modifica a membrana da célula, permitindo que o processo denominado lise celular (Gilbert *et al*., 2006; Hoshiba *et al*., 2010) possibilite a separação da célula da MEC. E, assim, essas células são removidas durante o processo de lavagem. Vários agentes químicos estão sendo aplicados no tecido ovariano, entre eles podemos destacar o SDS.

- **Dodecil sulfato de sódio**

O SDS é um detergente aniônico (Figure 3) que interage com as proteínas da membrana celular, facilitando o acesso do detergente aos lipídeos da membrana (Kragh-Hansen *et al*., 1998). Desta forma, solubiliza a membrana citoplasmática e a membrana do envelope nuclear da célula, resultando na lise celular (Faulk *et al*., 2014). Não obstante, é importante notar que o SDS também pode desnaturar, em alguma porcentagem, as proteínas da MEC do tecido durante o processo de descelularização (Faulk *et al*., 2014).

Apesar dessas limitações, o SDS tem sido utilizado na obtenção da MEC descelularizada do tecido ovariano devido aos resultados animadores.

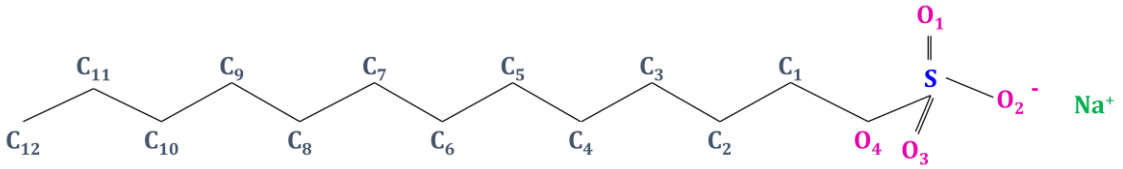

Figura 3. Estrutura do dodecil sulfato de sódio (Adaptado de Bruce et al., 2002).

A técnica de descelularização de tecido ovariano humano e bovino foi aplicada pela primeira vez em 2015 por Laronda *et al*. (2015). Nesse trabalho, o tecido ovariano de ambas as espécies foi submetido à descelularização usando 0,1% de SDS por 24 horas a temperatura ambiente, resultando na obtenção da MEC descelularizada do ovário humano e bovino. A MEC descelularizada do ovário bovino foi cultivada *in vitro* com células ovarianas de camundongo por 2 dias e, em seguida, esse conjunto foi transplantado ortotopicamente para fêmeas de camundongo ovariectomizadas. Esses animais recuperaram a produção de estradiol após 2 e 4 semanas do transplante (Laronda *et al*., 2015). A partir desse trabalho animador, foram realizadas mais investigações utilizando o SDS como agente químico de descelularização de tecido ovariano, tanto sozinho com em associação com outros agentes.

Liu *et al*. (2017) descrevem um protocolo de descelularização baseado na mistura de agentes químicos, físicos e enzimáticos para tecido ovariano de porca. Primeiramente, esse tecido foi congelado a -80°C e descongelado três vezes. Em seguida, foi colocado em solução de 1% de Triton X-100 por 9 horas e em solução de 0,5% de SDS por 3 horas. Por fim, o tecido foi colocado em 200 U/mL DNase I por 12 horas, conseguindo-se dessa forma a MEC descelularizada do tecido ovariano. Esta MEC descelularizada apresentou 20,92 ± 4,56 ng DNA/mg de peso seco em comparação ao tecido normal que foi de 701,62±469,28 ng DNA/mg de peso seco. Além disso, a MEC descelularizada foi transplantada heterotopicamente em ratos machos, e o excerto apresentou uma leve reação inflamatória após 2 e 4 semanas do transplante.

Alshaikh *et al*. (2019) descrevem os efeitos qualitativos e quantitativos da descelularização de ovário de camundongo. Nesse trabalho, os ovários foram congelados a -20°C e descongelados, em seguida, colocados em solução de 0,5% de SDS por 10 horas e em 40 units/mL DNase I por 30 min. Obtendo-se 145 ± 50 ng de DNA/ ovário no ovário descelularizado em comparação ao ovário natural que foi de 33,972 ± 5,163 ng de DNA/

ovário. Desta forma, os autores descreveram leves modificações nas fibras de colágeno e nas fibras de queratina, bem como, nos GAGs da MEC após a descelularização do tecido ovariano. Posteriormente, os mesmos autores testam essa MEC descelularizada no cultivo *in vitro* com células estromais mesenquimais por 14 dias, mostrando que, apesar dos danos gerados na MEC após a descelularização, esta é re-celularizada e as células se multiplicam (Alshaikh *et al*., 2020).

Eivazkhani *et al*. (2019) e Pennarossa *et al*. (2020) descrevem dois diferentes protocolos de descelularização para tecido ovariano que mantêm a integridade das fibras da MEC após a descelularização. Eivazkhani *et al*. (2019) trabalharam com fragmentos de ovários vitrificados de humanos e de ovelhas, e com ovários frescos de camundongos. O protocolo de descelularização consistiu em congelar as amostras a -80°C e após descongelar, um grupo de amostras foi colocado em solução de 1% de SDS e outro grupo de amostras em solução de 0,5 N de NaOH. Nessas soluções, os ovários de camundongos foram mantidos por 3 horas e os fragmentos de ovários de humanos e ovelhas foram mantidos *overnight*. Finalmente, as amostras foram colocadas numa solução de RNase/DNase, obtendo-se a MEC descelularizada para cada amostra (ambos grupos), as quais apresentaram conservação das fibras de colágeno e dos GAGs. Além disso, a MEC descelularizada de humano (Protocolo com NaOH) com células ovarianas de camundongos foram autotransplantada heterotopicamente por 1 mês; observou-se a proliferação de células ovarianas e estruturas semelhantes a folículos ovarianos após o transplante.

Pennarossa *et al*. (2020) trabalharam com ovário de porca. O ovário inteiro foi congelado a - 80°C e descongelado, colocado em solução de 0,5% de SDS por 3 horas, em solução de 1% de Triton X-100 por 9 horas e em solução de 2% de desoxicolato por 12 horas. Conseguiu-se, dessa forma, uma MEC descelularizada com 0,03 ± 0,01 μg DNA/mg, em comparação a 1,59 ± 0,08 μg DNA/mg de tecido não descelularizado. Também com esse protocolo, manteve-se a integridade das fibras de colágeno e de elastina, bem como os GAGs da MEC após a descelularização. Além disso, a MEC descelularizada foi cultivada *in vitro* com fibroblastos suínos de pele por 1, 3 e 7 dias, mostrando uma colonização completa da MEC descelularizada após 24 horas do cultivo e um aumento progressivo da proliferação das células no decorrer dos dias de cultivo.

Nikniaz *et al*. (2021) descelularizaram a região cortical do ovário de bovino e de humano. Todas as amostras foram congeladas a -80°C e descongeladas; este procedimento foi repetido três vezes. Por um lado, as amostras de tecido ovariano bovino foram submetidas a uma concentração de 0,1% de SDS: um grupo por 24 horas e outro grupo por

18 horas. Um terceiro grupo foi submetido a uma concentração de 0,5% de SDS por 3 horas e 1% Triton por 9 horas, e um quarto grupo foi com 0,5% de SDS por 2 horas e com uma mistura de 1% de Triton com 0,1% de hidróxido de amônio por 22 horas. Por outro lado, as amostras de tecido ovariano humano foram descelularizadas como foi descrito no quarto grupo. As amostras de bovino e de humano foram adequadamente descelularizadas com os protocolos utilizados; não obstante, as amostras de humanos apresentaram maior quantidade de DNA remanescente. Também, as MECs de ambas as espécies não apresentaram modificações qualitativas após a descelularização. Depois disso, foi realizado o cultivo *in vitro* de células fibroblásticas de camundongos nas MEC descelularizadas por 7 dias, apresentando uma maior viabilidade celular na MEC que foi descelularizada com os três tipos de agentes químicos (grupo 4). Além disso, nesse tipo de MEC descelularizada, foram inseridos folículos pré-antrais de camundongos misturados com a solução de 1% de alginato, e esta estrutura foi cultivada *in vitro* por 7 dias, resultando em um 85,9% de recuperação dos folículos pré-antrais após o cultivo.

Apesar de serem descritos resultados diferentes na MEC do tecido ovariano após a descelularização com SDS, Pors *et al*. (2019) comprovou a viabilidade deste tipo de MEC mediante o desenvolvimento folicular após o transplante do enxerto. Eles trabalharam com tecido ovariano de humano que foram colocados em solução de 0,1% de SDS, por 24 horas, no caso da região cortical criopreservada, e por 18 horas, no caso da região medular fresca. Após isso, os tecidos foram colocados em solução de 1 mg/ml de DNase I por 24 horas. Com esse protocolo, foi obtida a descelularização de ambas as regiões do ovário humano e a MEC descelularizada não apresentou variação na porcentagem de colágeno em comparação ao tecido ovariano sem descelularização. Além disso, na MEC descelularizada foram inseridos folículos pré-antrais humanos ou de camundongos; esses enxertos foram transplantados para camundongas ovarectomizadas, resultando em desenvolvimento folicular de folículos pré-antrais humanos a folículos secundários e de folículos pré-antrais de camundongos a folículos antrais, após 3 semanas do transplante. Além disso, taxas de recuperação folicular de 25% para folículos humanos e de 21% para folículos de camundongos foram obtidas.

- **Outros agentes químicos de descelularização no tecido ovariano**

Outros agentes químicos, descritos por Hassanpour *et al*. (2018), Buckenmeyer *et al*. (2020), Chiti *et al*. (2022) e Wu *et al.* (2022), foram usados nos protocolos de descelularização do tecido ovariano. Hassanpour *et al*. (2018) usaram lauril éter sulfato de sódio (SLES), enquanto Buckenmeyer *et al*. (2020) e Chiti *et al.* (2022) usaram EDTA,

Triton X-100 e desoxicolato de sódio (SDC) em seus protocolos de descelularização. A diferença entre os estudos é que Chiti *et al* (2022) também incorporaram tripsina no protocolo.

Hassanpour *et al*. (2018) trabalharam com ovário de humano congelado -80°C. A região cortical desse ovário foi submetida a 1% de SLES por 48 horas e a 500 U/ml de DNase I por 24 horas, resultando na descelularização do tecido com 40 ± 7,33 ng DNA/mg de peso seco, em comparação a 1296,26 ± 52,59 ng DNA/mg de peso seco no tecido não descelularizado. Além disso, as fibras de colágeno I e IV, fibras elásticas e GAGs (fibronectina e laminina) foram mantidas na MEC após a descelularização. Posteriormente, na MEC descelularizada, foram colocadas células ovarianas de ratas, e essa estrutura foi transplantada ortotopicamente em ratas ovário-histerectomizadas por 4 semanas. Após o período mencionado anteriormente, foram observadas formações de vasos sanguíneos e estruturas semelhantes a folículos primordiais e primários, bem como a produção de progesterona. No entanto, também foi observada uma reação inflamatória na estrutura após o transplante.

Buckenmeyer *et al*. (2020) descelularizaram tecido ovariano de porca. Esse tecido foi congelado a -20°C e armazenado a 4°C. Em seguida, foi colocado em solução de 0,02% de tripsina com 0,05% de EDTA por 1 hora e em solução de 3% de Triton X-100 por 1 hora. Finalmente, foi armazenado a 4°C e colocado em solução de 4% de desoxicolato de sódio por 1 hora. O procedimento resultou em 262,4 ± 59,96 ng dsDNA/mg de peso seco do tecido descelularizado, em comparação a 9126 ± 1988 ng dsDNA/mg de peso seco do tecido não descelularizado. Além disso, as fibras de colágenos I e IV, e GAGs (fibronectina e laminina) foram mantidas no tecido descelularizado. Posteriormente, foi obtido o hidrogel da MEC descelularizada, no qual foram misturados folículos de camundongos. Essa estrutura foi injetada na região cortical do ovário de camundongos com insuficiência ovariana primária, conseguindo-se descendentes provenientes desses folículos transplantados.

Chiti *et al*. (2022) descelularizaram o tecido ovariano de bovino, mas quando usaram o hidrogel de MEC descelularizada com folículos ovarianos humanos, observaram que não era possível a sobrevivência dos folículos após o cultivo. Nesse trabalho, os fragmentos de ovário foram congelados em nitrogênio líquido e armazenados a -80°C. Em seguida, foram incubados em solução de 0,05% tripsina e 0,02% EDTA por 1 h a 37°C, lavados com água deionizada e incubados em 3% Triton X-100 por 1 hora a temperatura ambiente. Depois, foram lavados com água deionizada, incubada em 4% de SDC por 1 hora

a temperatura ambiente e lavada com água deionizada, obtendo-se a MEC descelularizada e preservando as fibras de colágeno e dos GAGs. O hidrogel da MEC descelularizada foi misturado com folículos pré-antrais de humano e cultivado *in vitr*o por 1 semana. Nesse caso, foram formados quatro grupos de tratamento: (a) 100% de hidrogel de MEC descelularizada, (b) 90% de hidrogel de MEC descelularizada com 10% de alginato, (c) 75% de hidrogel de MEC com 25% de alginato e (d) 100% alginato, obtendo uma recuperação folicular de 0%, 23%, 65% e 85%, respectivamente.

Wu *et al*. (2022) descelularizaram o tecido ovariano de porca, mas a MEC descelularizada gerou uma reação inflamatória após o transplante. As amostras foram congeladas a -80°C, submersas em água destilada por 6 horas e, em seguida, misturadas em uma solução de 2% de SDC com 4% de Triton X-100 por 36 horas. Posteriormente, foram incubadas em 1% de SDS por 36 h, 80 U/mL de RNase/DNase por 6 horas a 37°C, e lavadas em água destilada por 24 horas. A MEC descelularizada apresentou uma concentração de 12,86 ± 1,707 ng/mg de DNA, fragmentos menores a 200pb de DNA, e a preservação das proteínas da MEC (diferentes tipos de colágeno, GAGs e glicoproteínas). Os pesquisadores também realizaram o transplante heterotópico da MEC descelularizada com células da granulosa e folículos ovarianos, ambos de camundongos, por 4 semanas, mas não houve recuperação da produção de hormônios sexuais no camundongo. Isso se deveu à grave reação inflamatória às mitocôndrias e endossomos residuais na MEC descelularizada nos dias 3 e 7 após o transplante.

Em resumo, os protocolos de descelularização atualmente empregados para tecido ovariano geralmente envolvem o uso conjunto de vários agentes de descelularização. A utilização desses múltiplos agentes pode resultar em modificações relevantes na estrutura e na função da MEC do ovário. Assim, é fundamental investigar novos protocolos de descelularização, mais suaves e eficientes, para avançar no campo da biotecnologia reprodutiva.

3. *Matrisome*

Matrisome é um conjunto de genes que codificam as proteínas da MEC. As proteínas da MEC são identificadas de acordo com seus domínios, e divididas em proteínas centrais do *matrisome* e proteínas associadas a *matrisome* (Figura 4) (Essas informações estão disponíveis em: <http://matrisomeproject.mit.ed>) (Hynes y Naba, 2012, Naba *et al*., 2012, 2016).

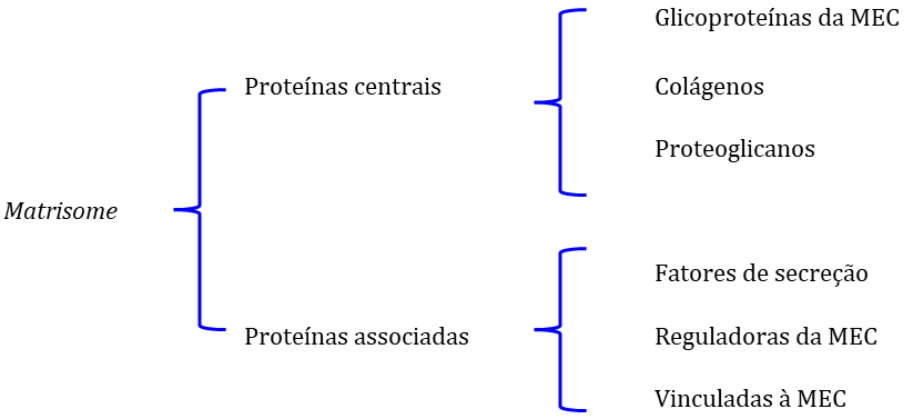

Figura 4. Esquema da divisão do *matrisome*. O *matrisome* é dividido em proteínas centrais, que incluem glicoproteínas da MEC, colágeno e proteoglicanos, e proteínas associadas, que englobam fatores de secreção, proteínas reguladoras da MEC e proteínas vinculadas à MEC.

3.1. Proteínas centrais do *matrisome*

As proteínas centrais são as proteínas que dão a estrutura à MEC e são classificadas em colágenos, proteoglicanos e glicoproteínas (Naba *et al*., 2012, 2016).

a. **Colágenos**: são proteínas caracterizadas por sequências repetitivas de glicina-X (frequentemente prolina) - Y (frequentemente 4-hidroxiprolina ou hidrosilisina) (Hynes e Naba, 2012), como cadeia alfa 2 de colágeno tipo IV e cadeia alfa 3 de colágeno VI (Figura 5).

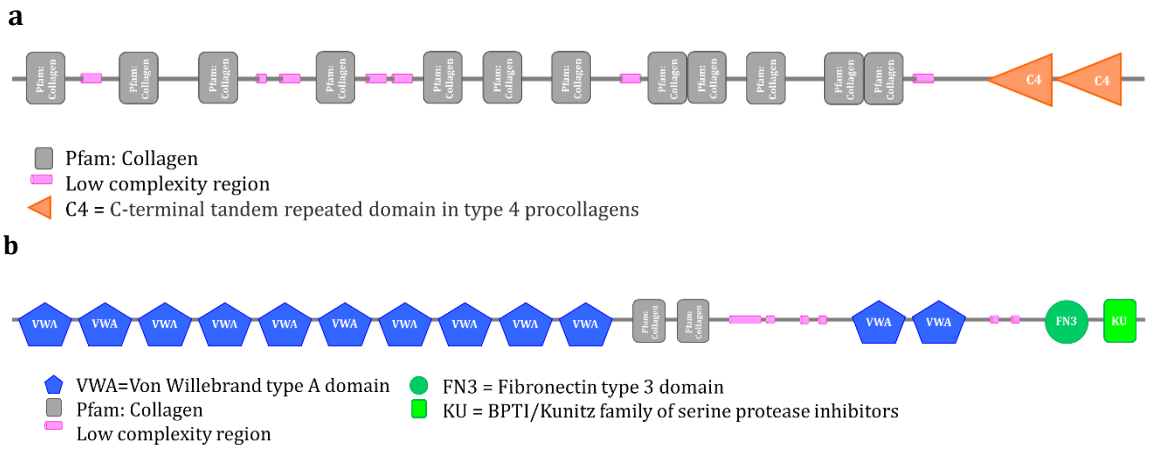

Figura 5. Representação esquemática de dois tipos de colágeno. (a) Cadeia alfa 2 de colágeno tipo IV e (b) cadeia alfa 3 de colágeno VI, cada um com seus respetivos domínios, obtidas da matriz extracelular descelularizada de ovário bovino (Adaptado de: <www.smart.embl.de>).

b. Proteoglicanos. são caraterizados por repetições ricas em leucinas (LRR), e por repetições de domínios de LINK e lectina tipo C (Hynes e Naba, 2012), como o *heparan sulfate proteoglycan 2*, *lumican*, etc (Figura 6).

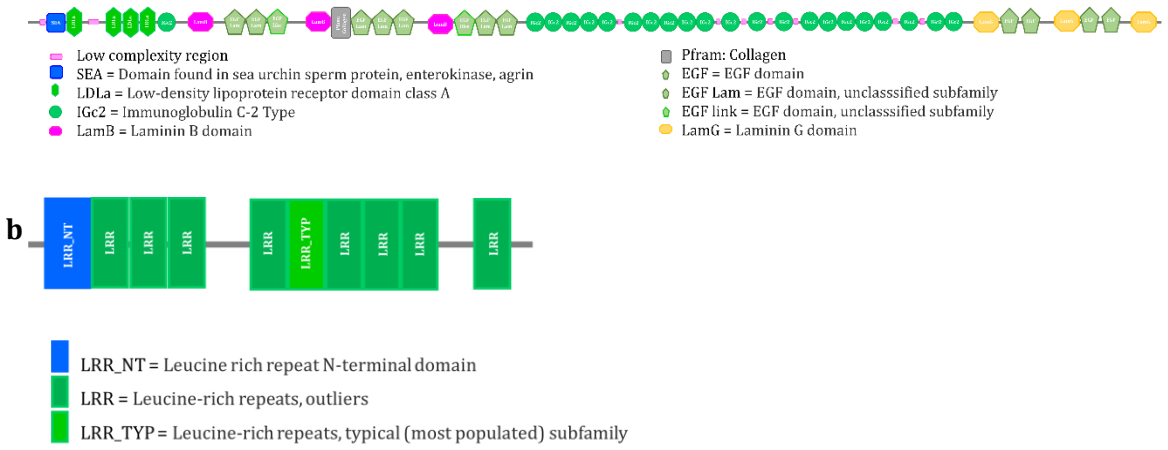

Figura 6. Representação esquemática de dois tipos de proteoglicanos. (a) *Heparan sulfate proteoglycan 2* e (b) *lumican*, cada um com seus respetivos domínios, obtidas da matriz extracelular descelularizada de ovário bovino (Adaptado de: <www.smart.embl.de>).

c. **Glicoproteínas da MEC**: são caracterizadas por múltiplos domínios de aminoácido (Hynes e Naba, 2012), como *laminin*, *tenascin XB*, etc. (Figura 7).

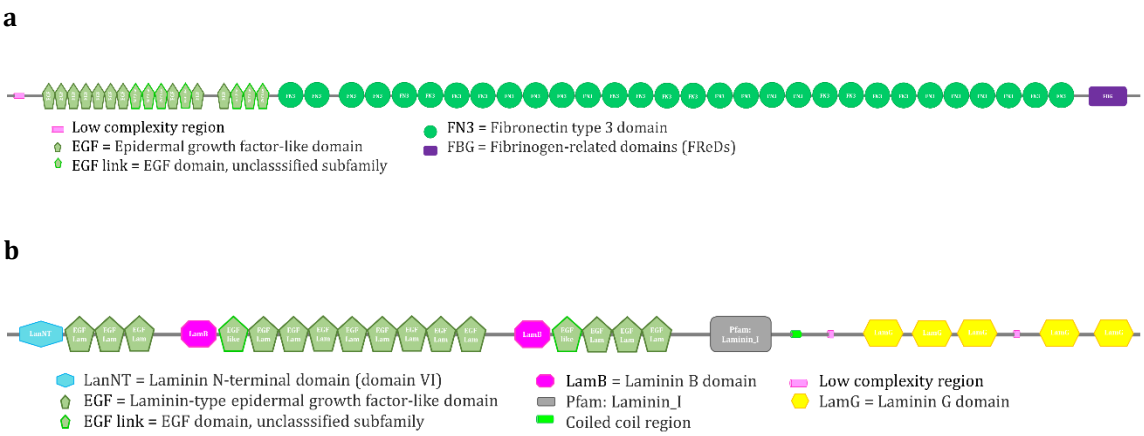

Figura 7. Representação esquemática de dois tipos de glicoproteínas. (a) *Tenascin XB* e (b) *laminin subunit alpha 1*, cada uma com seus respetivos domínios, obtidas da matriz extracelular descelularizada de ovário bovino (Adaptado de: <www.smart.embl.de>).

3.2. Proteínas associadas a *matrisome*

As proteínas associadas ao *matrisome* são proteínas que interagem com as proteínas centrais do matrisome e são classificadas em fatores de secreção, proteínas vinculadas à MEC e proteínas reguladoras da MEC (Naba *et al*., 2012, 2016).

a. **Fatores de secreção**: são proteínas que se ligam e modulam a sinalização da MEC, como citoquinas, fatores de crescimento, etc. (Naba *et al*., 2012, 2016) (Figura 8).

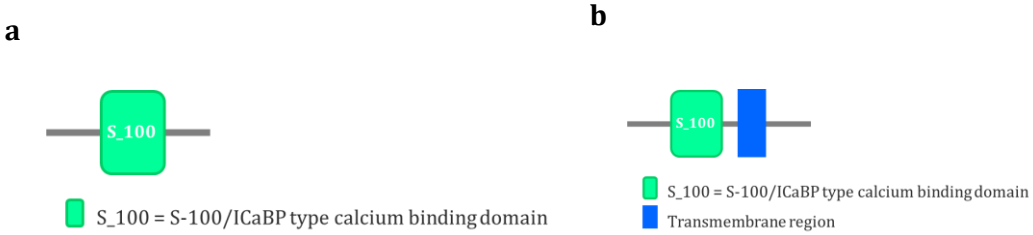

Figura 8. Representação esquemática de dois fatores de secreção. (a) *Protein S100-A16* e (b) *protein S100-A10*, cada uma com seus respetivos domínios, obtidas da matriz extracelular descelularizada de ovário bovino (Adaptado de: <www.smart.embl.de>).

b. **Proteínas reguladoras da MEC**: são enzimas que modificam a MEC e a regulam a sua estabilidade, como, proteases, inibidores de protease, etc. (Naba *et al*., 2012, 2016) (Figura 9).

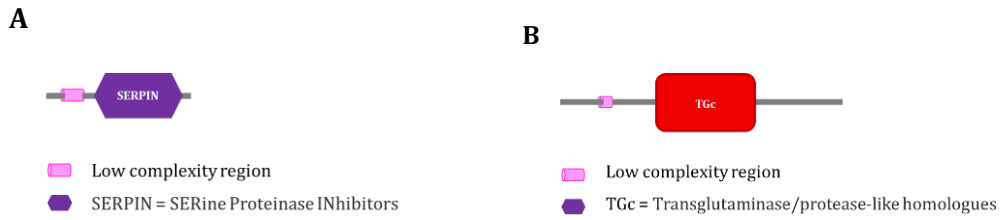

Figura 9. Representação esquemática de duas proteínas reguladoras. (a) *Serpin peptidase inhibitor, classe H, member 1* e (b) *protein-glutamine gamma-glutamytransferase 2*, cada uma com seus respetivos domínios, obtidas da matriz extracelular descelularizada de ovário bovino (Adaptado de: <www.smart.embl.de>).

c. **Proteínas vinculadas à MEC**: são proteínas que apresentam similaridades estruturais ou bioquímicas com as proteínas da MEC ou proteínas que não são incluídas nas outras categorias, mas que estão associadas às proteínas da MEC, como mucinas, galectinas, etc (Naba *et al*., 2012, 2016) (Figura 10).

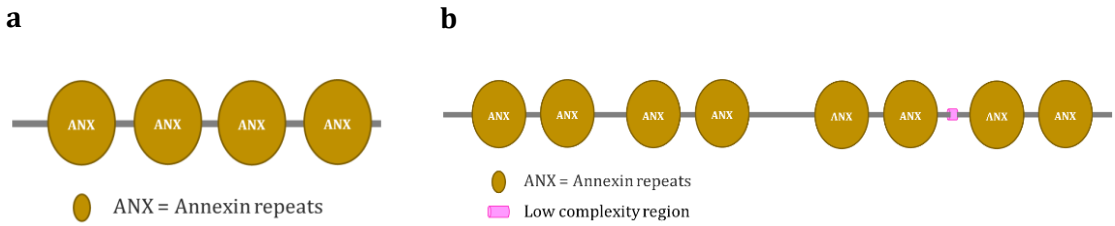

Figura 10. Representação esquemática de duas proteínas vinculadas à MEC. (a) *Annexin A2* e (b) *annexin A6*, cada uma com seus respetivos domínios, obtidas da matriz extracelular descelularizada de ovário bovino (Adaptado de: <www.smart.embl.de>).

3.3. *Matrisome* do ovário

As proteínas do *matrisome* foram identificadas em tecido ovariano de mulher (Ouni *et al*., 2019, 2020, 2022) e de porca (Henning *et al*., 2019). O *matrisome* de tecido ovariano de mulher foi descrito pela primeira vez por Ouni *et al*. (2019). Eles identificaram 85 proteínas no *matrisome*, especificamente do córtex ovariano fresco e criopreservado, das quais 46 eram proteínas principais do *matrisome* e 39 eram proteínas associadas à MEC. Nas proteínas centrais, foram identificadas 28 glicoproteínas da MEC (Tabela 1), 11 tipos diferentes de colágenos (Tabela 2) e 7 proteoglicanos (Tabela 3). Além disso, foram identificadas as proteínas mais abundantes em cada categoria, como *fibrilin 1*, cadeia alfa 3 de colágeno tipo VI e *osteoglycin*, respectivamente. Nas proteínas associadas à MEC, foram identificadas 23 proteínas reguladoras da MEC (Tabela 4), 12 proteínas vinculadas à MEC (Tabela 5) e 4 fatores de secreção (Tabela 6). Dessas categorias, as mais abundantes foram *serpin family A member 1*, *annexin A2* e *S100 calcium binding protein A11*. Anos mais tarde, outro *matrisome* de tecido ovariano de mulher foi descrito, mas com a diferença de que foi realizado nas diferentes etapas reprodutivas da mulher – pré-púbere, em idade reprodutiva, em menopausa (Ouni *et al*., 2022). Nesse *matrisome,* foram identificadas 120 proteínas no total, mas 98 proteínas foram identificadas nas diferentes etapas reprodutivas, das quais 51 eram proteínas principais do *matrisome* (27 glicoproteínas da MEC (Tabela 1), 16 tipos diferentes de colágenos (Tabela 2) e 8 proteoglicanos (Tabela 3)), e 47 eram proteínas associadas à MEC (22 proteínas reguladoras da MEC (Tabela 4), 16 proteínas de vinculadas à MEC (Tabela 5) e 9 fatores de secreção (Tabela 6)). Além disso, em cada etapa reprodutiva, os colágenos mais abundantes foram identificados, por exemplo, (i) em mulheres pré-púberes foi a cadeia alfa 3 de colágeno tipo VI, (ii) em mulheres em idade reprodutiva foi a cadeia alfa 1 de colágeno tipo I e (iii) em mulheres na menopausa foi a cadeia alfa 1 de colágeno tipo IV (Ouni *et al*. 2022).

O *matrisome* de tecido ovariano de porca, especificamente da MEC descelularizada, foi descrito por Henning *et al*. (2019). Eles identificam 82 proteínas no *matrisome*, mas 42 dessas proteínas variam de acordo com a profundidade do tecido ovariano. Por um lado, nas proteínas principais do *matrisome,* foram identificadas 55 proteínas, incluindo 36 glicoproteínas da MEC (Tabela 1), 11 tipos diferentes de colágenos (Tabela 2) e 8 proteoglicanos (Tabela 3). Por outro lado, nas proteínas associadas à MEC, foram identificadas 32 proteínas, das quais 16 eram proteínas reguladoras da MEC (Tabela 4), 11 eram de proteínas de vinculadas à MEC (Tabela 5) e 5 eram de fatores de secreção. Além disso, foram identificadas as proteínas mais abundantes em cada região do ovário. A região cortical do ovário (fatias de 0,5 mm) apresentou maior porcentagem de

glicoproteínas e proteínas associadas à MEC, enquanto a região medular do ovário (fatias de 1-3,5 mm) apresentou maior porcentagem da cadeia alfa 1 de colágeno tipo V, e*xtracellular matrix protein 1* e *laminin subunit gamma 1*.

Fazendo uma comparação entre o *matrisome* de ovário de mulher e de porca, obsrvamos que algumas proteínas foram identificadas apenas em cada espécie. Por um lado, o *matrisome* de ovário de mulher apresentou proteínas que não foram identificadas no *matrisome* de ovário descelularizado de porca, como, por exemplo, (i) 29 glicoproteínas, como a e*xtracellular matrix protein 2;* (ii) 7 colágenos, como a cadeia alfa 1 de colágeno tipo VIII; (iii) 3 proteoglicanos, como osteoglycin; (iv) 30 proteínas reguladoras da MEC, como c*athepsin B*; e (v) 11 proteínas vinculadas à MEC, como a *galectin-3*. Por outro lado, o *matrisome* de ovário descelularizado de porca apresentou proteínas que não foram identificadas no *matrisome* de ovário de mulher: (i) 9 glicoproteínas, como e*xtracellular matrix protein* 1; (ii) 3 tipos de colágeno, como a cadeia alfa 1 de colágeno tipo II; (iii) 1 proteína reguladora da MEC, a p*rotein-lysine 6-oxidase*; e (iv) 1 proteína vinculada à MEC, como *syndecan.*

Resumindo, as proteínas do *matrisome* de ovário são várias e há semelhanças e diferenças entre as diversas espécies estudadas. A compreensão dessas proteínas é fundamental para elucidar a verdadeira importância de conservar a MEC ovariana após a descelularização.

Tabela 1. Glicoproteínas da MEC identificadas na MEC de ovário de mulher e de porca.

Nome da proteína	Mulher	Porca
Adipocyte enhancer-binding protein 1 (AEBP1)	x[2]	x[3]
Cartilage intermediate layer protein 2 (CILP2)	x[1]	
Dermatopontin (DPT)	x[1,2]	x[3]
EGF-containing fibulin-like extracellular matrix protein 1 (EFEMP1)	x[2]	x[3]
EGF-containing fibulin-like extracellular matrix protein 2 (EFEMP2)	x[2]	
Elastin microfibril interfacer 1 (EMILIN1)	x[1,2]	x[3]
Elastin microfibril interfacer 3 (EMILIN3)	x[2]	x[3]
Extracellular matrix protein 1 (ECM1)		x[3]
Extracellular matrix protein 2 (ECM2)	x[2]	
Fibrilin 1 (FBN1)	x[1,2]	x[3]
Fibrinogen alpha chain (FGA)	x[1,2]	
Fibrinogen beta chain (FGB)	x[1,2]	
Fibrinogen gamma chain (FGG)	x[1,2]	
Fibulin 5 (FBLN5)	x[1,2]	
Fibulin-1 (FBLN1)	x[2]	
Insulin like growth factor binding protein 7 (IGFBP7)		x[3]
Insulin-like growth factor-binding protein acid labile subunit (IGFALS)	x[1]	
Isoform 3 of Tubulointerstitial nephritis antigen-loke (TINGL1)	x[1]	
Lactadherin (MFGE8)	x[2]	x[3]
Laminin subunit alpha 2 (LAMA2)	x[1,2]	
Laminin subunit alpha 4 (LAMA4)	x[1,2]	
Laminin subunit alpha 5 (LAMA5)	x[1,2]	
Laminin subunit beta 1 (LAMB1)	x[1,2]	x[3]
Laminin subunit beta 2 (LAMB2)	x[1,2]	
Laminin subunit gamma 1 (LAMC1)	x[1,2]	x[3]
Latent transforming growth factor beta binding protein 1 (LTBP1)		x[3]
Latent-transforming growth factor beta-binding protein 2 (LTBP2)	x[2]	

Latent-transforming growth factor beta-binding protein 4 (LTBP4)	x[2]	
Leucine-rich alpha-2-glycoprotein (LRG1)	x[2]	
Microfibrillar-associated protein 2 (MFAP2)	x[1,2]	x[3]
Microfibrillar-associated protein 4 (MFAP4)	x[1,2]	
Nidogen 1 (NID1)	x[1,2]	
Nidogen 2 (NID2)	x[1,2]	
Peroxidasin homolog (PXDN)	x[2]	
Procollagen C-endopeptidase enhancer (PCOLCE)	x[1,2]	
Profilin-1 (FN1)	x[1,2]	x[3]
Somatomedin-B and thrombospondin type-1 domain-containing protein (SBSPON)	x[2]	
SPARC	x[2]	
Sushi repeat containing protein, X-linked 2 (SRPX2)		x[3]
Target of Nesh-SH3 (ABI3BP)	x[2]	
Tenascin XB (TNXB)	x[1,2]	
Thrombospondin 1 (THBS1)	x[1,2]	
Transforming growth factor beta induced (TGFBI)	x[1,2]	x[3]
Uncharacterized protein (AGRN)		x[3]
Vitronectin (VTN)	x[1,2]	x[3]
Von Willebrand factor A domain containing 1 (VWA1)		x[3]
Von Willebrand fator (VWF)	x[1]	
WNT1-inducible-signaling pathway protein 2 (WISP2)	x[2]	
Zona pellucida sperm-binding protein 2 (ZP2)		x[3]
Zona pellucida sperm-binding protein 3 (ZP3)		x[3]
Zona pellucida sperm-binding protein 4 (ZP4)		x[3]

[1] = Ouni *et al*. (2019), [2] = Ouni *et al*. (2020), [3] = Henning *et al.* (2019).

Tabela 2. Tipos de colágenos identificados na MEC de ovário de mulher e de porca.

Nome da proteína	Mulher	Porca
Collagen type I alpha 1 chain (COL1A1)	x[1,2]	
Collagen type I alpha 2 chain (COL1A2)	x[1,2]	x[3]
Collagen type II alpha 1 chain (COL2A1)		x[3]
Collagen type III alpha 1 chain (COL3A1)	x[2]	x[3]
Collagen type IV alpha 1 chain (COL4A1)	x[1,2]	x[3]
Collagen type IV alpha 2 chain (COL4A2)	x[1,2]	x[3]
Collagen type V alpha 1 chain (COL5A1)	x[2]	x[3]
Collagen type V alpha 2 chain (COL5A2)		x[3]
Collagen type VI alpha 1 chain (COL6A1)	x[1,2]	
Collagen type VI alpha 2 chain (COL6A2)	x[1,2]	x[3]
Collagen type VI alpha 3 chain (COL6A3)	x[1,2]	
Collagen type VI alpha 5 chain (COL6A5)		x[3]
Collagen type VIII alpha 1 chain (COL8A1)	x[1]	
Collagen type XII alpha 1 chain (COL12A1)	x[1,2]	
Collagen type XIV alpha 1 chain (COL14A1)	x[1,2]	x[3]
Collagen type XV alpha 1 chain (COL15A1)	x[2]	
Collagen type I alpha 1 chain (COL18A1)	x[1,2]	

[1] = Ouni *et al*. (2019), [2] = Ouni *et al*. (2020), [3] = Henning *et al.* (2019).

Tabela 3. Proteoglicanos identificadas na MEC de ovário de mulher e de porca.

Nome da proteína	Mulher	Porca
Biglycan (BGN)	x[2]	x[3]
Decorin (DCN)	x[1,2]	x[3]
Fibromodulin (FMOD)	x[1,2]	x[3]
Heparan sulfate proteoglycan 2 (HSPG2)	x[1,2]	
Lumican (LUM)	x[1,2]	x[3]
Osteoglycin (OGN)	x[1,2]	
Podocan (PODN)	x[1,2]	
Proline and arginine rich leucin rich repeat protein (PRELP)	x[1,2]	x[3]
Versican (VCAN)	x[2]	x[3]

[1] = Ouni *et al*. (2019), [2] = Ouni *et al*. (2020), [3] = Henning *et al.* (2019).

Tabela 4. Proteínas reguladoras da MEC identificadas na MEC de ovário de mulher e de porca.

Nome da proteína	Mulher	Porca
Alpha-2-macroglobulin (A2M)	x[1,2]	x[3]
Alpha-1-microglobulin (AMBP)	x[1,2]	x[3]
Angiotensinogen (AGT)	x[1,2]	
Cathepsin B (CTSB)	x[1,2]	
Cathepsin D (CTSD)	x[1,2]	x[3]
Cathepsin Z (CTSZ)	x[2]	
Cathepsin-B (CSTB)	x[1,2]	
Coagulation factor XIII A chain (F13A1)	x[2]	
Cystatin-A (CSTA)	x[2]	
Dipeptidyl peptidase 1 (CTSC)	x[2]	
Histidine-rich glycoprotein (HRG)	x[1,2]	x[3]
Inter-alpha-trypsin inhibitor heavy chain H1 (ITIH1)	x[1,2]	x[3]
Inter-alpha-trypsin inhibitor heavy chain H2 (ITIH2)	x[1,2]	x[3]
Isoform 4 of Inter-alpha-trypsin inhibitor heavy chain H4 (ITIH4)	x[1,2]	
Lysosomal protective protein (CTSA)	x[2]	
Lysyl oxidase homolog 1 (LOXL1)	x[2]	
Lysyl-bradykinin (KNG1)	x[2]	x[3]
Metalloproteinase inhibitor 3 (TIMP3)	x[2]	
Plasminogen (PLG)	x[1,2]	x[3]
Pro-cathepsin H (CTSH)	x[2]	
Procollagen-lysine,2-oxoglutarate 5-dioxygenase 3 (PLOD3)	x[2]	
Prolyl 4-hydroxylase subunit alpha-1 (P4HA1)	x[2]	
Prolyl 4-hydroxylase subunit alpha-1 (PLOD1)	x[2]	
Protein-glutamine gamma-glutamyltransferase 2(TGM2)	x[2]	x[3]
Protein-glutamine gamma-glutamyltransferase E (TGM3)	x[2]	
Protein-lysine 6-oxidase (LOX)		x[3]
Prothrombin (F2)	x[2]	
Serpin family A member 1 (SERPINA1)	x[1,2]	x[3]
Serpin family A member 3 (SERPINA3)	x[1,2]	x[3]
Serpin family A member 4 (SERPINA4)	x[1]	
Serpin family A member 6 (SERPINA6)	x[2]	

Serpin family A member 7 (SERPINA7)	x[2]	
Serpin family B member 1 (SERPINB1)	x[1,2]	
Serpin family B member 12 (SERPINB12)	x[2]	
Serpin family B member 3 (SERPINB3)	x[2]	
Serpin family B member 6 (SERPINB6)	x[1,2]	
Serpin family B member 9 (SERPINB9)	x[2]	
Serpin family C member 1 (SERPINC1)	x[1,2]	x[3]
Serpin family D member 1 (SERPIND1)	x[1,2]	x[3]
Serpin family E member 2 (SERPINE2)	x[1,2]	
Serpin family F member 1 (SERPINF1)	x[1,2]	
Serpin family F member 1 (SERPINF2)	x[1,2]	
Serpin family G member 1 (SERPING1)	x[1,2]	
Serpin family H member 1 (SERPINH1)	x[1,2]	

[1] = Ouni *et al*. (2019), [2] = Ouni *et al*. (2020), [3] = Henning *et al.* (2019).

Tabela 5. Proteínas vinculadas à MEC identificadas na MEC de ovário de mulher e de porca.

Nome da proteína	Mulher	Porca
Annexin A1 (ANXA1)	x[1,2]	x[3]
Annexin A2 (ANXA2)	x[1]	x[3]
Annexin A3 (ANXA3)	x[2]	
Annexin A4 (ANXA4)	x[1,2]	x[3]
Annexin A5 (ANXA5)	x[1,2]	x[3]
Annexin A6 (ANXA6)	x[1,2]	
Annexin A7 (ANXA7)	x[1,2]	x[3]
Annexin A11 (ANXA11)	x[1,2]	x[3]
Complement C1q subcomponent subunit B (C1QB)	x[2]	
Complement C1q subcomponent subunit C (C1QC)	x[2]	
Galectin-1 (LGALS1)	x[1,2]	x[3]
Galectin-3 (LGALS3)	x[1,2]	
Galectin-1 (LGALS7)	x[2]	
Glypican 1 (GPC1)	x[2]	x[3]
Hemopexin (HPX)	x[1,2]	
Plexin domain-containing protein 2 (PLXDC2)	x[2]	

Plexin-B2 (PLXNB2)	x[1,2]	
Protein ERGIC-53 (LMAN1)	x[2]	
Syndecan (SDC2)		x[3]
Tetranectin (CLEC3B)	x[1,2]	

[1] = Ouni *et al*. (2019), [2] = Ouni *et al*. (2020), [3] = Henning *et al.* (2019).

Tabela 6. Fatores de secreção identificadas na MEC de ovário de mulher

Nome da proteína	Mulher
Host cell factor 1 (HCFC1)	x[1,2]
Filaggrin (FLG)	x[2]
Filaggrin-2 (FLG2)	x[2]
Hornerin (HRNR)	x[2]
Protein S100-A6 (S100A6)	x[1,2]
Protein S100-A7 (S100A7)	x[2]
Protein S100-A8 (S100A8)	x[2]
Protein S100-A9 (S100A9)	x[2]
Protein S100-A10 (S100A10)	x[2]
Protein S100-A11 (S100A11)	x[1,2]
Protein S100-A13 (S100A13)	x[1,2]
Protein S100-A16 (S100A16)	x[2]
Protein Wnt-2b (WNT2B)	x[2]

[1] = Ouni *et al*. (2019), [2] = Ouni *et al*. (2020).

II. REFERÊNCIAS BIBLIOGRÁFICAS

Alberts, B.; Johnson, A.; Lewis, J.; Morgan, D.; Raff, M.; Roberts, K.; Walter, P.; Wilson, J.; Hunt, T. (2017). Junções celulares e matriz extracelular In: (Ed.) Biologia Molecular da Célula. 6: Artmed Editora, cap. 1057-1089.

Alshaikh, A.B.; Padma, A.M.; Dehlin, M.; Akouri, R.; Song, M. J.; Brännström, M.; Hellström, M. (2020). Decellularization and recellularization of the ovary for bioengineering applications; studies in the mouse. Reproductive Biology and Endocrinology, 18(1), 1-10. https://doi.org/10.1186/s12958-020-00630-y

Alshaikh, A.B.; Padma, A.M.; Dehlin, M.; Akouri, R.; Song, M.J.; Brännström, M.; Hellström, M. (2019). Decellularization of the mouse ovary: comparison of different scaffold generation protocols for future ovarian bioengineering. Journal of ovarian research, 12(1), 1-9. https://doi.org/10.1186/s13048-019-0531-3

Amorim, C.A.; Shikanov, A. (2016). The artificial ovary: current status and future perspectives. Future oncology, 12(19), 2323-2332. https://doi.org/10.2217/fon-2016-0202

Anitua, E.; Prado, R.; Azkargorta, M.; Rodriguez-Suarez, E.; Iloro. I.; Casado-Vela, J.; Elortza, F.; Orive, G. (2013). High-throughput proteomic characterization of plasma rich in growth factors (PRGF-Endoret)-derived fibrin clot interactome. Journal of Tissue Engineering Regenerative Medical, 9 (11), E1-E12. https://doi.org/10.1002/term.1721

Bacha, W.J.; Bacha, L.M. (2017). Female Reproductive System In: (Ed.) Color Atlas of Veterinary Histology. 3: Wiley-Blackwell, cap. 243-265.

Badylak, S.F. (2002). The extracellular matrix as a scaffold for tissue reconstruction. In Seminars in cell & developmental biology, 13(5), 377-383. https://doi.org/10.1016/S1084952102000940

Berkholtz, C.B.; Lai, B.E.; Woodruff, T.K.; Shea, L.D. (2006). Distribution of extracellular matrix proteins type I collagen, type IV collagen, fibronectin, and laminin in mouse folliculogenesis. Histochemistry and Cell Biology, 126(5), 583-592. http://doi.org/10.1007/s00418-006-0194-1

Bruce, C.D.; Berkowitz, M.L.; Perera, L.; Forbes, M.D. (2002). Molecular dynamics simulation of sodium dodecyl sulfate micelle in water: micellar structural characteristics and counterion distribution. The Journal of Physical Chemistry B, 106(15), 3788-3793. https://doi.org/10.1021/jp013616z

Buckenmeyer, M.J.; Sukhwani, M.; Iftikhar, A.; Nolfi, A.L.; Xian, Z.; Dadi, S.; Case, Z.W.; Steimer, S.R.; D' more, A.; Orwig, K.E.; Brown, B.N. (2020). Bioengineering an *in situ* ovary (ISO) for fertility preservation. bioRxiv. https://doi.org/10.1101/2020.01.03.893941

Camargo, C.P.; Carvalho, H.A.; Maluf, F.C.; Sousa, A.A.D.C.; Perin, P.O.M.; Perin, M.M.; Besteiro, J.M; Gemperli, R. (2021). Light-emitting diode stimulates radiodermatitis recovery. Acta Cirúrgica Brasileira, 36(3). https://doi.org/10.1590/ACB3603014

Carroll, J.; Gosden, R.G. (1993). Transplantation of frozen—thawed mouse primordial follicle. Human Reproduction, 8(8), 1163-1167. https://doi.org/10.1093/oxfordjournals.humrep.a138221

Chiti, M.C.; Dolmans, M.M.; Orellana, R.; Soares, M.; Paulini, F.; Donnez, J.; Amorim, C.A. (2016). Influence of follicle stage on artificial ovary outcome using fibrin as a matrix. Human Reproduction, 31(2), 427-435. https://doi.org/10.1093/humrep/dev299

Chiti, M.C.; Vanacker, J.; Ouni, E.; Tatic, N.; Viswanath, A.; Des Rieux, A.; Dolmans, M.M.; White, L.J.; Amorim, C.A. (2022) Ovarian extracellular matrix-based hydrogel for human ovarian follicle survival in vivo: A pilot work. J Biomed Mater Res B Appl Biomater, 110(5),1012-1022. https://doi.org/10.1002/jbm.b.34974

Corazza, A.V.; Jorge, J.; Kurachi, C.; Bagnato, V.S. (2007). Photobiomodulation on the angiogenesis of skin wounds in rats using different light sources. Photomedicine and laser surgery, 25(2), 102-106. https://doi.org/10.1089/pho.2006.2011

Crapo, P.M.; Gilbert, T.W.; Badylak, S.F. (2011). An overview of tissue and whole organ decellularization processes. Biomaterials, 32(12), 3233-3243. https://doi.org/10.1016/j.biomaterials.2011.01.057

De Robertis, E.; Hib, J. (2004). La unión de las células entre sí y con la matriz extracelular In: (Ed.) Fundamentos de Biología Celular y Molecular De Robertis. 4: El Ateneo, Cap. 109–113.

Dolmans, M.M.; Falcone, T.; Patrizio, P. (2020). Importance of patient selection to analyze in vitro fertilization outcome with transplanted cryopreserved ovarian tissue. Fertility and sterility, 114(2), 279-280. https://doi.org/10.1016/j.fertnstert.2020.04.050

Dolmans, M.M.; Martinez-Madrid, B.; Gadisseux, E.; Guiot, Y.; Yuan, W.Y.; Torre, A.; Camboni, A.; Langendonck, A.V.; Donnez, J. (2007). Short-term transplantation of isolated human ovarian follicles and cortical tissue into nude mice. Reproduction, 134(2), 253-262. https://doi.org/10.1530/REP-07-0131

Dolmans, M.M.; Yuan, W.Y; Camboni, A.; Torre, A; Van Langendonckt, A.; Martinez-Madrid, B.; Donnez, J. (2008). Development of antral follicles after xenografting of isolated small human preantral follicles. Reproductive biomedicine online, 16(5), 705-711. https://doi.org/10.1016/S1472-6483(10)60485-3

Donnez, J.; Dolmans, M.M. (2017). Fertility preservation in women. New England Journal of Medicine, 377(17), 1657-1665. https://doi.org/10.1056/NEJMra1614676

Eivazkhani, F.; Abtahi, N.S.; Tavana, S.; Mirzaeian, L.; Abedi, F.; Ebrahimi, B.; Montazeri, L.; Valojerdi, R.M.R.; Fathi, R. (2019). Evaluating two ovarian decellularization methods in three species. Materials Science and Engineering: C, 102, 670-682. https://doi.org/10.1016/j.msec.2019.04.092

Faulk, D.M.; Johnson, S.A.; Zhang, L.; Badylak, S.F. (2014). Role of the extracellular matrix in whole organ engineering. Journal of cellular physiology, 229(8), 984-989. https://doi.org/10.1002/jcp.24532

Gilbert, T.W.; Sellaro, T.L.; Badylak, S.F. (2006). Decellularization of tissues and organs. Biomaterials, 27(19), 3675-3683. https://doi.org/10.1016/j.biomaterials.2006.02.014

Gobbi, G.; Vitale, M. (2012). Platelet-rich plasma preparations for biological therapy: applications and limits. Operative Techniques in Orthopaedics, 22(1), 10-15. https://doi.org/10.1053/j.oto.2012.01.002

Gosden, R.G. (1990). Restitution of fertility in sterilized mice by transferring primordial ovarian follicles. Human Reproduction, 5(2), 117-122. https://doi.org/10.1093/oxfordjournals.humrep.a137053

Guruswamy, D.R.; Vermette, P. (2018). Tissue and organ decellularization in regenerative medicine. Biotechnology progress, 34(6), 1494-1505. https://doi.org/10.1002/btpr.2699

Hafez, E.S.E.; Hafez, B. (2004). Foliculogênese, Maduração, Ovocitária e Ovulação In: (Ed.) Reprodução Animal.7: Manole, cap. 69-91.

Hassanpour, A.; Talaei-Khozani, T.; Kargar-Abarghouei, E.; Razban, V.; Vojdani, Z. (2018). Decellularized human ovarian scaffold based on a sodium lauryl ester sulfate (SLES)-treated protocol, as a natural three-dimensional scaffold for construction of bioengineered ovaries. Stem cell research & therapy, 9(1), 1-13. https://doi.org/10.1186/s13287-018-0971-5

He, H.; Teng, H.; Zhou, T.; Guo, Y.; Wang, G.; Lin, M.; Sun, Y.; Si, W.; Zhou, Z.; Guo, X; Huo, R. (2014). Unravelling the proteome of adult rhesus monkey ovaries. Molecular BioSystems, 10(3), 653-662. http://doi.org/10.1039/c3mb70312f

Henning, N.F.; LeDuc, R.D.; Even, K. A.; Laronda, M.M. (2019). Proteomic analyses of decellularized porcine ovaries identified new matrisome proteins and spatial differences across and within ovarian compartments. Scientific reports, 9(1), 1-12. https://doi.org/10.1038/s41598-019-56454-3

Hoshiba, T.; Lu, H.; Kawazoe, N.; Chen, G. (2010). Decellularized matrices for tissue engineering. Expert opinion on biological therapy, 10(12), 1717-1728. https://doi.org/10.1517/14712598.2010.534079

Hrebikova, H.; Diaz, D.; Mokry, J. (2015). Chemical decellularization: a promising approach for preparation of extracellular matrix. Biomed Pap Med Fac Univ Palacky Olomouc Czech Repub, 159(1), 12-17. http://dx.doi.org/10.5507/bp.2013.076

Hynes, R.O.; Naba, A. (2012). Overview of the matrisome—an inventory of extracellular matrix constituents and functions. Cold Spring Harbor perspectives in biology, 4(1), a004903. http://doi.org/10.1101/cshperspect.a004903

Irving-Rodgers, H.F.; Rodgers, R.J. (2006). Extracellular matrix of the developing ovarian follicle. In: Seminars in reproductive medicine, 24(4), 195-203. http://doi.org/10.1055/s-2006-948549

Kim, J.; Perez, A.S.; Claflin, J.; David, A.; Zhou, H.; Shikanov, A. (2016). Synthetic hydrogel supports the function and regeneration of artificial ovarian tissue in mice. NPJ Regenerative medicine, 1(1), 1-8. http://dx.doi.org/10.1038/npjregenmed.2016.10

Kinnear, H.M.; Tomaszewski, C.E.; Chang, F.L.; Moravek, M.B.; Xu, M.; Padmanabhan, V.; Shikanov, A. (2020). The ovarian stroma as a new frontier. Reproduction, 160(3), R25-R39. https://doi.org/10.1530/REP-19-0501

Kniazeva, E.; Hardy, A.N.; Boukaidi, S.A.; Woodruff, T.K.; Jeruss, J.S.; Shea, L.D. (2015). Primordial follicle transplantation within designer biomaterial grafts produce live births in a mouse infertility model. Scientific reports, 5(1), 1-11. http://doi.org/10.1038/srep17709

Koeppen, B.M; Stanton, B.A. (2018). The male and female reproductive systems In: (Ed.) Berne & Levy Physiology. 7: Elvevier, cap. 793-809.

Kragh-Hansen, U.; le Maire, M.; Møller, J.V. (1998). The mechanism of detergent solubilization of liposomes and protein-containing membranes. Biophysical Journal, 75(6), 2932-2946. https://doi.org/10.1016/S0006-3495(98)77735-5

Laronda, M.M.; Jakus, A.E.; Whelan, K.A.; Wertheim, J.A.; Shah, R.N.; Woodruff, T.K. (2015). Initiation of puberty in mice following decellularized ovary transplant. Biomaterials, 50, 20-29. https://doi.org/10.1016/j.biomaterials.2015.01.051

Liu, W.Y.; Lin, S.G.; Zhuo, R.Y.; Xie, Y.Y.; Pan, W.; Lin, X.F.; Shen, F.X. (2017). Xenogeneic decellularized scaffold: a novel platform for ovary regeneration. Tissue Engineering Part C: Methods, 23(2), 61-71. https://doi.org/10.1089/ten.tec.2016.0410

Maltaris, T., Seufert, R., Fischl, F., Schaffrath, M., Pollow, K., Koelbl, H., & Dittrich, R. (2007). The effect of cancer treatment on female fertility and strategies for preserving fertility. European Journal of Obstetrics & Gynecology and Reproductive Biology, 130(2), 148-155. https://doi.org/10.1016/j.ejogrb.2006.08.006

Mescher, A.L. (2016). The Female Reproductive System In: (Ed.) Junquira´s Basic Histology Text and Atlas. 4: McGraw-Hill Education, cap. 460-470.

Naba, A.; Clauser, K.R.; Ding, H.; Whittaker, C.A.; Carr, S.A.; Hynes, R.O. (2016) The extracellular matrix: Tools and insights for the "omics" era. Matrix Biol, 49,10-24. https://doi.org/10.1016/j.matbio.2015.06.003

Naba, A.; Clauser, K.R.; Hoersch, S.; Liu, H.; Carr, S.A.; Hynes, R.O. (2012). The matrisome: in silico definition and in vivo characterization by proteomics of normal and tumor extracellular matrices. Molecular & Cellular Proteomics, 11(4), M111-014647. https://doi.org/10.1074/mcp.M111.014647

Nelson, D.L.; Cox, M.M. (2014). Carboidratos e Glicobiologia In: (Ed.) Princípios de Bioquímica de Lehninger. 6: Artmed Editora, cap. 243-276.

Nikniaz, H.; Zandieh, Z.; Nouri, M.; Daei-Farshbaf, N.; Aflatoonian, R., Gholipourmalekabadi, M.; Jameie, S.B. (2021). Comparing various protocols of human and bovine ovarian tissue decellularization to prepare extracellular matrix-alginate scaffold for better follicle development in vitro. BMC biotechnology, 21(1), 1-8. https://doi.org/10.1186/s12896-020-00658-3

Ouni, E.; Bouzin, C.; Dolmans, M.M.; Marbaix, E.; Pyr dit Ruys, S.; Vertommen, D.; Amorim, C.A. (2020). Spatiotemporal changes in mechanical matrisome components of the human ovary from prepuberty to menopause. Human Reproduction, 35(6), 1391-1410. https://doi.org/10.1093/humrep/deaa100

Ouni, E.; Vertommen, D.; Chiti, M.C.; Dolmans, M.M.; Amorim, C.A. (2018). A draft map of the human ovarian proteome for tissue engineering and clinical applications. Molecular & Cellular Proteomics, 18(1), S159-S173. https://doi.org/10.1074/mcp.RA117.000469

Paulini, F.; Vilela, J.M.; Chiti, M.C.; Donnez, J.; Jadoul, P.; Dolmans, M.M.; Amorim, C.A. (2016). Survival and growth of human preantral follicles after cryopreservation of ovarian tissue, follicle isolation and short-term xenografting. Reproductive biomedicine online, 33(3), 425-432. https://doi.org/10.1016/j.rbmo.2016.05.003

Pawlina, W.; Ross, M. H. (2018). Female genial system In:(Ed.) Histology: a text and atlas: with correlated cell and molecular biology. 7: Lippincott Williams & Wilkins., cap. 898-912.

Pennarossa, G.; Ghiringhelli, M.; Gandolfi, F.; Brevini, T.A. (2020). Whole-ovary decellularization generates an effective 3D bioscaffold for ovarian bioengineering.

Journal of Assisted Reproduction and Genetics, 37(6), 1329-1339. https://doi.org/10.1007/s10815-020-01784-9

Pors, S.E.; Ramløse, M.; Nikiforov, D.; Lundsgaard, K.; Cheng, J., Andersen, C.Y.; Kristensen, S.G. (2019). Initial steps in reconstruction of the human ovary: survival of pre-antral stage follicles in a decellularized human ovarian scaffold. Human Reproduction, 34(8), 1523-1535. https://doi.org/10.1093/humrep/dez077

Rajabzadeh, A.R.; Eimani, H.; Koochesfahani, H.M.; Shahvardi, A.H.; Fathi, R. (2015). Morphological study of isolated ovarian preantral follicles using fibrin gel plus platelet lysate after subcutaneous transplantation. Cell Journal (Yakhteh), 17(1), 145-152. https://dx.doi.org/10.22074%2Fcellj.2015.521

Rodgers, R.J.; Irving-Rodgers, H.F.; Russell, D.L. (2003). Extracellular matrix of the developing ovarian follicle. Reproduction, 126(4), 415-424.

Shaw, J.M.; Bowles, J.; Koopman, P.; Wood, E.C.; Trounson, A.O. (1996). Ovary and Ovulation: Fresh and cryopreserved ovarian tissue samples from donors with lymphoma transmit the cancer to graft recipients. Human Reproduction, 11(8), 1668-1673. https://doi.org/10.1093/oxfordjournals.humrep.a019467

Smith, R.M.; Shikanov, A.; Kniazeva, E.; Ramadurai, D.; Woodruff, T.K.; Shea, L.D. (2014). Fibrin-mediated delivery of an ovarian follicle pool in a mouse model of infertility. Tissue Engineering Part A, 20(21-22), 3021-3030. https://doi.org/10.1089/ten.tea.2013.0675

Sonmezer, M.; Oktay, K. (2010). Orthotopic and heterotopic ovarian tissue transplantation. Best Practice & Research Clinical Obstetrics & Gynaecology, 24(1), 113-126. https://doi.org/10.1016/j.bpobgyn.2009.09.002

Telfer, E.; Torrance, C.; Gosden, R.G. (1990) Morphological study of cultured preantral ovarian follicles of mice after transplantation under the kidney capsule. Reproduction, 89(2), 565-571. https://doi.org/10.1530/jrf.0.0890565

Vanacker, J.; Camboni, A.; Dath, C.; Van Langendonckt, A.; Dolmans, M.M.; Donnez, J.; Amorim, C. A. (2011). Enzymatic isolation of human primordial and primary ovarian follicles with Liberase DH: protocol for application in a clinical setting. Fertility and sterility, 96(2), 379-383. https://doi.org/10.1016/j.fertnstert.2011.05.075

Vanacker, J.; Dolmans, M.M.; Luyckx, V.; Donnez, J.; Amorim, C.A. (2014). First transplantation of isolated murine follicles in alginate. Regenerative medicine, 9(5), 609-619. https://doi.org/10.2217/rme.14.33

Woodruff, T.K.; Shea, L.D. (2007). The role of the extracellular matrix in ovarian follicle development. Reproductive sciences, 14(8), 6-10. http://doi.org/10.1177/1933719107309818.

Wu, T.; Gao, Y.Y. ; Tang, X.N.; Zhang, J.J.; Wang, S.X. Construction of Artificial Ovaries with Decellularized Porcine Scaffold and Its Elicited Immune Response after Xenotransplantation in Mice. J Funct Biomater. 2022 Sep 28;13(4):165. https://doi.org/10.3390/jfb13040165

Zhao, Y.; Luck, M.R. (1995). Gene expression and protein distribution of collagen, fibronectin and laminin in bovine follicles and corpora lutea. Reproduction, 104(1), 115-123. https://doi.org/10.1530/jrf.0.1040115

III. JUSTIFICATIVA

A construção de um OAT, no qual folículos pré-antrais isolados sejam inseridos em uma MEC descelularizada, poderá possibilitar a manutenção da fertilidade em mulheres diagnosticadas com câncer e submetidas a terapias gonadotóxicas para tratamento da doença. Apesar do grande interesse mundial nesta abordagem, até o momento, os estudos prévios têm mostrado que as matrizes testadas apresentam a capacidade de sustentar o desenvolvimento folicular completo apenas em camundongos, e ainda assim com uma baixa taxa de sobrevivência folicular.

Os métodos de obtenção da MEC descelularizada em geral não foram otimizados, e utilizam tempos longos de incubação e concentrações elevadas de detergentes, além da combinação de vários fatores. Tudo isso pode causar danos à estrutura da MEC, levando a perdas de funções e dificuldades na recelularização e desenvolvimento folicular. Assim, o desenvolvimento e otimização de um protocolo de descelularização menos agressivo, que utilize concentrações e tempos mínimos necessários para a descelularização do tecido, é interessante. Um método assim desenvolvido pode conservar melhor as características da MEC e facilitar o seu uso posterior.

O ovário bovino é um bom modelo animal para o ovário humano, por apresentar diversas semelhanças na fisiologia reprodutiva, permitindo o estudo e desenvolvimento de métodos, sem a necessidade de material humano. Além disso, a obtenção de uma MEC descelularizada de ovário bovino pode ser utilizada para humanos, visto que não promove reação imunológica, como é o caso de outros tecidos bovinos descelularizados que já são utilizados. Por exemplo, temos o pericárdio bovino descelularizado usado como bypass de vasos de membros inferiores para humanos ou fêmur bovino descelularizado usado em enxertos ósseos em outros animais.

A composição da MEC ovariana de bovinos ainda não é conhecida. Já se sabe que há diferenças nas proteínas do *matrisome* ovariano entre espécies. Portanto, é importante conhecer o *matrisome* ovariano bovino, bem como verificar a sua composição após descelularização.

Por isso, o presente projeto propõe desenvolver um protocolo de descelularização com menor concentração e menor tempo de incubação de SDS, para obter uma matriz descelularizada diretamente do tecido ovariano bovino. Além disso, o estudo visa identificar as proteínas que constituem a MEC nativa e descelularizada do tecido ovariano bovino.

IV. OBJETIVOS

- **OBJETIVO GERAL**

Otimizar um protocolo de descelularização para obter uma matriz extracelular descelularizada de córtex ovariano bovino e descrever suas características morfológicas e seu perfil proteico.

- **OBJETIVOS ESPECÍFICOS**

- Obter uma matriz extracelular descelularizada de córtex ovariano de bovino mediante a aplicação do dodecil sulfato de sódio otimizando sua concentração e tempo de incubação;

- Verificar a descelularização da matriz por histologia, quantificação de DNA e eletroforese de gel de agarose;

- Caracterizar a estrutura morfológica da matriz descelularizada obtida por microscopia de luz e eletrônica de varredura;

- Avaliar a citotoxicidade da matriz descelularizada ovariana mediante o cultivo *in vitro* de células ovarianas de humano;

- Identificar as proteínas e as funções da matriz extracelular nativa do ovário bovino por análise proteômica;

- Identificar as proteínas e as funções da matriz extracelular descelularizada do córtex ovariano bovino e compará-la à matriz nativa;

V. CAPÍTULO I

O capítulo I consistiu em desenvolver um protocolo otimizado de descelularização eficiente para córtex ovariano bovino, com concentrações mínimas de SDS e tempos mínimos de incubação com o detergente. Com base nesse objetivo, foi desenvolvido o primeiro artigo, conforme apresentado a seguir.

Minimum sodium dodecyl sulfate concentration and incubation period to decellularize ovarian tissue

Authors/Affiliations

Cecibel M. León-Félix[1], Andrea Q. Maranhão[2], Christiani A. Amorim[3], Carolina M. Lucci[1,*]

[1]Institute of Biological Sciences, Department of Physiology, University of Brasilia, Brasilia, Brazil

[2]Institute of Biological Sciences, Department of Cellular Biology, University of Brasilia, Brasilia, Brazil

[3]Institut de Recherche Expérimentale et Clinique, Department of Gynecology, Université Catholique de Louvain, Brussels, Belgium

***Co-corresponding author:**

Prof. Carolina M. Lucci

Address: Instituto de Biologia, Universidade de Brasília, Campus Darcy Ribeiro, Asa Norte, Brasília – DF. Brazil. 70910-900

E-mail: carollucci@gmail.com

Abstract

This study aimed to obtain decellularized extracellular matrix (dECM) from bovine ovarian tissue using sodium dodecyl sulfate (SDS) at a minimum concentration in the shortest incubation time. A stock decellularization solution was prepared with 1% SDS (w/v) (Sigma-Aldrich, Brazil) and 0.2M NaOH in distilled water, subsequently diluted to the desired concentrations. The respective SDS and NaOH concentrations investigated were 1% and 0.2M; 0.5% and 0.1M; 0.1% and 0.02M, and 0.05% and 0.01M, with 24, 12, and 6 h incubation periods. Samples were individually incubated in 10 mL of the solution under constant stirring (100 rpm) at room temperature for the duration defined for each treatment, after which time they were washed in 50 mL of distilled water for 6 h. Histological analysis confirmed decellularization and Mallory's trichrome staining showed the conservation of collagen in all samples following treatment. Furthermore, the lowest SDS and NaOH concentrations that showed no DNA remaining during electrophoresis analysis were 0.1% and 0.02M when incubated for 24 and 12 h. DNA quantification resulted in < 0.2 ng DNA/mg ovarian tissue using these protocols. In addition, the coculture of dECM (obtained by 0.1% SDS and 0.02M NaOH for 12 h) with ovarian cells showed that there was no toxic effect for the cells up to 72 h. In conclusion, the protocol involving 0.1% SDS and 0.02M NaOH for 12 h incubation decellularizes bovine ovarian tissue, generating a dECM that preserves the native ECM morphology which is non-toxic to ovarian cells.

Keywords:

ovary, SDS, decellularization, extracellular matrix, dECM

Impact Statement

Ovarian decellularized extracellular matrix (dECM) is being investigated with the aim of developing a transplantable artificial ovary. The most used agent for decellularization protocols for ovarian tissue is sodium dodecyl sulfate (SDS), but there is currently no optimized protocol for its use. This study evaluated different SDS concentrations and incubation times to determine the lowest concentration and shortest incubation time capable of successfully promoting decellularization of ovarian tissue. We established an efficient protocol utilizing 0.1% SDS and 0.02M NaOH for 12 h incubation, which resulted in a dECM with preserved morphological structure and no toxic effects to ovarian cells.

Introduction

Although cancer remains one of the leading causes of death in women, cancer patient survival rates after treatment have increased considerably.[1,2] That said, the most commonly used treatments - radiotherapy and/or chemotherapy - can cause infertility in these patients.[3] Alternative strategies employed to conserve fertility include the cryopreservation of embryos, immature or mature oocytes, and ovarian tissue cryopreservation and transplantation.[4] Unfortunately, not all of these alternatives are applicable to all patients, for example prepubertal patients or those requiring immediate treatment. The only viable alternative treatment for the aforementioned patients is ovarian tissue cryopreservation for future autotransplantation,[5] a technique that has already resulted in the birth of > 200 human babies.[6] Nevertheless, in some cases, this alternative poses a risk of reintroducing cancer cells into the patient,[5,7] especially when the cancer type has a moderate/high probability of metastasizing to the ovary, such as in the case of leukemia, neuroblastoma, ovarian cancer, hemangiosarcoma, among others.[4] Therefore, new alternatives are emerging to preserve fertility, ensuring that primary cancer cells are not reintroduced into the patient, for instance a transplantable artificial ovary (TAO).[8]

The TAO strategy consists of providing an extracellular matrix (ECM) and colonizing it with isolated preantral follicles and ovarian cells to permit full follicular development.[9,10] To achieve this, various non-synthetic materials, including collagen,[11] plasma clot,[12–15] fibrin[16–19] and alginate,[20] together with synthetic materials such as polyethylene glycol,[21] have been investigated as potential matrices to establish a

functional TAO.[22] Unfortunately, these materials have certain limitations, such as (i) relatively low follicular survival rates following transplantation;[15,19,20,23] (ii) a lack of comprehensive understanding regarding the composition of all their components, particularly in the plasma clot, and (iii) rapid degradation after transplantation, as in the cases of alginate and fibrin.[16,20] Moreover, none of these materials have demonstrated the ability to fully replicate all the functions of the native ovarian ECM, including cell support and regulation. Therefore, to overcome these obstacles, the use of decellularized ovarian tissues from an animal model as a matrix for TAO could be considered. This approach aims to preserve the acellular components and properties of the native ovarian ECM.[24,25], while addressing the limitations associated with the availability of human ovarian samples.

Decellularized extracellular matrix (dECM) use has already been studied in relation to the transplantation of different organs. Recellularization of dECM with tissue-specific native cells presented promising results regarding tissue function restoration in various organs, including the heart,[26] lungs,[27] kidneys,[28] liver,[29] uterus,[30] and testis.[31] The strategy of obtaining dECM from ovarian tissue could benefit TAO development. Indeed, progress has been made in this field, with dECM obtained from the ovaries and/or ovarian tissue from women,[25,32,33] cows,[25] sheep,[34] sows,[35–37] and mice[38,39] with recellularization, hormone production (e.g. estradiol and progesterone) and the growth of follicle-like structures. However, it is important to note that the human preantral follicle recovery rate following dECM transplantation remained at 25%, and no antral follicles were obtained.[33]

Decellularization methods involve the use of physical, chemical, and/or biological agents. Specifically in the case of chemical agents, various substances have been employed, including Triton-X,[35] sodium lauryl ester sulfate,[32] sodium deoxycholate solution,[39] sodium hydroxide,[34] EDTA,[36] deoxycholate,[37] ammonium hydroxide,[40] and the most used sodium dodecyl sulfate (SDS).[25,33–35,37–40] Despite its more frequent use, it has been reported that SDS denatures tissue ECM proteins during the decellularization process.[41] Additionally, complete SDS removal is challenging, leaving residues in the resulting ECM[42–44] which can be detrimental to the recellularization process and transplantation. Furthermore, decellularization protocols for ovary and/or ovarian tissue using SDS[25,33,34,39,40] have utilized arbitrary concentrations ranging from 0.1 to 1%. These protocols also exhibit variations in terms of incubation time (ranging from 3 to 24h), associations with other decellularization agents (chemical and/or biological, such as DNase I and/or RNase), and the removal method employed. However, no comprehensive survey has been conducted to determine the minimum SDS concentration capable of achieving effective decellularization of ovarian tissue. Therefore, the aim of this study was to evaluate different SDS

concentrations and incubation times to determine the lowest concentration and shortest incubation time capable of successfully promoting decellularization of ovarian tissue.

Materials and Methods

Bovine ovarian tissue decellularization

Bovine ovaries without *corpus luteum* were obtained from a local slaughterhouse and transported in PBS at 37 °C to the laboratory. On arrival, the ovaries were cleaned and stored at -20 °C. After thawing, antral follicles were punctured with a needle, and the capsule and medullary region of the ovary removed using a scalpel. Slices (10 mm x 5 mm x 1 mm) were taken from the ovary cortical region, weighed, and distributed to the experimental treatment groups.

A stock decellularization solution was prepared with 1% SDS (w/v) (L3771-100G, Sigma-Aldrich, USA) and 0.2M NaOH in distilled water and subsequently diluted to achieve the desired concentrations. The respective SDS and NaOH concentrations used were 1% and 0.2M; 0.5% and 0.1M; 0.1% and 0.02M; 0.05% and 0.01M, with 24 h, 12 h, and 6 h incubation times. Samples were immersed in 10 mL of decellularization solution under constant agitation (100 rpm) in an orbital shaker at room temperature for the defined treatment duration. Each sample was then washed 10 times in 50 mL of distilled water that was replaced every 30 min. The ECM samples resulting from each experimental treatment were stored at -20 °C for subsequent DNA extraction or fixed for morphological analysis.

Residual DNA Analysis

DNA from each sample was isolated using the PAXgene™ Blood DNA kit (761133, PreAnalytic, Germany) adapted from the manufacturer's instructions. Each sample was frozen in liquid nitrogen and ground. The resulting powder was homogenized in 1.5 mL of BG1 buffer, collected in an Eppendorf tube, centrifuged at 2500 x g for 3 min and the supernatant discarded. The pellet was then resuspended in 130 µL of BG3 buffer supplemented with 5 µL of PreAnalytiX Protease, incubated at 65 °C for 10 min, and centrifuged for 1 min. Subsequently, 200 µL of isopropanol was added and the sample centrifuged for 3 min. The supernatant was discarded and the isopropanol allowed to evaporate. Ethanol (70%, 200 µL v/v) was added, followed by 3 min centrifugation, and

the supernatant discarded. BG4 buffer (50 µL) was added and the samples were incubated for 1 h at 65 °C. Electrophoresis (0.8% agarose gel) was performed to analyze the remaining DNA which was visualized and photographed using the E-Gel Imager (Life Technologies™, USA).

DNA quantification

DNA concentration was determined by the Qubit 2.0 Fluorometer (Thermo Fisher Scientific, USA) using the Qubit® dsDNA HS Assay Kit (Q32851, Thermo Fisher Scientific) according to the manufacturer's instructions. A 1-µL aliquot of each isolated DNA sample was used to calculate the residual DNA expressed as ng/mg ovarian tissue weight.

dECM Morphology Evaluation

dECM morphology was analyzed by classical microscopy and scanning electron microscopy (SEM). Classical microscopy samples were fixed in Carnoy´s solution for 30 min, dehydrated in increasing ethanol concentrations, clarified in xylene, soaked, infiltrated in Paraplast® and embedded. Each sample was cut (5 µm thick) with sections mounted on glass slides and hematoxylin-eosin (H&E) stained to evaluate ovarian ECM general appearance in addition to Mallory's trichrome to assess collagen fiber content.

SEM samples were fixed in Karnovsky's solution at 4 °C for 24 h and post-fixed in 2% osmium tetroxide for 1 h. After washing with distilled water, dehydration in increasing acetone concentrations, and drying to the critical point (Balzers CPD 30, Liechtenstein), samples were mounted on stubs, metalized with a layer of colloidal gold and observed under a scanning electron microscope (JEOL JSM-7001F, Japan).

Human ovarian Cell Isolation

Ovaries were collected from deceased multi-organ donors following approval granted by the Université Catholique de Louvain's Institutional Review Board for the use of human ovaries on May 25, 2019 (IRB reference 2018/19DEC/475). The collected ovaries were immediately frozen according to the protocol described by Amorim *et al.*[45] To isolate ovarian cells, the samples were thawed and subjected to our routine digestion protocol as previously described.[46] Briefly, tissue fragments were mechanically minced and digested in Dulbecco's Phosphate Buffered Saline (DPBS, 14040-091, Thermo Scientific) with Ca^{2+} and Mg^{2+}, 0.28 Wünsch units/mL Liberase DH (05401089001, Sigma

Aldrich), and 8 Kunitz units/mL DNase (89836, Thermo Scientific). The mixture was pipetted every 15 min and incubated at 37 °C for 75 min with a 150 rpm agitation rate. A DPBS solution (without Ca^{2+} and Mg^{2+}) containing 10% heat-inactivated fetal bovine serum (HI FBS, 16140-071, Thermo Scientific) was added in equal amounts to PBS without Ca^{2+} and Mg^{2+} to inactivate the enzymes. The suspension was filtered sequentially through 80 μm (NY8002500, Sigma Aldrich) and 30 µm (NY3002500, Sigma Aldrich) nylon net filters to remove remaining tissue fragments. The resulting suspension was centrifuged for 10 min at 500 g. After cell counting using trypan blue (T8154, Sigma Aldrich) and a Bürker chamber, the pellet was resuspended in cell culture medium, including Dulbecco's modified Eagle's medium F-12 nutrient mixture (DMEM/F12, 21041-025, Thermo Scientific), 10% HI FBS, and 1% antibiotics and antimycotic (AA, 15240-062, Thermo Scientific). The cells were cultured at 37 °C in a humidified incubator with 5% CO_2 and the culture medium renewed every other day. Cells were subcultured on reaching confluence.

Cell Toxicity Test

According to the qualitative and quantitative results from the experiments, the dECM obtained by incubating with 0.1% SDS and 0.02M NaOH for 12 h was selected to assess the possible toxic effects of SDS residues on cells. For this, dECM samples (n = 4) were sterilized in 1 mL of 1% AA diluted in DMEM/F-12 for 30 min at 37 °C with 5% CO_2. Samples were subsequently equilibrated in 12-well plates containing 1 mL of culture medium consisting of DMEM/F-12 supplemented with 50 µg/mL L-ascorbic acid (A4403, Sigma-Aldrich), 10% HI FBS, 1% insulin-transferrin-selenium (41400045, Gibco, USA) and 1% AA for 4 h in a humidified incubator at 37 °C with 5% CO_2. The equilibrium medium was then removed and each dECM sample cocultured with 7 x 10^4 human ovarian stromal cells in 1 mL of culture medium for 72 h at 37 °C in a humidified incubator with 5% CO_2. During this period, 50% of the medium was replaced every 24 h. The control group (n=2) consisted of 7 x 10^4 human ovarian stromal cells cultured under the same conditions as described above but without dECM.

Cell viability was analyzed after 24 and 72 h of *in vitro* co-culture using PrestoBlue™ HS (P50200, Invitrogen, USA), prepared according to the manufacturer's instructions. The culture medium was removed and 1 mL of PrestoBlue solution (1:10) was added to each well. Samples were incubated for 1 h at 37 °C with 5% CO_2. Finally, 100 µL of the solution (in triplicate) were transferred to the 96-well cell culture plate (Corning, USA) and read at a wavelength of 570 nm using a fluorescence microplate reader (Perkin Elmer Victor™ X4 2030 Multilabel Reader, USA).

Statistical Analysis

Cell viability data (mean ± SD) were analyzed by Student's t distribution using the Prism v.8 software (GraphPad Software, USA). P-values less than 0.05 were considered statistically significant.

Experiment Results

The histological analysis of dECM confirmed the absence of cells/nuclear material and the conservation of collagen fibers in samples incubated with 0.1% SDS and 0.02M NaOH for 24, 12 and 6 h, also observed 0.05% SDS and 0.01 M NaOH samples incubated for 24 and 12 h (Fig. 11).

Meanwhile, the electrophoresis results indicated that the lowest SDS concentration without detectable DNA remaining was 0.1% SDS and 0.02M NaOH, for both the 24- and 12-h incubation periods (Fig. 1). However, incubation with 0.1% SDS and 0.02M NaOH for 6 h, as well as incubation with 0.05% SDS and 0.01M NaOH (all incubation periods) resulted in DNA remaining as confirmed by electrophoresis (Fig. 12).

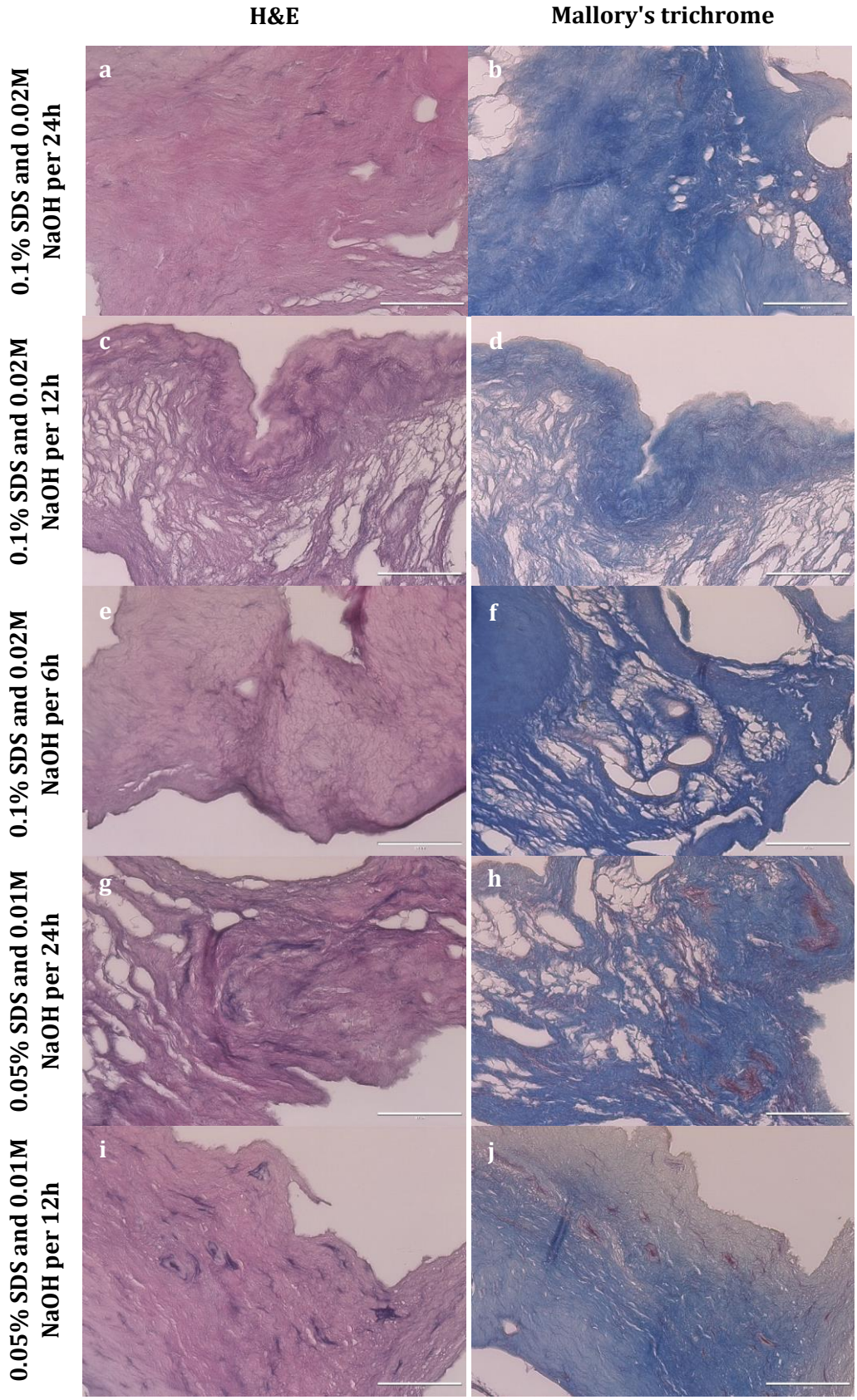

Figure 11. Histology of ovarian tissue after experimental treatment with 0.1% SDS and 0.02M NaOH for 24 h (a and b), 12 h (c and d), 6 h (e and f), and 0.05% SDS and 0.01M NaOH for 24 h (g and h) and 12 h (i and j). H&E staining (a, c, e, g, i) and Mallory trichrome staining (b, d, f, h, j) - Collagen fibers are stained blue. Bars = 100 μm.

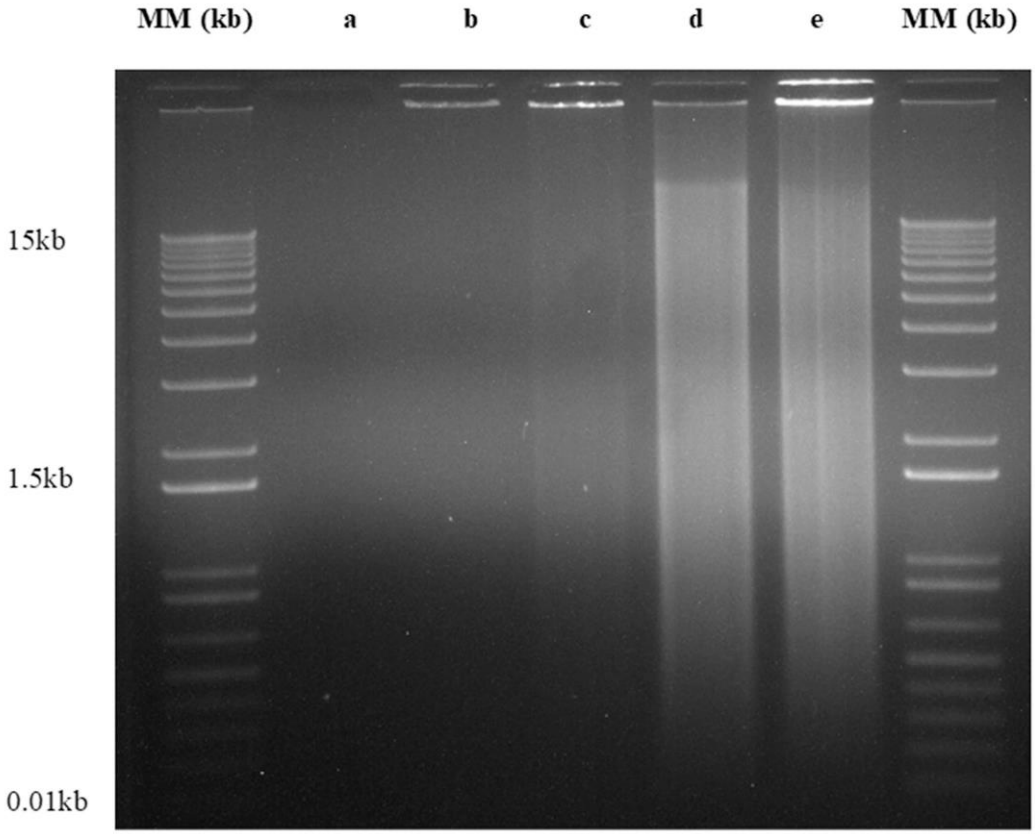

Figure 12. Residual DNA Analysis. Samples obtained from ovarian tissue with different experimental treatments were analyzed by 0.8% (w/v) agarose gel electrophoresis. Samples treated with 0.1% SDS and 0.02M NaOH for (a) 24 h, (b) 12 h, (c) 6 h, and 0.05% SDS and 0.01M NaOH for (d) 24 h, and (e) 12 h are shown. MM = TrackItTM 1kb Ladder molecular size standard (104888-085, Thermo Fisher Scientific, USA).

DNA quantification in the dECM samples with 0.1% and 0.02 NaOH (24 h) revealed a range of 0.002 to 0.194 ng DNA/mg ovarian tissue; the 0.1% SDS and 0.02 NaOH (12 h) samples ranged from 0.001 to 0.302 ng DNA/mg ovarian tissue; the 0.1% SDS and 0.02 NaOH (6 h) samples ranged from 0.368 to 0.419 ng DNA/mg ovarian tissue; the 0.05% SDS and 0.01 NaOH (24 h) ranged from 1.55 to 2.31 ng DNA/mg ovarian tissue; the 0.05% SDS and 0.01M NaOH (12 h) range was 1.25 to 2.31 ng DNA/mg ovarian tissue (Table 7).

Table 7. Quantification (mean ± SD) of remaining DNA in decellularized ovarian tissue samples.

Experimental Treatment	N° samples	ng DNA/mg decellularized ovarian tissue*
0.1% SDS and 0.02M NaOH per 24 h	n = 3	0.103 ± 0.10
0.1% SDS and 0.02M NaOH per 12 h	n = 4	0.173 ± 0.15
0.1% SDS and 0.02M NaOH per 6 h	n = 3	0.390 ± 0.03
0.05% SDS and 0.01M NaOH per 24 h	n = 3	> 1.953 ± 0.38
0.05% SDS and 0.01M NaOH per 12 h	n = 4	> 1.708 ± 0.47

Based on these experiment findings, we decided to perform SEM analysis on the native ovarian tissue (control group) and samples treated with 0.1% SDS and 0.02M NaOH for 12 h (dECM group). The SEM demonstrated preserved integrity of ECM fibers after decellularization (Fig. 13). The fibers in dECM were similar to the native ovarian tissue in both appearance and organization.

According to the established criteria, successful tissue decellularization requires that 3 specific conditions are met: 1) <50 ng DNA per mg dry weight of ECM; 2) <200 bp DNA fragment size, and 3) absence of nuclear material in the tissue when stained with H&E.[47] Based on the aforementioned criteria, incubation in 0.1% SDS and 0.02M NaOH for 24 h and 12 h successfully decellularized the tissue. However, the experimental treatment involving 0.1% SDS and 0.02M NaOH for 12 h demonstrated the lowest SDS concentration and shortest incubation time. Consequently, *in vitro* culture with stroma cells was conducted using the dECM obtained after tissue incubation in 0.1% SDS and 0.02M NaOH for 12 h, aiming to assess potential residual SDS-induced toxicity.

Cell viability analysis demonstrated that dECM obtained after incubation in 0.1% SDS and 0.02M NaOH for 12 h did not exhibit cytotoxic effects during *in vitro* culture (Fig.

14). Comparison between the control group and the dECM group after culturing for 24 h and 72 h did not show any significant difference in cell viability (Fig. 15).

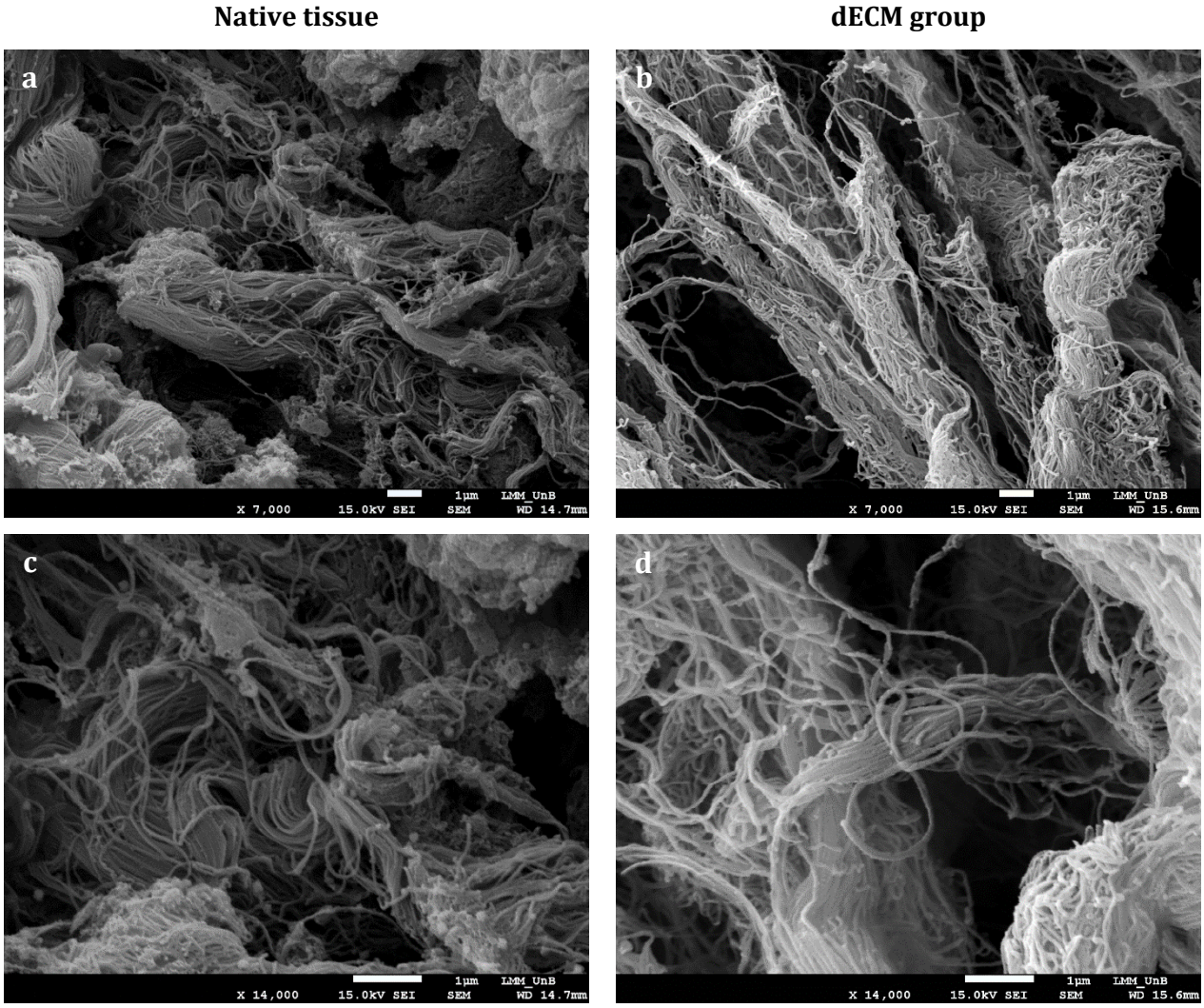

Figure 13. Scanning electron micrographs of native bovine ovarian tissue (a and c) and dECM using 0.1% SDS and 0.02M NaOH for 12 h (b and d). Bars = 1 µm.

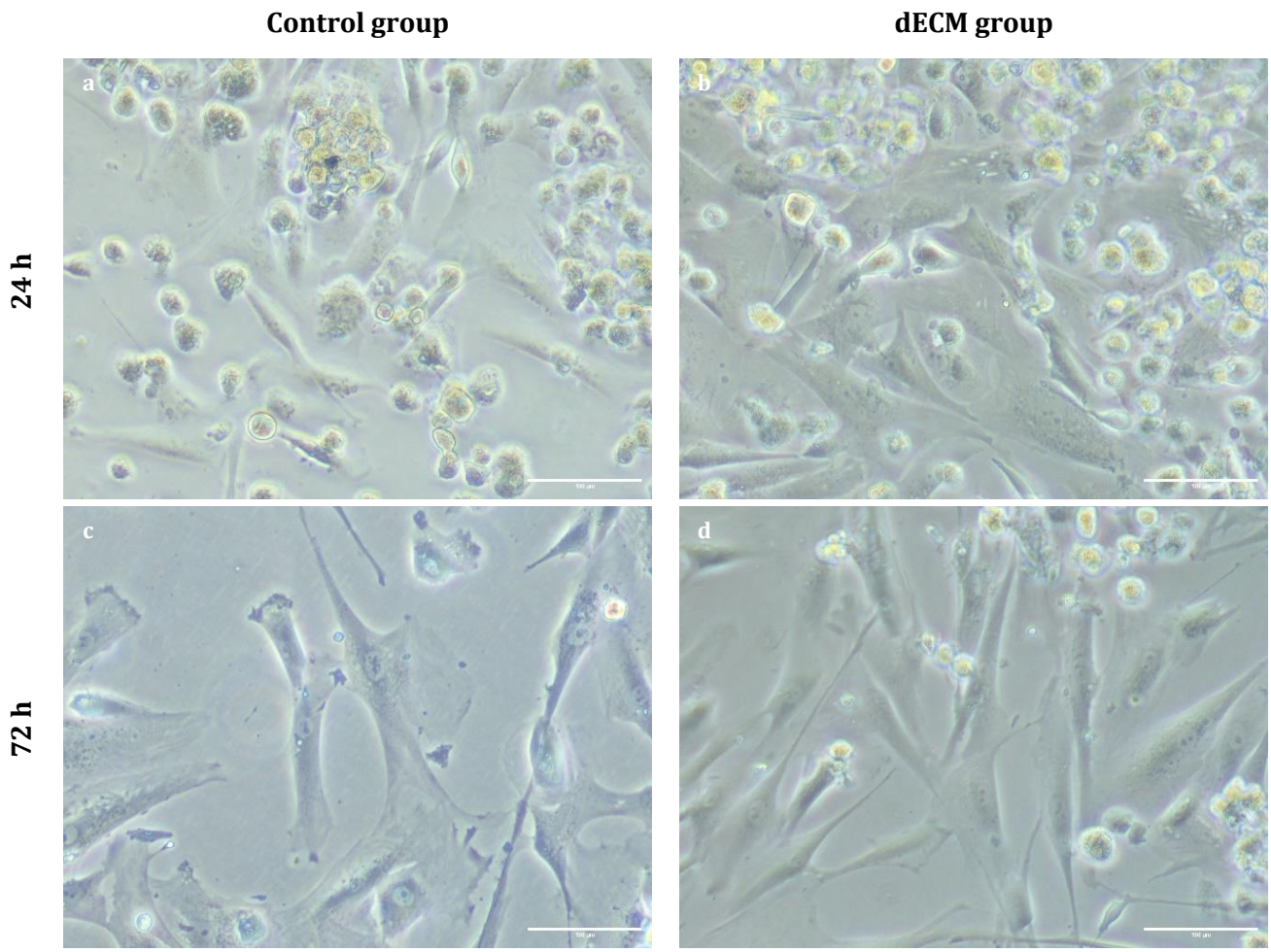

Figure 14. Appearance of human ovarian stromal cells cultured *in vitro* for 24 h (a and b) and 72 h (c and d) alone (control group) or with dECM derived from bovine ovarian cortex incubated with 0.1% SDS and 0.02M NaOH for 12 h. Bars = 100 µm. (Leica inverted fluorescence microscope).

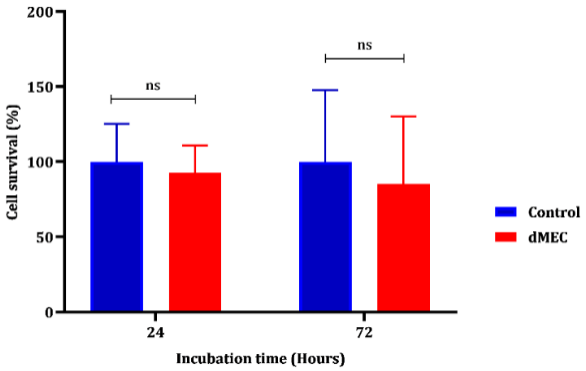

Figure 15. Cell viability after in vitro culture in the control group (blue bars) after decellularization of bovine ovarian cortex with 0.1% SDS and 0.02M NaOH for 12 h. P > 0.05.

Discussion

We tested different SDS concentrations with the aim of developing a decellularization protocol to obtain dECM from bovine ovarian tissue. Our objective was to achieve a protocol with the minimum SDS concentration and the shortest incubation time necessary for successful decellularization. The resulting ovarian tissue dECM presented the characteristics of a decellularized tissue, specifically: 1) <50 ng of DNA per mg dry weight of ECM; 2) <200 bp of DNA fragment size, and 3) absence of nuclear material in the tissue when H&E stained.[47] The lowest SDS concentration and shortest incubation time resulting in a dECM from bovine ovarian tissue was 0.1% SDS and 0.02M NaOH for 12 h incubation. Under these experimental conditions, the dECM displayed similar morphology to the native ECM in both the histological and scanning electron microscopy analysis. In addition, the obtained dECM showed no toxicity to human ovarian cells when cocultured for up to 72 h.

Ovary and/or ovarian tissue decellularization has been previously performed using SDS concentrations of 1%, 0.5% and 0.1%, albeit with the aid of other chemical and/or biological agents and prolonged incubation times, potentially affecting the morphology and disrupting the chemical composition of the extracellular matrix. For instance, the use of 1% SDS was combined with RNase/DNase,[34] while other authors reported use of 0.5% SDS in conjunction with 1% Triton X-100 and 200 U/mL DNase I;[35] 40 IU/mL DNase I;[39] 1% Triton X-100 and 2% deoxycholate,[37] and 1% Triton X-100 and 1% ammonium hydroxide.[40] Moreover, the 0.1% SDS concentration was used with an incubation time of 24 h,[25,40] followed by incubation with 1 mg/mL DNase for an additional 24 h.[33] The selection of SDS concentration and incubation time in all of these studies appear to have been arbitrary without investigating different concentrations or incubation times. In our study, we performed an optimization process, testing different SDS concentrations and different incubation times. In contrast to the previous protocols, we successfully obtained a dECM from ovarian tissue using only 0.1% SDS and 0.02M NaOH, as the decellularization agent, and a 12-h incubation period. It is important to highlight that by decreasing the concentration and tissue exposure time to SDS, we were able to reduce denaturation of extracellular proteins and possibly the presence of residual SDS in the resulting dECM.[41,43]

Classical histological analysis showed the absence of cells and preservation of collagen fibers (the main component of native ovarian ECM) in dECM after incubation in 0.1% SDS and 0.02M NaOH for 12 h. Moreover, the SEM analysis demonstrated conservation of ECM fiber integrity following decellularization. Thus, we can affirm that the protocol employing 0.1% SDS and 0.02M NaOH for 12 h not only decellularizes the

ovarian tissue, but also preserves characteristics in a similar manner to the native ECM. Preservation of the ECM morphological characteristics after decellularization was also reported using: 0.1% SDS and 0.02M NaOH for 24 h;[25] 1% SLES (sodium lauryl ester sulfate) for 24 h followed by 24 h incubation with DNase I,[32] and using 0.5% SDS for 10 h or 2% SDC (sodium deoxycholate solution) for 16 h followed by 30 min incubation with DNase I.[38]

One crucial aspect to consider when using SDS to decellularize tissues is the challenge of complete detergent removal from the dECM and the potential toxicity associated with its residues.[48,49] With this in mind, we decided to perform 10 agitation-based washes after the incubation period, replacing the solution every 30 min, as studies have shown that cellular cytotoxicity and residual concentrations of chemical agents in dECM decrease with an increased number of washes.[48–50] For instance, the viability of cells cultured on lung dECM increased when the SDS concentration decreased and the number of washes increased.[50] Cebotari *et al*.[48] obtained a heart valve dECM using 1% SDS, and after 10 consecutive washes, the washing solution showed a residual detergent concentration of < 50 mg/L and 17±3% cytotoxicity. Another study, focused on decellularizing kidney tissue with 1% SDS, obtained a very low residual SDS concentration (0.0001%) in the washing solution after 10 washing cycles of kidney dECM, resulting in 87.4% cell viability after *in vitro* culture.[49] Our toxicity experiment using human ovarian stromal cells demonstrated viability after 24 h and 72 h of *in vitro* culture with dECM, with no significant difference compared to cells cultured alone, evidencing absence of dECM toxicity. This favorable result can be attributed to the solution changes during washing and the low concentration of SDS used.

In addition, prior to conducting the present study, we performed preliminary experiments (unpublished results) evaluating the effect of: 1) removing the ovarian capsule or not before decellularization; 2) renewing the SDS solution every 4 h, and 3) adding a further 1 h incubation at 37 °C with deoxyribonuclease I (DNase I, 1 mg/mL, 10104159001, Roche Diagnostics GmbH, Germany) after incubation with SDS and NaOH. Our experiments (data not shown) revealed the importance of removing the ovarian capsule to successfully obtain decellularized ovarian tissue. Furthermore, renewing the SDS and NaOH solution did not make the decellularization protocol more efficient, while the use of DNase I after SDS and NaOH incubation did not favor the decellularization process. Regardless of the SDS concentration employed, with or without an additional 1-h incubation at 37 °C with DNase I, the same results were obtained in the electrophoresis. Also, the DNase I-treated samples presented a viscous consistency making manipulation more difficult. This altered consistency could be due to the modification of extracellular

matrix proteins by the endonuclease at the time of cell death.[51] Consequently, the use of DNase I was excluded from our protocol.

In conclusion, we established an efficient decellularization protocol for bovine ovarian tissue utilizing SDS as the sole decellularization agent, employing both minimum detergent concentration and incubation time. The application of 0.1% SDS and 0.02M NaOH for 12 h resulted in a dECM with preserved morphological structure and no detrimental effects on human ovarian stromal cells *in vitro*. Further investigations are needed to assess the conservation of different ovarian ECM proteins post-decellularization and explore the potential use of this dECM in the development of a TAO.

Acknowledgments

We thank EMBRAPA-CENARGEN for donating the bovine ovaries, especially Nayara Ribeiro Kussano and Ligiane de Oliveira Leme. We are also grateful to the Microscopy and Microanalysis Laboratory of the University of Brasilia for use of the scanning electron microscope, especially Ingrid Gracielle M. da Silva. Finally, we express our gratitude to the Kidney and Pancreatic Transplantation Unit of UCLouvain's Saint-Luc Hospital for donating the human ovaries used in this study, from which the stromal cells were obtained.

Author Contributions

Cecibel M. León-Félix: Conceptualization; methodology; formal analysis, investigation; writing - original draft. Andrea Q. Maranhão: Conceptualization; methodology; writing - reviewing and editing. Christiani A. Amorim: Conceptualization; methodology; writing - reviewing and editing. Carolina M. Lucci: Conceptualization; methodology; writing - reviewing and editing.

Competing Interests

The authors declare that they have no known competing financial interests or personal relationships that could have appeared to influence the work reported in this paper.

Funding

This study was supported by grants from the *Coordenação de Aperfeiçoamento de Pessoal de Nível Superior - Brasil* (CAPES) (Finance Code 001), Erasmus+ Dimension internationale (convention grant no. DS/VM/CAI45-1011 awarded to C.A.A.) and Southeast Asia – Europe Joint Funding Scheme for Research and Innovation (FNRS PINT, convention grant no. R.8002.21 awarded to C.A.A.).

References

1. Sung H, Ferlay J, Siegel RL, et al. Global Cancer Statistics 2020: GLOBOCAN Estimates of Incidence and Mortality Worldwide for 36 Cancers in 185 Countries. CA Cancer J Clin 2021;71(3):209–249; doi: 10.3322/caac.21660.

2. Siegel RL, Miller KD, Fuchs HE, et al. Cancer statistics, 2022. CA Cancer J Clin 2022;72(1):7–33; doi: 10.3322/caac.21708.

3. Maltaris T, Seufert R, Fischl F, et al. The effect of cancer treatment on female fertility and strategies for preserving fertility. European Journal of Obstetrics & Gynecology and Reproductive Biology 2007;130(2):148–155; doi: 10.1016/j.ejogrb.2006.08.006.

4. Donnez J, Dolmans M-M, Pellicer A, et al. Restoration of ovarian activity and pregnancy after transplantation of cryopreserved ovarian tissue: a review of 60 cases of reimplantation. Fertil Steril 2013;99(6):1503–1513; doi: 10.1016/j.fertnstert.2013.03.030.

5. Donnez J, Dolmans M-M. Fertility Preservation in Women. New England Journal of Medicine 2017;377(17):1657–1665; doi: 10.1056/NEJMra1614676.

6. Dolmans M-M, Falcone T, Patrizio P. Importance of patient selection to analyze in vitro fertilization outcome with transplanted cryopreserved ovarian tissue. Fertil Steril 2020;114(2):279–280; doi: 10.1016/j.fertnstert.2020.04.050.

7. Sonmezer M, Oktay K. Orthotopic and heterotopic ovarian tissue transplantation. Best Pract Res Clin Obstet Gynaecol 2010;24(1):113–126; doi: 10.1016/j.bpobgyn.2009.09.002.

8. Böttcher B, Winkler-Crepaz K. Future perspectives of fertility preservation in women. memo - Magazine of European Medical Oncology 2020;13(4):416–420; doi: 10.1007/s12254-020-00626-9.

9. Amorim CA, Shikanov A. The artificial ovary: current status and future perspectives. Future Oncology 2016;12(20):2323–2332; doi: 10.2217/fon-2016-0202.

10. Dolmans M-M, Amorim CA. FERTILITY PRESERVATION: Construction and use of artificial ovaries. Reproduction 2019;158(5):F15–F25; doi: 10.1530/REP-18-0536.

11. Telfer E, Torrance C, Gosden RG. Morphological study of cultured preantral ovarian follicles of mice after transplantation under the kidney capsule. Reproduction 1990;89(2):565–571; doi: 10.1530/jrf.0.0890565.

12. Gosden RG. Restitution of fertility in sterilized mice by transferring primordial ovarian follicles. Human Reproduction 1990;5(2):117–122; doi: 10.1093/oxfordjournals.humrep.a137053.

13. Carroll J, Gosden RG. Physiology: Transplantation of frozen—thawed mouse primordial follicles. Human Reproduction 1993;8(8):1163–1167; doi: 10.1093/oxfordjournals.humrep.a138221.

14. Dolmans M-M, Martinez-Madrid B, Gadisseux E, et al. Short-term transplantation of isolated human ovarian follicles and cortical tissue into nude mice. Reproduction 2007;134(2):253–262; doi: 10.1530/REP-07-0131.

15. Dolmans M-M, Yuan WY, Camboni A, et al. Development of antral follicles after xenografting of isolated small human preantral follicles. Reprod Biomed Online 2008;16(5):705–711; doi: 10.1016/S1472-6483(10)60485-3.

16. Smith RM, Shikanov A, Kniazeva E, et al. Fibrin-Mediated Delivery of an Ovarian Follicle Pool in a Mouse Model of Infertility. Tissue Eng Part A 2014;20(21–22):3021–3030; doi: 10.1089/ten.tea.2013.0675.

17. Chiti MC, Dolmans MM, Orellana R, et al. Influence of follicle stage on artificial ovary outcome using fibrin as a matrix. Human Reproduction 2015;dev299; doi: 10.1093/humrep/dev299.

18. Kniazeva E, Hardy AN, Boukaidi SA, et al. Primordial Follicle Transplantation within Designer Biomaterial Grafts Produce Live Births in a Mouse Infertility Model. Sci Rep 2015;5(1):17709; doi: 10.1038/srep17709.

19. Paulini F, Vilela JMV, Chiti MC, et al. Survival and growth of human preantral follicles after cryopreservation of ovarian tissue, follicle isolation and short-term xenografting. Reprod Biomed Online 2016;33(3):425–432; doi: 10.1016/j.rbmo.2016.05.003.

20. Vanacker J, Dolmans M-M, Luyckx V, et al. First transplantation of isolated murine follicles in alginate. Regenerative Med 2014;9(5):609–619; doi: 10.2217/rme.14.33.

21. Kim J, Perez AS, Claflin J, et al. Synthetic hydrogel supports the function and regeneration of artificial ovarian tissue in mice. NPJ Regen Med 2016;1(1):16010; doi: 10.1038/npjregenmed.2016.10.

22. Dadashzadeh A, Moghassemi S, Shavandi A, et al. A review on biomaterials for ovarian tissue engineering. Acta Biomater 2021;135:48–63; doi: 10.1016/j.actbio.2021.08.026.

23. Rajabzadeh AR, Eimani H, Koochesfahani HM, et al. Morphological Study of Isolated Ovarian Preantral Follicles Using Fibrin Gel Plus Platelet Lysate after Subcutaneous Transplantation. Cell Journal (Yakhteh) 2015;17(1):145–152; doi: 10.22074/cellj.2015.521.

24. Hrebikova H, Diaz D, Mokry J. Chemical decellularization: a promising approach for preparation of extracellular matrix. Biomedical Papers 2015;159(1):012–017; doi: 10.5507/bp.2013.076.

25. Laronda MM, Jakus AE, Whelan KA, et al. Initiation of puberty in mice following decellularized ovary transplant. Biomaterials 2015;50:20–29; doi: 10.1016/j.biomaterials.2015.01.051.

26. Hochman-Mendez C, Mesquita FCP, Morrissey J, et al. Restoring anatomical complexity of a left ventricle wall as a step toward bioengineering a human heart with human induced pluripotent stem cell-derived cardiac cells. Acta Biomater 2022;141:48–58; doi: 10.1016/j.actbio.2021.12.016.

27. Kawai N, Ouji Y, Sakagami M, et al. Induction of lung-like cells from mouse embryonic stem cells by decellularized lung matrix. Biochem Biophys Rep 2018;15:33–38; doi: 10.1016/j.bbrep.2018.06.005.

28. Kajbafzadeh A-M, Khorramirouz R, Nabavizadeh B, et al. Whole organ sheep kidney tissue engineering and in vivo transplantation: Effects of perfusion-based decellularization on vascular integrity. Materials Science and Engineering: C 2019;98:392–400; doi: 10.1016/j.msec.2019.01.018.

29. Panahi F, Baheiraei N, Sistani MN, et al. Analysis of decellularized mouse liver fragment and its recellularization with human endometrial mesenchymal cells as a

candidate for clinical usage. Prog Biomater 2022;11(4):409–420; doi: 10.1007/s40204-022-00203-9.

30. Li X, Wang Y, Ma R, et al. Reconstruction of functional uterine tissues through recellularizing the decellularized rat uterine scaffolds by MSCs in vivo and in vitro. Biomedical Materials 2021;16(3):035023; doi: 10.1088/1748-605X/abd116.

31. Kargar-Abarghouei E, Vojdani Z, Hassanpour A, et al. Characterization, recellularization, and transplantation of rat decellularized testis scaffold with bone marrow-derived mesenchymal stem cells. Stem Cell Res Ther 2018;9(1):324; doi: 10.1186/s13287-018-1062-3.

32. Hassanpour A, Talaei-Khozani T, Kargar-Abarghouei E, et al. Decellularized human ovarian scaffold based on a sodium lauryl ester sulfate (SLES)-treated protocol, as a natural three-dimensional scaffold for construction of bioengineered ovaries. Stem Cell Res Ther 2018;9(1):252; doi: 10.1186/s13287-018-0971-5.

33. Pors SE, Ramløse M, Nikiforov D, et al. Initial steps in reconstruction of the human ovary: survival of pre-antral stage follicles in a decellularized human ovarian scaffold. Human Reproduction 2019;34(8):1523–1535; doi: 10.1093/humrep/dez077.

34. Eivazkhani F, Abtahi NS, Tavana S, et al. Evaluating two ovarian decellularization methods in three species. Materials Science and Engineering: C 2019;102:670–682; doi: 10.1016/j.msec.2019.04.092.

35. Liu W-Y, Lin S-G, Zhuo R-Y, et al. Xenogeneic Decellularized Scaffold: A Novel Platform for Ovary Regeneration. Tissue Eng Part C Methods 2017;23(2):61–71; doi: 10.1089/ten.tec.2016.0410.

36. Buckenmeyer MJ, Sukhwani M, Iftikhar A, et al. Bioengineering an in situ ovary (ISO) for fertility preservation. bioRxiv 2020;01; doi: 10.1101/2020.01.03.893941.

37. Pennarossa G, Ghiringhelli M, Gandolfi F, et al. Whole-ovary decellularization generates an effective 3D bioscaffold for ovarian bioengineering. J Assist Reprod Genet 2020;37(6):1329–1339; doi: 10.1007/s10815-020-01784-9.

38. Alshaikh AB, Padma AM, Dehlin M, et al. Decellularization and recellularization of the ovary for bioengineering applications; studies in the mouse. Reproductive Biology and Endocrinology 2020;18(1):75; doi: 10.1186/s12958-020-00630-y.

39. Alshaikh AB, Padma AM, Dehlin M, et al. Decellularization of the mouse ovary: comparison of different scaffold generation protocols for future ovarian bioengineering. J Ovarian Res 2019;12(1):58; doi: 10.1186/s13048-019-0531-3.

40. Nikniaz H, Zandieh Z, Nouri M, et al. Comparing various protocols of human and bovine ovarian tissue decellularization to prepare extracellular matrix-alginate scaffold for better follicle development in vitro. BMC Biotechnol 2021;21(1):8; doi: 10.1186/s12896-020-00658-3.

41. Faulk DM, Johnson SA, Zhang L, et al. Role of the Extracellular Matrix in Whole Organ Engineering. J Cell Physiol 2014;229(8):984–989; doi: 10.1002/jcp.24532.

42. Zvarova B, Uhl FE, Uriarte JJ, et al. Residual Detergent Detection Method for Nondestructive Cytocompatibility Evaluation of Decellularized Whole Lung Scaffolds. Tissue Eng Part C Methods 2016;22(5):418–428; doi: 10.1089/ten.tec.2015.0439.

43. White LJ, Taylor AJ, Faulk DM, et al. The impact of detergents on the tissue decellularization process: A ToF-SIMS study. Acta Biomater 2017;50:207–219; doi: 10.1016/j.actbio.2016.12.033.

44. Kraft L, Ribeiro VST, de Nazareno Wollmann LCF, et al. Determination of antibiotics and detergent residues in decellularized tissue-engineered heart valves using LC–MS/MS. Cell Tissue Bank 2020;21(4):573–584; doi: 10.1007/s10561-020-09856-x.

45. Amorim CA, Van Langendonckt A, David A, et al. Survival of human pre-antral follicles after cryopreservation of ovarian tissue, follicular isolation and in vitro culture in a calcium alginate matrix. Human Reproduction 2009;24(1):92–99; doi: 10.1093/humrep/den343.

46. Vanacker J, Camboni A, Dath C, et al. Enzymatic isolation of human primordial and primary ovarian follicles with Liberase DH: protocol for application in a clinical setting. Fertil Steril 2011;96(2):379-383.e3; doi: 10.1016/j.fertnstert.2011.05.075.

47. Crapo PM, Gilbert TW, Badylak SF. An overview of tissue and whole organ decellularization processes. Biomaterials 2011;32(12):3233–3243; doi: 10.1016/j.biomaterials.2011.01.057.

48. Cebotari S, Tudorache I, Jaekel T, et al. Detergent Decellularization of Heart Valves for Tissue Engineering: Toxicological Effects of Residual Detergents on Human Endothelial Cells. Artif Organs 2010;34(3):206–210; doi: 10.1111/j.1525-1594.2009.00796.x.

49. Ghorbani F, Ekhtiari M, Moeini Chaghervand B, et al. Detection of the residual concentration of sodium dodecyl sulfate in the decellularized whole rabbit kidney extracellular matrix. Cell Tissue Bank 2022;23(1):119–128; doi: 10.1007/s10561-021-09921-z.

50. Ghorbani F, Abdihaji M, Roudkenar MH, et al. Development of a Cell-Based Biosensor for Residual Detergent Detection in Decellularized Scaffolds. ACS Synth Biol 2021;10(10):2715–2724; doi: 10.1021/acssynbio.1c00321.

51. Fahmi T, Wang X, Zhdanov DD, et al. DNase I Induces Other Endonucleases in Kidney Tubular Epithelial Cells by Its DNA-Degrading Activity. Int J Mol Sci 2020;21(22):8665; doi: 10.3390/ijms21228665.

VI. CAPÍTULO II

O segundo capítulo consistiu na caracterização proteômica da MEC do córtex ovariano bovino nativa e descelularizada utilizando o protocolo desenvolvido no Capítulo I. Essa análise incluiu a identificação das proteínas presentes em ambas as matrizes, bem como a aplicação de ferramentas de bioinformática para uma investigação das suas funções. Com esse propósito, foi elaborado o segundo artigo, apresentado a seguir, que ainda não está submetido para publicação.

Protein characterization of extracellular matrix from bovine ovarian cortex before and after decellularization

Authors:

Cecibel M. León-Félix[1], Emna Ouni[2], Gaëtan Herinckx[3], Didier Vertommens[3], Christiani A. Amorim[2], Carolina M. Lucci[1,*]

Affiliations:

[1]Institute of Biological Sciences, Department of Physiology, University of Brasilia, Brasilia, Brazil

[2]Institut de Recherche Expérimentale et Clinique, Department of Gynecology, Université Catholique de Louvain, Brussels, Belgium

[3]de Duve Institute, Université Catholique de Louvain, Brussels, Belgium

***Co-corresponding author:**

Prof. Carolina M. Lucci

Address: Instituto de Biologia, Universidade de Brasília, Campus Darcy Ribeiro, Asa Norte, Brasília – DF. Brazil. 70910-900

TEL: +55 61 98581-4662

E-mail: carollucci@gmail.com

Abstract

Recent approaches of regenerative reproductive medicine investigate the decellularized extracellular matrix to develop a transplantable artificial ovary (TAO). However, a full proteomic analysis is not usually performed after the decellularization process to evaluate the preservation of the extracellular matrix (ECM). In this study, the ECM of bovine ovarian cortex was analyzed before and after decellularization using mass spectrometry and bioinformatics. A total of 155 matrisome proteins were identified on the bovine ovarian cortex native ECM, while 145 matrisome proteins were identified on the decellularized ECM. After decellularization, only 10 matrisome proteins were lost, and none of them belonged to the category of reproductive biological processes. Additionally, bioinformatic analyses revealed that those proteins, present in both native and decellularized ECM, are involved in 12 biological processes, 19 cellular components, and 13 molecular functions. Also, the general morphology of both native and decellularized ECM was accessed through histology and histochemistry analyses, along with the identification of the most abundant ECM proteins. Moreover, we demonstrated that collagen type VI alpha 3 and heparan sulfate proteoglycan 2 were the most abundant components of bovine ovarian ECM. These findings contribute to a better understanding of the composition of both native and decellularized ECM and may have important implications in the development of a TAO.

Keywords:

Matrisome, proteomics, proteins, ECM, ovary.

Introduction

In recent years, advances in the field of regenerative medicine applied to reproduction have introduced new assisted reproductive technologies (ART) for infertility treatment (Zegers-Hochschild *et al*., 2009). Cancer patients undergoing chemotherapy and/or radiotherapy may experience ovarian function loss after treatment (Maltaris *et al*., 2007) and may benefit from those ART. However, patients diagnosed with cancer and with a probability of ovarian metastasis (Donnez *et al*., 2013) face challenges in accessing these technologies, such as ovarian tissue cryopreservation for future autotransplantation, due to the risk of reintroducing cancerous cells (Sonmezer and Oktay, 2010; Donnez and Dolmans, 2017). To address these issues, researchers are investigating the transplantable artificial ovary (TAO) as a new possibility to restore female fertility and hormonal production.

The TAO is based on the interaction between a three-dimensional structure with ovarian cells and isolated preantral follicles, with the purpose of facilitating the complete development of follicles and oocyte maturation, as well as promoting adequate production of female sex hormones (Amorim and Shikanov, 2016; Dolmans and Amorim, 2019). To achieve this, it is necessary the microenvironment of a native ovarian extracellular matrix (ECM), as the ECM plays a dynamic and essential role in folliculogenesis and steroidogenesis in the ovary (Rodgers *et al*., 2003; Woodruff and Shea, 2007). To obtain a cell-free native ECM while simultaneously preserving the inherent characteristics of the ovarian tissue's ECM, the decellularization technique has been employed in ovarian tissue (for a review see Wu *et al*., 2023). Recently, we developed a mild decellularization protocol for bovine ovarian cortex, that proved to provide a decellularized ECM (dECM) morphologically similar to the native ovarian ECM and was not toxic to human ovarian cells (see Capítulo 1).

The development of a dECM from an animal model is extremely important due to the limited availability of human ovarian samples. The bovine ovary, due to its striking resemblance to the human ovary in numerous aspects (Adams and Piersont, 1995; Malhi *et al*., 2005), presents a viable alternative. A successfully dECM lacks nuclear material, preventing immunological reactions in the recipient (Wu *et al*., 2022; Talaei-Khozani and Yaghoubi, 2022). In fact, it has already been demonstrated that dECM derived from other bovine tissues does not induce immune responses in other species (Arhuidese *et al*., 2015; Gardin *et al*., 2015), as evidenced in bone grafting utilizing decellularized bovine femur (Gardin *et al*., 2015), guided bone regeneration using decellularized bovine pericardium

(Gardin *et al*., 2015), and lower limb vessel bypass for humans using decellularized bovine carotid artery (Artegraf®). So, the dECM derived from the bovine ovarian cortex could be used as a potential scaffold from human OAT.

Another important aspect to consider when using dECM from an animal model is the conservation of ECM molecules across different species, a topic well-documented in the literature (Bernard *et al*., 1983; Constantinou *et al*., 1991). The dECM are usually evaluated by other ways, such as morphologically, through immunohistochemistry and scanning electron microscopy, and quantitatively, using colorimetric techniques to examine certain ECM components (Liu *et al*., 2017; Alshaikh *et al*., 2019; Eivazkhani *et al*., 2019). However, none of these evaluations provide a detailed assessment of the preservation of ovarian ECM components. Therefore, the main objective of this study was to conduct a comprehensive proteomic analysis of the bovine ovarian tissue ECM components before and after the decellularization process using our protocol of 0.1% SDS concentration with 0.02M NaOH for a 12-hour incubation period (see Capítulo 1). Moreover, we conducted a parallel comparative analysis of our bovine ovarian matrisome findings with those of other species.

Material and Methods

Ovarian tissue

Ovaries from bovine were collected from local slaughterhouses (Frigoias and Bom Corte, Anapolis and Formosa-GO, Brazil) and transported to the laboratory in PBS at 37 °C. In the laboratory, the ovaries were carefully cleaned and stored at -20 °C. Prior to the experimentation, the ovaries were thawed, the antral follicles were aspirated, and the epithelial and medullary layers of the ovary were meticulously removed with the aid of a scalpel. Subsequently, samples measuring 10 mm x 5 mm x 1 mm were extracted from the cortical region, weighed, and evenly distributed among control and decellularized group (decell group).

Decellularization protocol

The samples assigned to the decell group underwent decellularization using a protocol previously described by León-Félix *et al*. (see Capítulo 1). Briefly, the tissue

samples were incubated in 10 mL of 0.1% sodium dodecyl sulfate (SDS; L3771-100G, Sigma-Aldrich, USA) and 0.02M sodium hydroxide (NaOH, 106467, Sigma-Aldich, USA) in distilled water for 12 h at room temperature under constant stirring (100 rpm). Then, the samples were washed in 50 mL of distilled water for 6 h, under constant stirring, with the water being changed every 30 min. The samples designated for the control group underwent treatment with distilled water alone, following the same procedure as the decell group. Finally, all samples were lyophilized and stored for subsequent analyses.

Protein extraction

All samples (n=5 per group) were processed following the protocol established by Ouni *et al*. (2022). Briefly, each sample was transferred to an empty 2mL FastPrep® Lysing matrix tube (MP Biomedicals) and covered with 100 µL lysing buffer containing 0.2 % RapiGest SF (Water Corp, Milford, MA, USA), 300 mM NaCl, 25 mM HEPES, 0.25 mM sodium orthovanadate, 50 mM NaF, 0.25 mM PMSF, 1X halts protease inhibitor cocktail (Thermo Scientific, San Jose, CA, USA) and 5 mM EDTA. Mechanical lysis was performed using 0.3 mm-diameter stainless steel beads (Full Moon, BioSystems, Sunnyvale, CA, USA) with homogenization carried out at 4 ˚C with Precellys Evolution (Bertin Technologies, Montighny-le-Breton-neux, France). The homogenate was eluted with the needle technique following by centrifugation at 3000 *g* for 5 min at 4 °C. The resulting eluate was then subjected to another round of centrifugation at 16,000 *g* for 30 min at 4 °C to recover the supernatant. Total protein content of this fraction was quantified using the Pierce™ BCA Protein Assay Kit (23225, Thermo Scientific).

Peptide extraction

A total of 100 µg of total supernatant proteins was reduced with 5 mM 1,4-Dithiothreitol (DTT), incubated for 30 min at 56 °C and then alkylated with 25 mM chloroacetamide for 25 min at room temperature in the dark. Then, the proteins were precipitated using methanol-chloroform, resuspended in 50 mM TEAB (pH 8), and subjected to digestion using Lys-C/Trypsin (V507A, Thermo Scientific) at the enzyme-to-substrate ratio of 1:25 [wt/wt] overnight at 37 °C. The resulting mixture was then centrifuged at 16,000 *g* for 10 min at 4 °C. The recovered peptides were quantified using the Pierce™ Quantitative Colorimetric Peptide Assay (23275, Thermo Scientific).

Liquid chromatography –tandem-mass-spectrometry (LC-MS/MS)

One μg of peptides dissolved in solvent A (0.1% TFA in 2% ACN) was directly loaded onto a reversed-phase pre-column (Acclaim PepMap 100, Thermo Scientific) and eluted in backflush mode. Peptide separation was achieved using a reversed-phase analytical column (Acclaim PepMap RSLC, 0.075 x 250 mm, Thermo Scientific) with a 140 min linear gradient of 4%-32% solvent B (0.1% TFA in 80% ACN) for 99 min, 32%-60% solvent B for 10 min, 60%-95% for 1 min and holding at 95% for the last 10 min at a constant flow rate of 300 nL/min on an Ultimate 3000 RSLN nanoHPLC system (Thermo Scientific). The peptides were analyzed by an Orbitrap Fusion Lumos tribrid mass spectrometer (Thermo Fisher Scientific) with enabled advanced peak determination (APD) and relative quantification either by MS2 or SPS MS3. The peptides were subjected to a nanospray ionization source, followed by MS/MS in the Fusion Lumos coupled online to the UPLC. Intact peptides were detected in the Orbitrap at a resolution of 120,000 with a scan range m/z from 375 to 1500 and an AGC target of 4x105, maximum injection time was set to 50 ms. A data-dependent procedure of MS/MS scans was applied for the top precursor ions above a threshold ion count of 5.0 x 103 in the MS survey scan with 60 s dynamic exclusion. The total cycle time was set to 3 s. For MS2 quantification of the TMT reporter ions, MS/MS spectra were acquired in the Orbitrap at a resolution of 50,000 after HCD fragmentation at 35% with an AGC target of 1 x 105 ions and a maximum injection time of 120 ms. For MS3 quantification, MS/MS spectra were first acquired in the Ion Trap after CID fragmentation at 30%, 10 precursors were synchronously selected (SPS MS3) for HCD fragmentation at 55%, and the MS3 spectra was acquired in the Orbitrap at a resolution of 50,000 with an AGC of 2 x 105 and a maximum injection time of 120 ms. MS/MS spectra was exported using the following settings: peptide mass range: 350-5000 Da, minimal total ion intensity: 500.

Proteomic data and statistical analysis

All proteins identified with ≥ 2 unique peptides were compared with the human *in-silico* matrisome (http://matrisomeproject.mit.edu/). These proteins were characterized according to Naba *et al*. (2012, 2016) based on core-matrisome proteins, including ECM glycoproteins, collagens and proteoglycans, as well as matrisome-associated proteins, such as ECM-affiliated proteins, ECM regulators and secreted factors, using the Matrisome

Annotator (http://matrisomeproject.mit.edu/analytical-tools/matrisome-annotator/). Bioinformatic analysis was performed using JMP® Pro 16 Statistical Software and WebGestalt online (htt://WebGestalt.org)., and statistical analysis, including Pearson's correlation analysis and Student´s t-distribution ($p < 0.05$), was conducted using GraphPad Prism® 9 Statistical Software to quantify and compare the proteins between both groups and each quantified protein. A comprehensive protocol is illustrated on Figure 16.

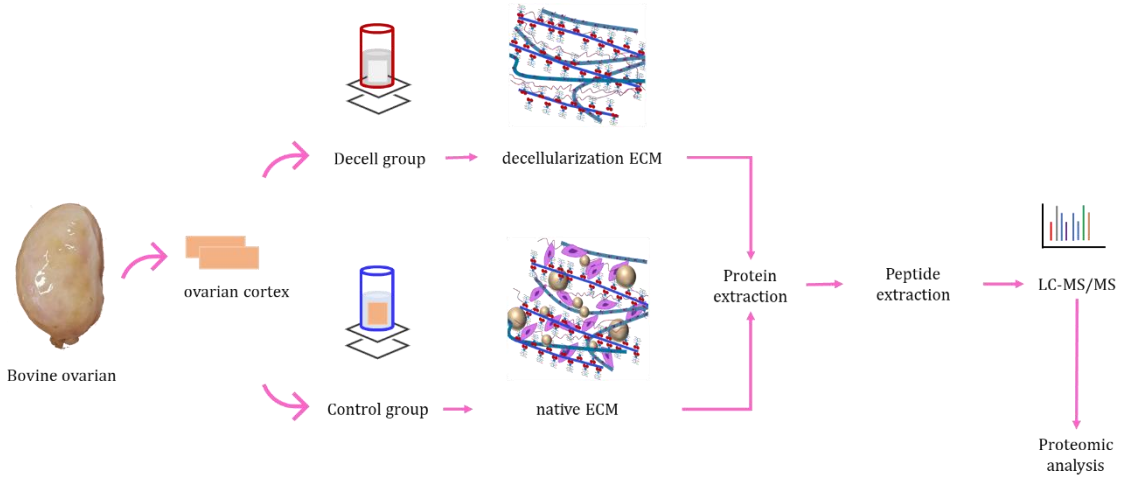

Figure 16. Schematization of the decellularization process and proteomic analysis. Bovine ovarian cortex samples were divided into two groups: the control group (without decellularization process) and the decell group (exposed to the decellularization process). The proteins present in each sample were reduced to peptides and subsequently analyzed using liquid chromatography – tandem mass spectrometry, enabling the detection of the components of the extracellular matrix in the bovine ovarian cortex. Finally, each of the components was identified and analyzed statistically and bioinformatically. ECM = extracellular matrix; LC-MS/MS = Liquid chromatography – tandem mass spectrometry.

Histological and Immunohistochemical analysis

Histological analysis was conducted on both control and decell group samples (n=5 per group). Samples were fixed in 4% paraformaldehyde, dehydrated, embedded in paraffin, and cut into 5 μm-thick sections. Sections from each sample was stained with hematoxylin-eosin (Sigma, Hannover, Germany), Masson's trichrome (Goldner,1938) and Alcian blue satin (pH 2.5) staining (Hayat, 1993) in order to assess the general appearance of the ovarian ECM, the content of collagen fibers and carboxylated and sulfated glycosaminoglycans, respectively.

Additional sections were used for immunohistochemical analyses. Sections were deparaffinized with Histosafe (Yvsolab SA, Beerse, Belgium) and rehydrated in alcohol. Endogenous peroxidase was blocked with 3% H_2O_2, epitope unmasking with 0.01 M citrate buffer (0.019 M citric acid, 0.082 M sodium citrate dihydrate, and 20% TritonX100, pH 6,) at 96°C for 75 min. Nonspecific reactions were blocked with 10% normal goat serum (NGS) and 1 % bovine serum albumin (BSA) for 30 min.

Primary rabbit antibodies used in this study included collagen type VI alpha 3 (1/100 dilution, PA549914, ThermoFisher), EMILIN1 (1/100 dilution, HPA002822, Sigma-Aldrich), fibrilin1 (1/100 dilution, HPA017759, Sigma-Aldrich) and elastin (1/100 dilution, PA599418, ThermoFisher). These antibodies were diluted in TBS containing 1% NGS and 0.1% BSA, and the slides were incubated with the primary antibodies overnight at 4 °C. The secondary antibodies were horseradish peroxidase (HRP)-conjugated anti-rabbit (K003, EnVision™+, Dako) for 1 h at room temperature. After, the slides were treated with 3,3'-diaminobenzidine (DAB) substrate chromogen system (K3468, EnVision™+, Dako) for 15 min, followed by counterstaining with hematoxylin. Slides were mounted with DPX mounting medium. Positive controls consisting of human ovarian tissue were utilized, while negative controls were prepared without the addition of the primary antibodies.

Results

Quantification of proteins

The quantification of soluble proteins was determined to be 3.5 ± 0.3 µg/µL (mean ± SD) in the control group (n = 5), and 2.1 ± 0.2 µg/µL (mean ± SD) in the decell group (n = 5). These results demonstrate a statistically significant difference ($p < 0.05$) between the two groups (Fig. 17).

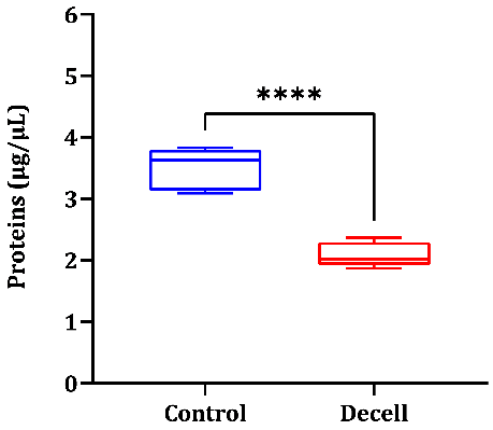

Figure 17. Quantification of soluble proteins in the control group and decell group. Student´s t-distribution was applied to compare both groups (mean ± SD, **** $p \leq 0.0001$).

Total ovarian proteome analysis

A total of 3311 proteins were detected with a false discovery rate (FDR) below 5%. Among them, 2195 proteins were identified based on a minimum score of ≥ 2 unique peptides. These proteins were then compared with a curated *in-silico* protein set of the human matrisome obtained from the Matrisome Project (http://matrisomeproject.mit.edu/), resulting in the identification of 155 matches. The pool of matrisome proteins identified was further characterized for the control and decell groups. In the control group, a total of 155 matrisome proteins were found, consisting of 87 core-matrisome proteins. Among the core-matrisome proteins, 37.42% were ECM glycoproteins, 11.60% were collagens, and 7.10% were proteoglycans. Additionally, 68 matrisome-associated proteins were identified in the control group, including 21.29% ECM regulators, 17.42% ECM-affiliated proteins, and 5.16% secreted factors (Table 8). In the decell group, a total of 145 matrisome proteins were identified, comprising 84 core-matrisome proteins. Among the core-matrisome proteins, 37.93% were ECM glycoproteins, 12.41% were collagens, and 7.59% were proteoglycans. Furthermore, 61 matrisome-associated proteins were found in the decell group, which included 21.38% ECM regulators, 16.55 % ECM-affiliated proteins, and 4.14% secreted factors (Table 8).

Table 8. Matrisome protein categories in the control and the decell groups.

Group	Core-matrisome			Matrisome-associated			Total
	ECM glycoproteins	**Collagens**	**Proteoglycans**	**ECM regulators**	**ECM-affiliated proteins**	**Secreted factors**	
Control	58	18	11	33	27	8	155
	(37.42%)	(11.61%)	(7.10%)	(21.29%)	(17.42%)	(5.16%)	
Decell	55	18	11	31	24	6	145
	(37.93%)	(12.41%)	(7.59%)	(21.38%)	(16.55%)	(4.14%)	

Ovarian ECM Proteome Map of the control group and decell group

The matrisome composition is shown in Figure 18 to 23. Each identified protein was subjected to statistic comparison ($p < 0.05$) between the control group and the decell group based on the abundance (log10 [mean of each group]) and corresponding peptide spectrum matches (PSM). Following decellularization, ten proteins were found to be absent. These included three ECM glycoprotein proteins (SPARC, homologous peroxidasin, and multimerin 2), one ECM regulator protein (procollagen-lysine,2-oxoglutarate 5-dioxygenase 3), three ECM-affiliated protein proteins (glypican 1, plexin A4 and plexin B1) and two secreted factors (angiopoietin-like 2 and angiopoietin-4). However, the number of collagen and proteoglycan proteins remained the same in both groups.

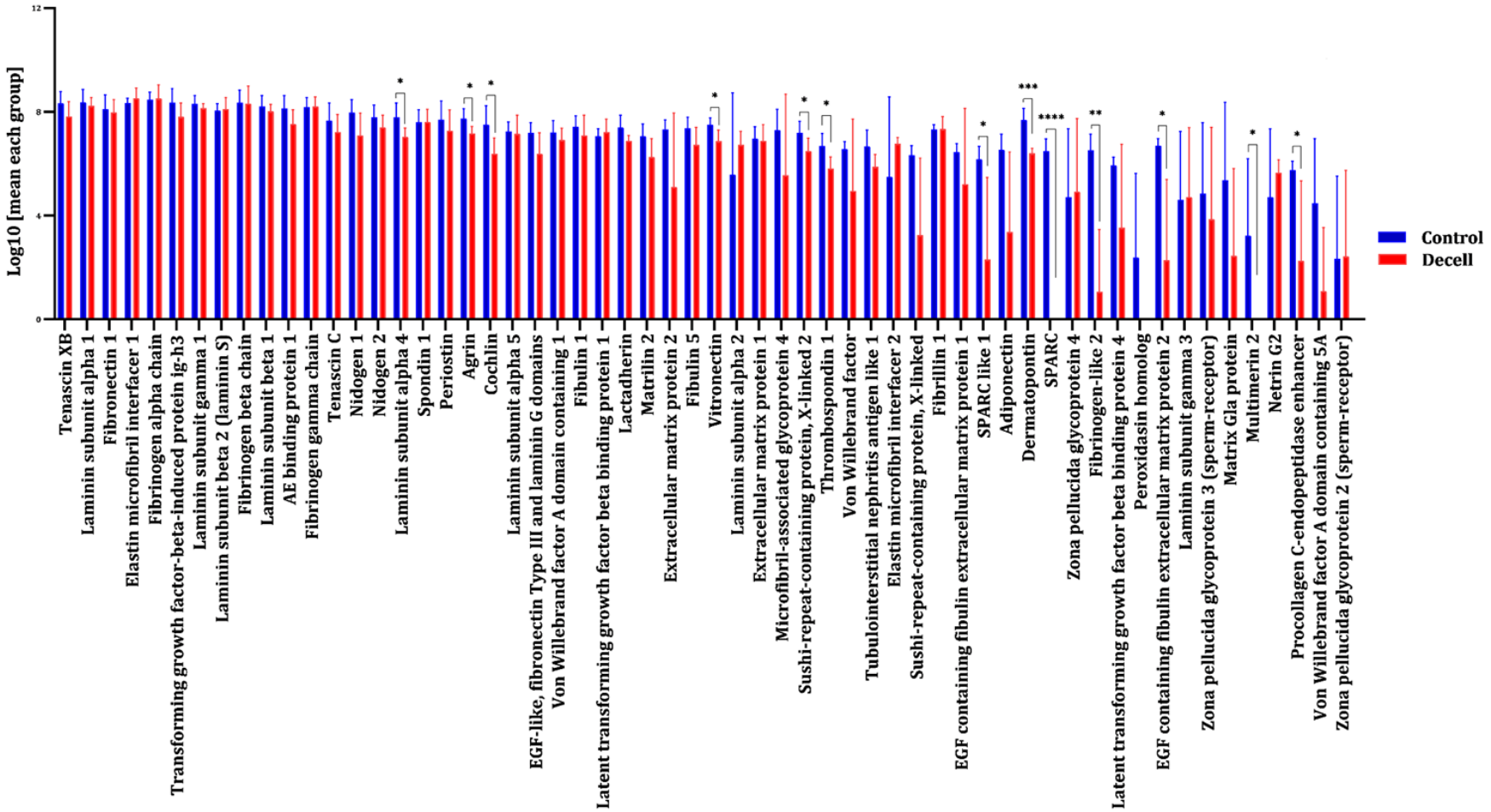

Figure 18. Ovarian matrisome of glycoproteins were identified in the control group (blue) and decell group (red) and quantified (mean ±SD). Student´s t-distribution (*p ≤ 0.05, **p ≤ 0.01, ***p ≤ 0.001, **** p ≤ 0.0001) was made for each protein.

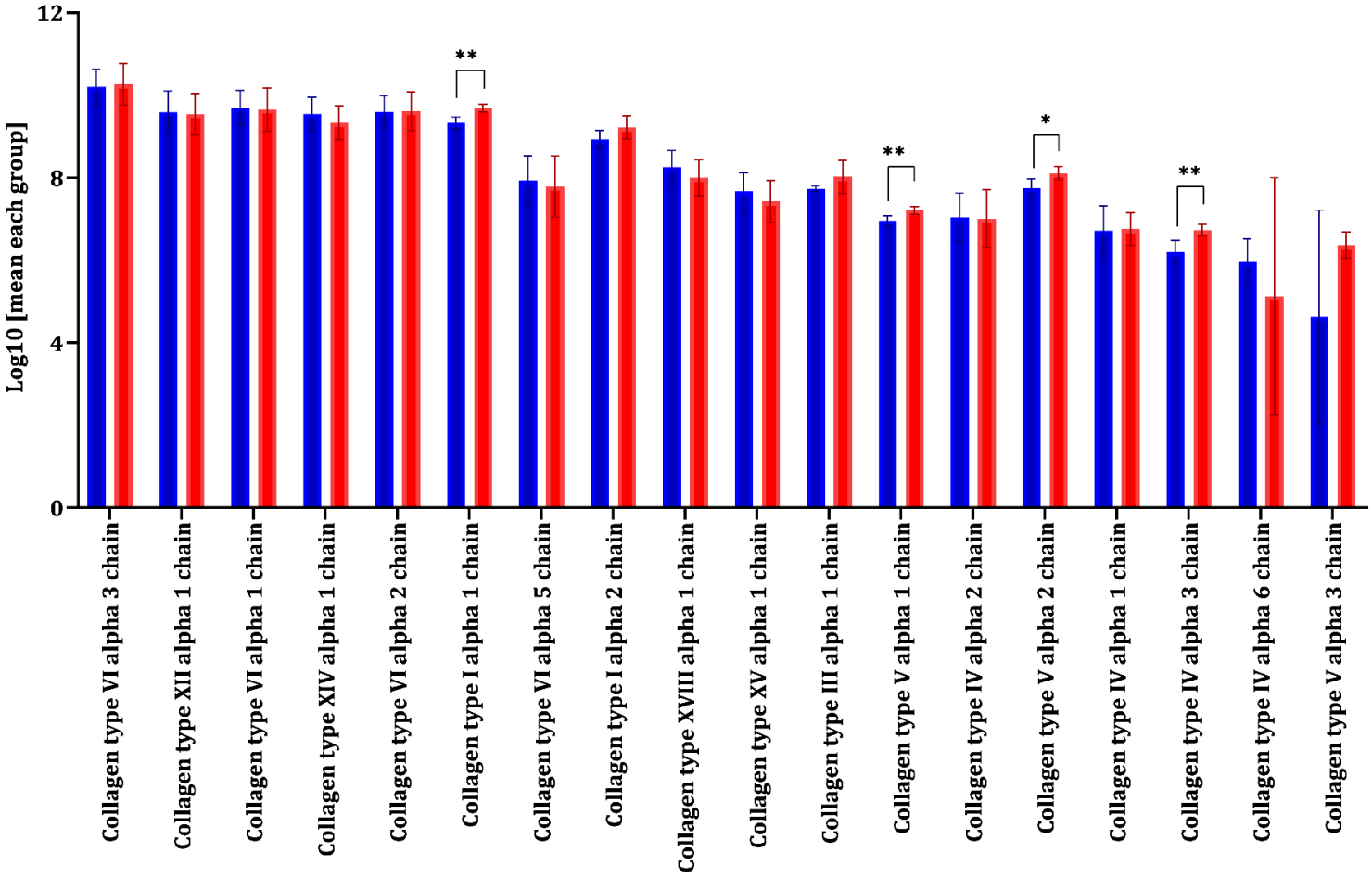

Figure 19. Ovarian matrisome of collagens were identified in the control group (blue) and decell group (red) and quantified (mean ±SD). Student´s t-distribution (*p ≤ 0.05, **p ≤ 0.01, ***p ≤ 0.001, **** p ≤ 0.0001) was made for each protein.

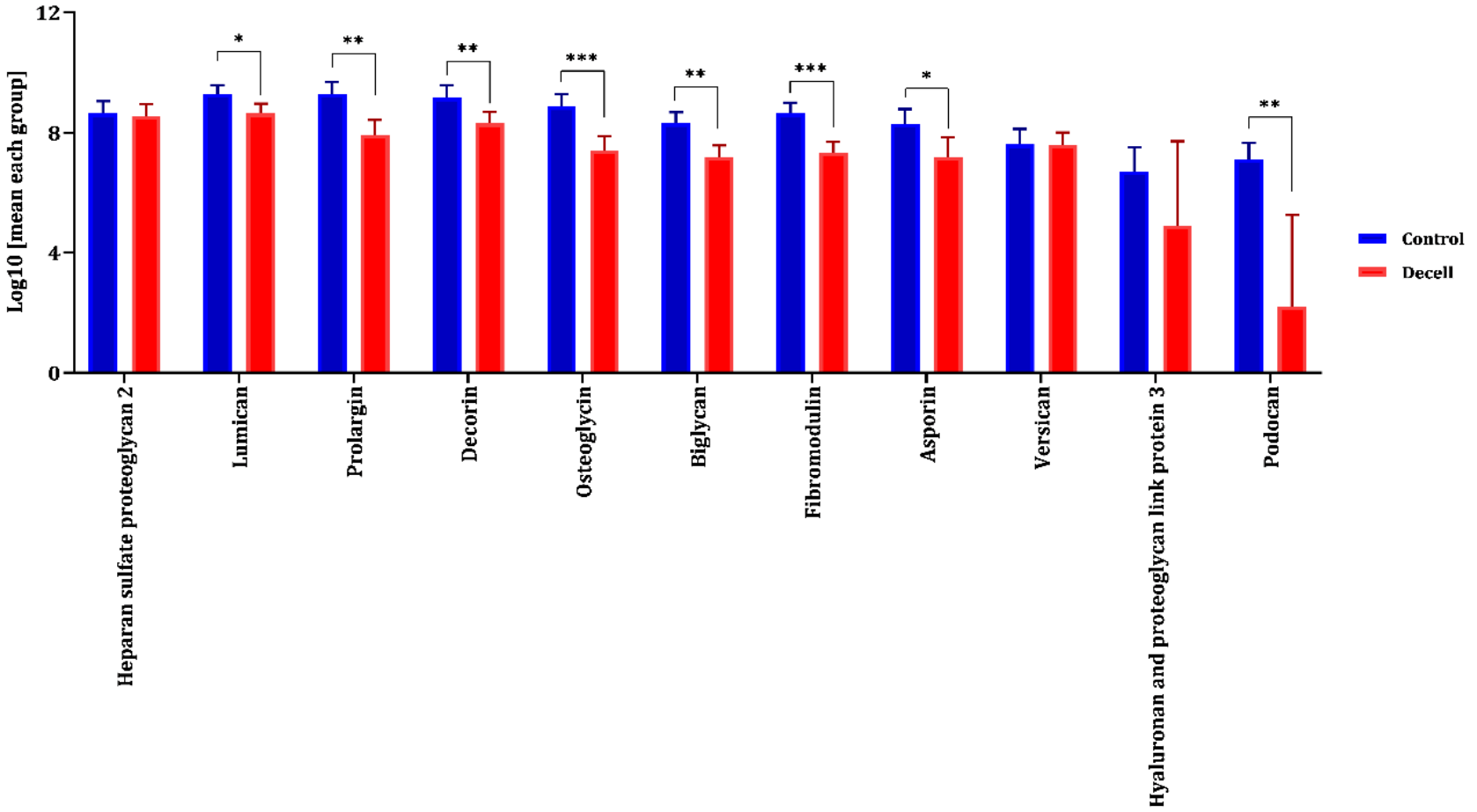

Figure 20. Ovarian matrisome of proteoglycans were identified in the control group (blue) and decell group (red) and quantified (mean ±SD). Student´s t-distribution (*p ≤ 0.05, **p ≤ 0.01, ***p ≤ 0.001, **** p ≤ 0.0001) was made for each protein.

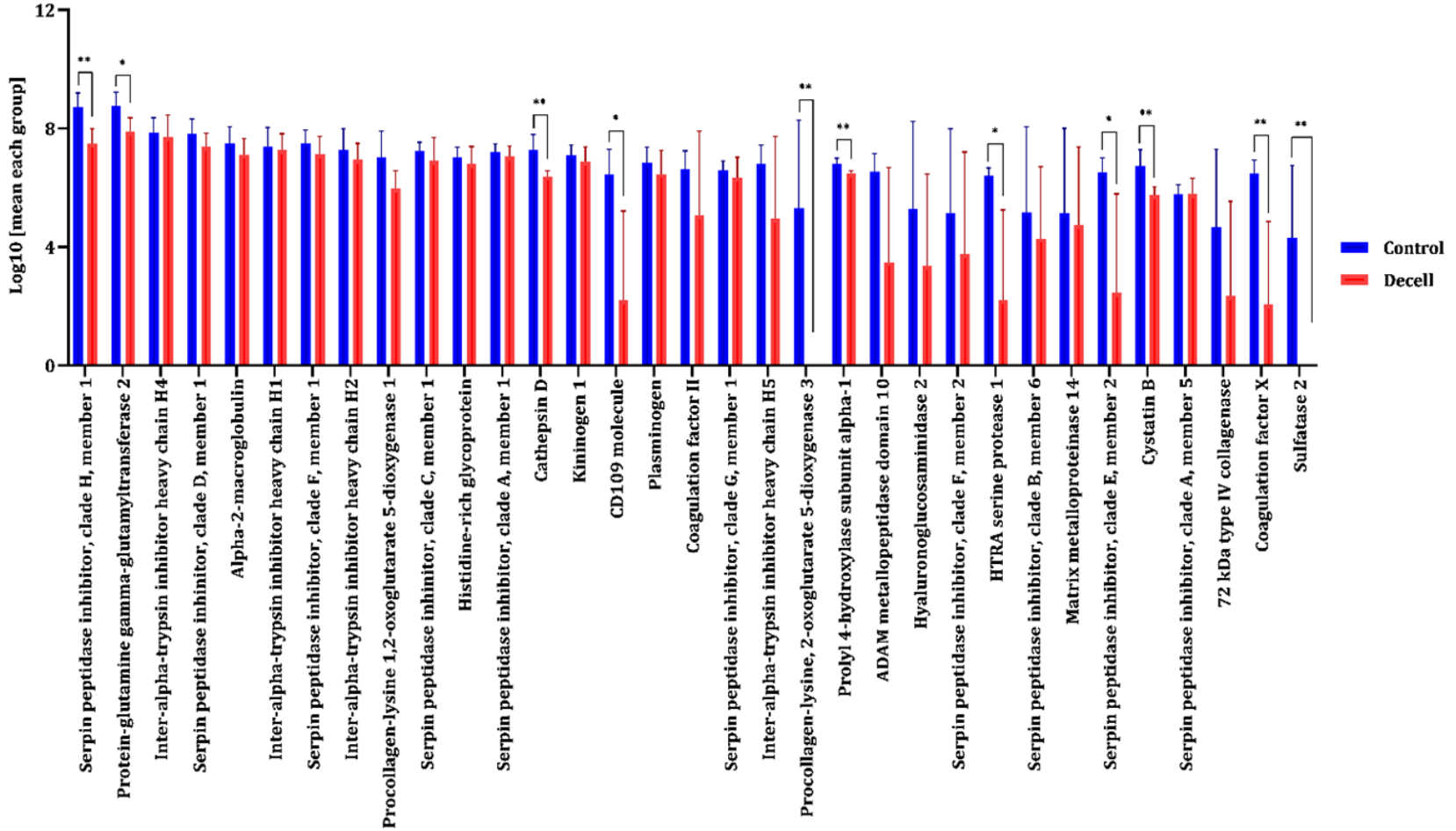

Figure 21. Ovarian matrisome of ECM regulators were identified in the control group (blue) and decell group (red) and quantified (mean ±SD). Student´s t-distribution (*p ≤ 0.05, **p ≤ 0.01, ***p ≤ 0.001, **** p ≤ 0.0001) was made for each protein.

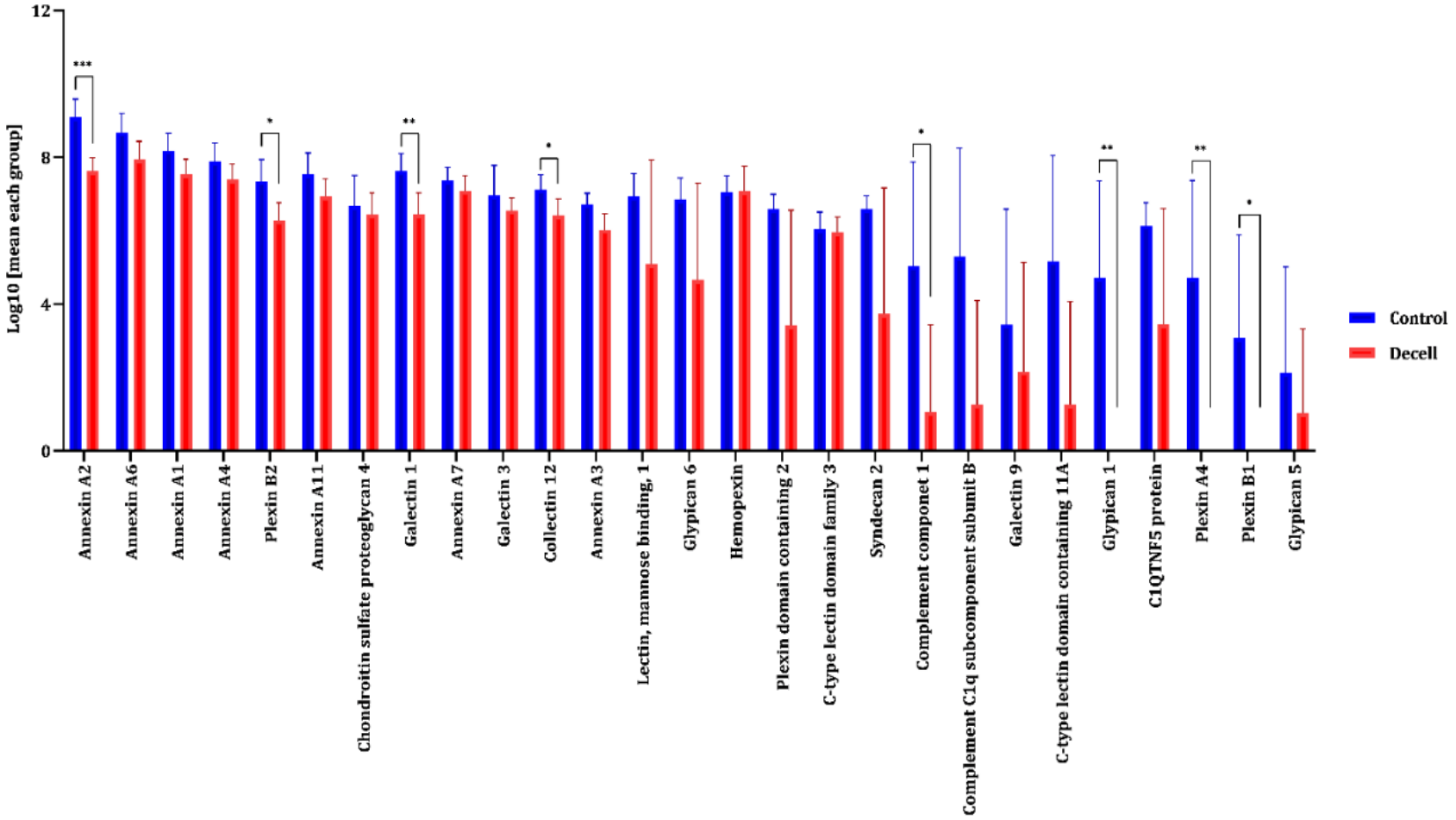

Figure 22. Ovarian matrisome of ECM-affiliated proteins were identified in the control group (blue) and decell group (red) and quantified (mean ±SD). Student´s t-distribution (*p ≤ 0.05, **p ≤ 0.01, ***p ≤ 0.001, **** p ≤ 0.0001) was made for each protein.

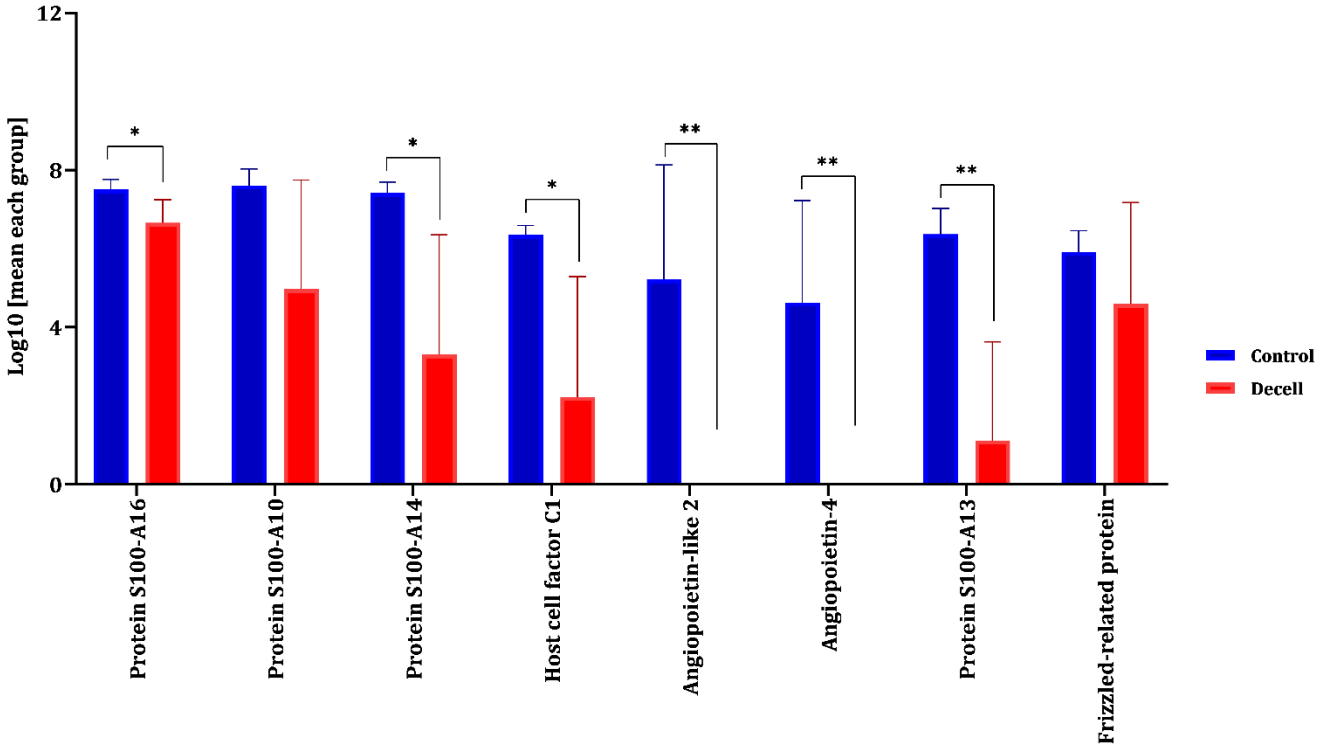

Figure 23. Ovarian matrisome of secreted factors were identified in the control group (blue) and decell group (red) and quantified (mean ±SD). Student´s t-distribution (*p ≤ 0.05, **p ≤ 0.01, ***p ≤ 0.001, **** p ≤ 0.0001) was made for each protein.

Top 58 detected proteins

The identification of the most abundant proteins in both the control group and decell group was based on the number of PSM (Fig. 24). The most abundant proteins observed were type VI collagen, heparan sulfate proteoglycan 2, the ECM glycoprotein Tenascin XV, the ECM-affiliated protein annexin A2 and the ECM regulator serpin H1.

Gene ontology analysis of Ovarian ECM Proteome of the control group and decell group

All gene symbols of each protein identified the control and decell groups (mentioned above) were analyzed WebGestalt online (htt://WebGestalt.org). The following criteria were selected: *Bos taurus* as the organism of interest and Over-representation analysis (ORA) as the method of interest. The result was the division of proteins into 12 biological processes (Fig. 25a),19 cellular components (Fig. 25b), and 13 molecular functions (Fig. 25c).

Histological and Immunohistochemical Analyses

Histological and histochemistry evaluations showed the preservation of the general morphology of ECM and the two most important groups of ECM proteins (collagen and glycoproteins) after decellularization of the bovine ovarian ECM (Fig. 26). Furthermore, immunohistochemistry analysis showed the preservation of specific proteins after decellularization: type VI alpha 3 collagen, a significant member of the collagen group, as well as emilin-1, fibrillin-1, and elastin, which are ECM glycoproteins (Fig. 27), confirming the proteomics results.

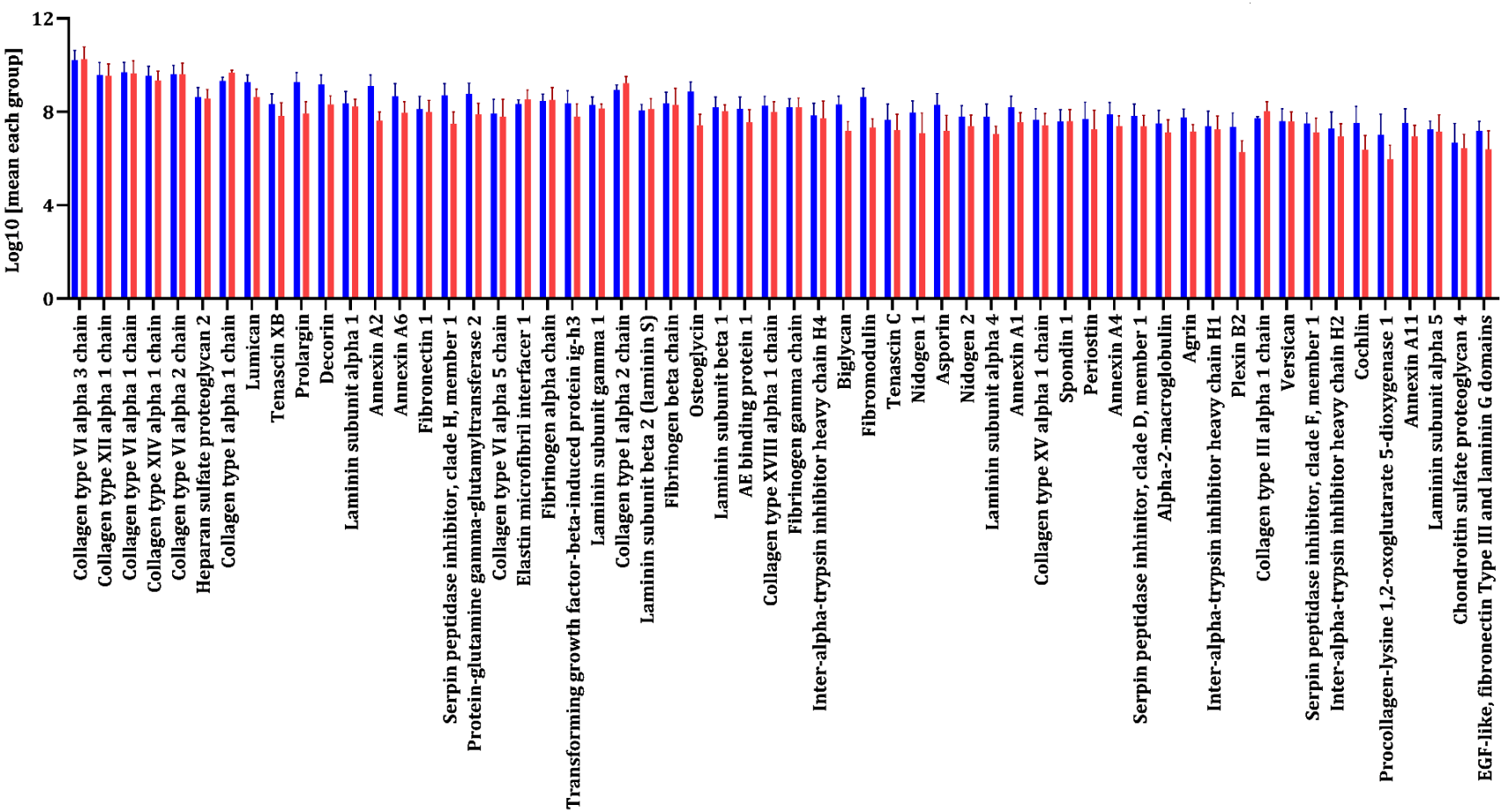

Figure 24. Top 58 most abundant proteins. All samples of the control group (blue) and decell group (red) were organized based on their peptide spectrum matches.

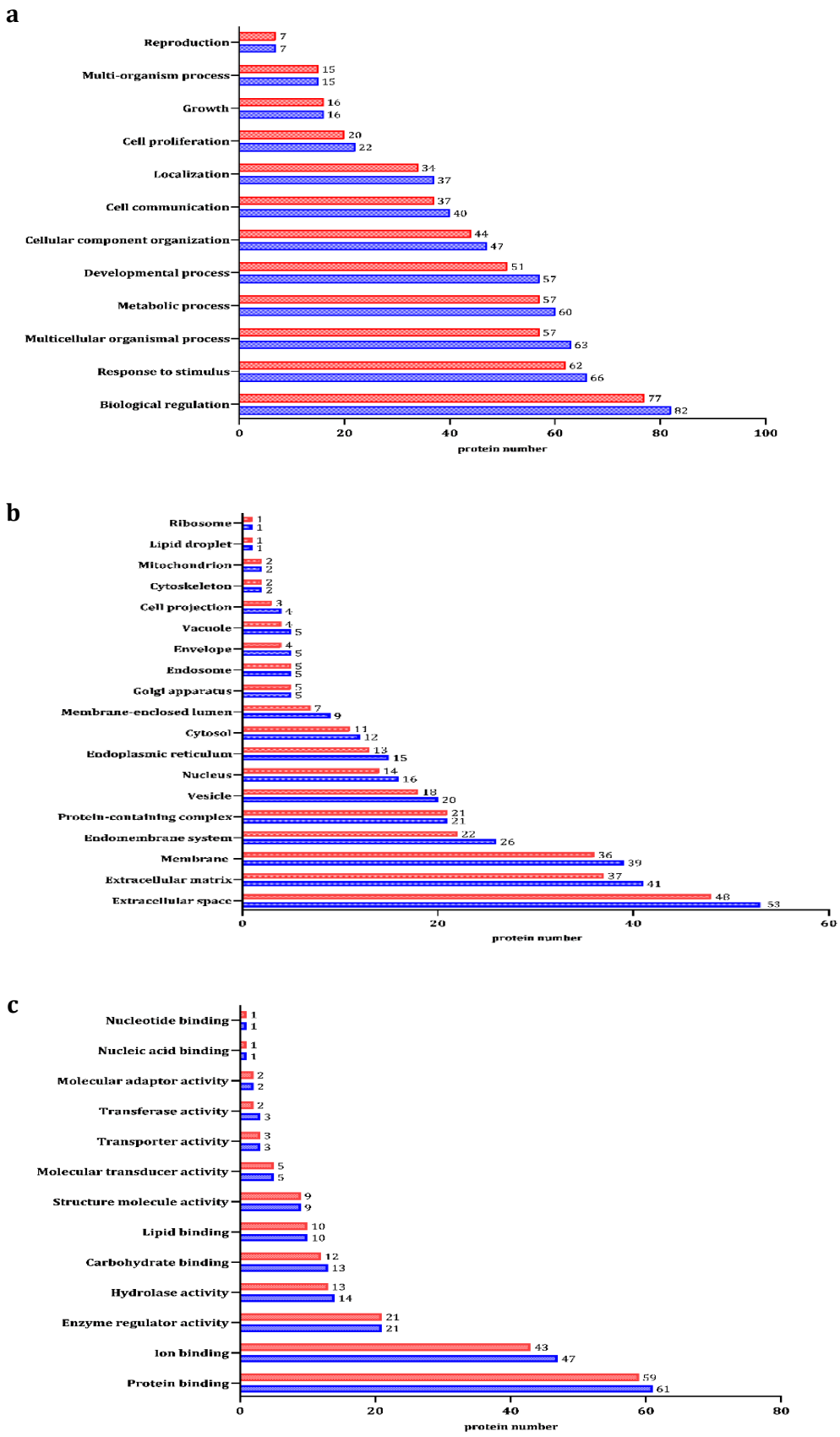

Figure 25. Number of proteins identified in control group (blue) and decell group (red). (a) Biological process, (b) cellular component, and (c) molecular function categories.

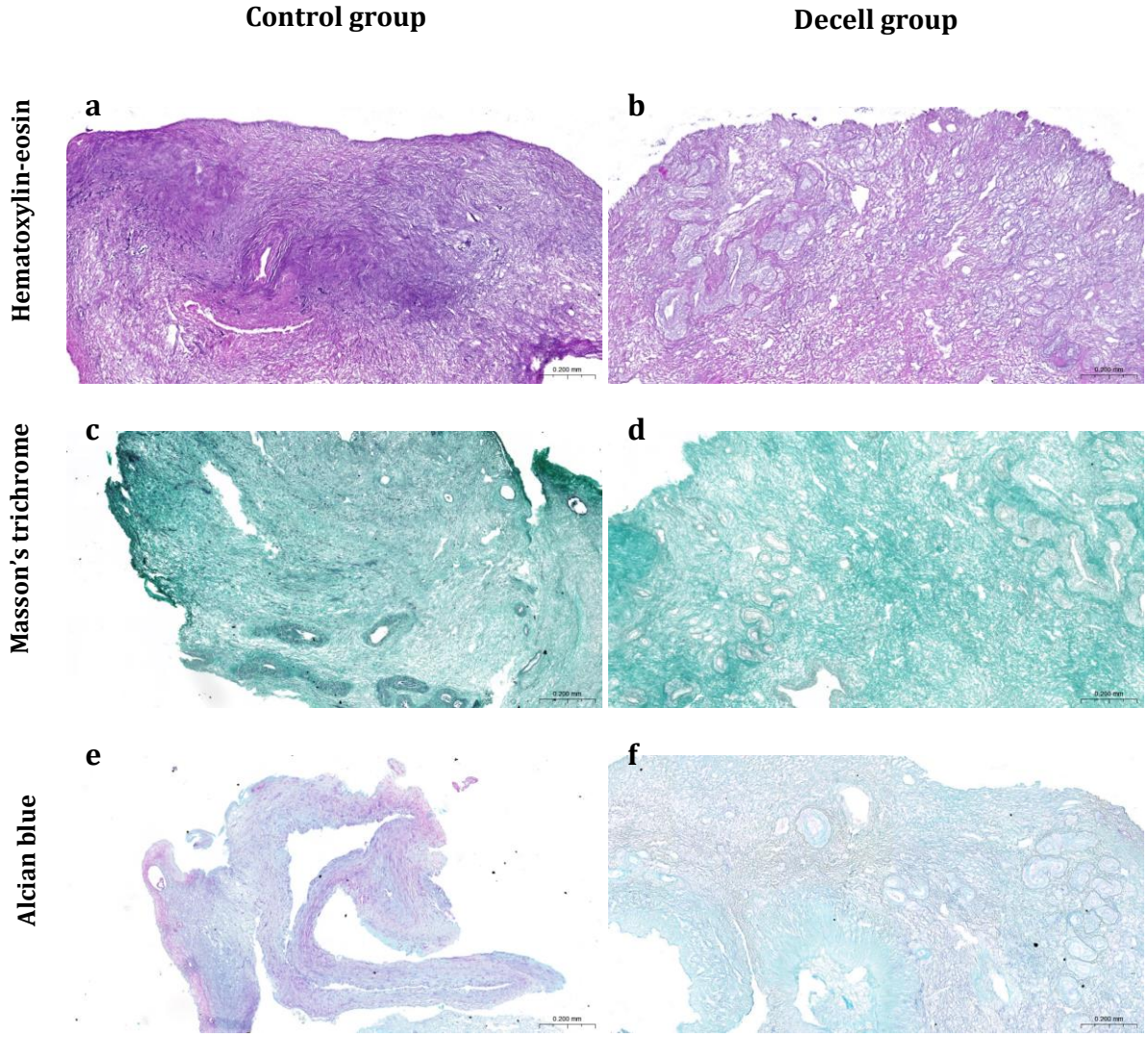

Figure 26. Histological staining in the control group and decell group. (a,b) Hematoxylin-eosin, showing the general morphology of ECM, while (c,d) Masson's trichrome, showing the collagen fibers (green) in both groups, demonstrating their conservation post decellularization. (e,f). Alcian blue (pH 2.5), showing proteoglycans (blue) in both groups and showed their conservation post decellularization. Scale bars = 200μm.

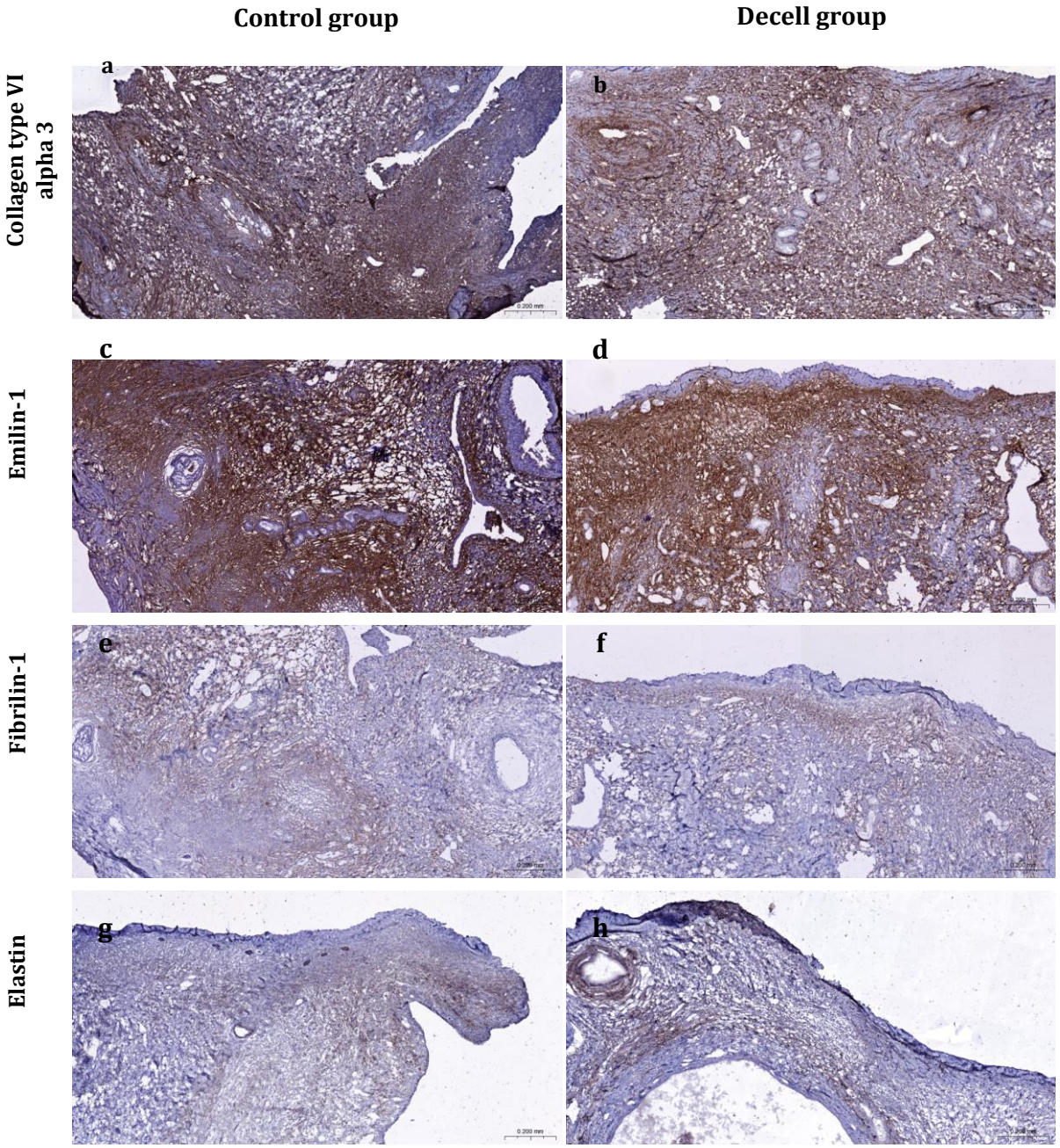

Figure 27. Immunohistochemical staining in control group and decell group. (a,b) Type VI alpha 3 collagen was selected as the most important proteins identified of the collagen group, and to confirm the proteomics result. (c,d) Emilin-1, (e,f) Fibrilin-1 and elastin (g,h), components of the ECM-glycoproteins, were selected to confirm the proteomics result. Scale bars = 200μm.

Discussion

The present study described for the first time the extracellular matrix proteins from the bovine ovarian cortex. This matrisome profile was used to further analyze a method recently described for the decellularization of bovine ovarian cortex using a minimum SDS concentration and incubation period (Capitulo 1). Previously, we demonstrated that this optimized decellularization protocol using 0.1% SDS with 0.02M NaOH for 12 h incubation period, effectively removed cellular components while preserving the structural integrity of the ovarian tissue. In the present study, we report that this gentle decellularization protocol retained approximately 93.5% of the matrisome proteins, showcasing its efficacy and potential for tissue engineering applications.

Other decellularization protocols described for the ovary and/or ovarian tissue commonly use morphological and colorimetric analysis to assess the integrity of the ECM post-decellularization. The morphological evaluation typically includes (1) classical histology with hematoxylin and eosin staining (for general appearance), Mallory or Masson's trichrome staining (both for collagen visualization), alcian blue staining (for glycosaminoglycans detection), Verhoeff Van Gieson staining (for elastin visualization), among others; (2) immunohistochemistry to observe specific ECM proteins, for example, collagen types I, III, and IV, fibronectin and laminin; and (3) scanning electron microscopy to provide high-resolution images of the ECM's structural characteristics (Liu *et al*., 2017; Hassanpour *et al*., 2018; Alshaikh *et al*., 2019; Buckenmeyer *et al*., 2020; Pennarossa *et al*., 2020). Moreover, colorimetric methods have been the most widely used to determine the total protein content and the main components of the ECM, such as glycosaminoglycans and collagen (Alshaikh *et al*., 2019; Eivazkhani *et al*., 2019; Liu *et al*., 2017). These colorimetric techniques enable the quantitative evaluation of certain ECM constituents after the decellularization process. However, it is important to note that while the colorimetric methods allow for overall quantification, they do not provide identification of individual proteins. While the morphological methods allow the identification and localization of some ECM components, but not a reliable quantification.

For example, Alshaikh *et al*. (2019) described that protein levels were significantly reduced from 109.4 ± 11.5 µg protein/2 ovaries in native ovaries to 3.6 ± 2.4 µg protein/2 ovaries in decellularized mice ovaries using 0.5% SDS for 10 hours followed by 40 UI/mL DNase I for 30 minutes. Similarly, glycoprotein levels were significantly reduced from 85.1 ± 12.5 µg/mg dry weight in native ovarian tissues to 44.4 ± 17.8 µg/mg dry weight in decellularized porcine ovarian tissues after decellularization with 1% Triton X-100 for 9

hours, 0.5% SDS for 3 hours, and 200 U/mL DNase I at 37°C for 12 hours (Liu *et al*., 2017). Additionally, collagen levels were significantly reduced in human ovaries after a decellularization protocol using 1% SDS overnight with RNase/DNase (Eivazkhani *et al*., 2019). However, none of these works thoroughly analyzed the effect of decellularization on the ovarian ECM, especially quantitatively for each component of the ovarian ECM.

In our work, we analyzed the bovine ovarian cortex before and after decellularization with 0.1% SDS and 0.02M NaOH using LC-MS/MS. We identified 155 ECM proteins before decellularization and 145 ECM proteins after decellularization. Although there is a statistical difference in some proteins, we only completely lost 10 ECM proteins after decellularization. From those lost proteins, 3 belonged to the core-matrisome category and 7 to the matrisome-associated proteins (according to Naba *et al*., 2012, 2016), and none of them belonged to the reproductive biological process category.

The proteins lost after the decellularization process play molecular functions related to ion binding, protein binding, transferase activity, carbohydrate binding, and hydrolase activity. One example of these proteins is procollagen-lysine,2-oxoglutarate 5-dioxygenase 3, which plays a crucial role in collagen synthesis in the ECM. This protein encodes the enzyme lysyl hydroxylase, which catalyzes the hydroxylation of hydroxyproline, allowing the formation of procollagen before its final conversion into collagen (Qi and Xu, 2018). Another relevant example is plexin-A4 and B1, which act as transmembrane receptors for signaling proteins of the semaphorin family. Both proteins form complexes that play a role in signal transduction, angiogenesis, and immune response (Kigel *et al*., 2011; Takamatsu and Kumanogoh, 2012).

The proteins that presented a decrease of ≥50% in their abundance after the decellularization process exhibit diverse molecular functions. These functions include: collagen binding, extracellular matrix structural constituent, glycosaminoglycan binding, calcium ion binding, and hydrolase activity. Of particular relevance is the role played by latent transforming growth factor beta binding protein 4 and adiponectin, both ECM glycoproteins, and serpin peptidase inhibitor clade E member 2, an ECM regulator in steroidogenesis and folliculogenesis (UniProtKB).

In general, the identification of ECM proteins highlights a dynamic interaction mediated by biochemical signals between the ovarian follicle and the ovarian ECM. This interaction is essential for the recruitment and follicular dominance phase, as well as for oocyte maturation and the production of the required sex hormones to carry out these processes. Furthermore, it has been observed that the interaction between both ovarian

components is also necessary for new blood vessel formation in the ECM and constant ECM remodeling. However, it is important to note that the decrease in abundance and loss of some proteins from ECM after the decellularization process may not significantly affect the various processes occurring during folliculogenesis and steroidogenesis, because the functions of ECM are not exclusively carried out by a single protein, instead several proteins play similar roles. Nevertheless, it is not clear how the slight modification of the ECM composition after the decellularization process will affect its functions. What we do know is that our decellularization method is quite conservative, providing a dECM that closely resembles the native ECM.

Besides comparing the matrisome composition before and after decellularization, our study delved into the biological and molecular functions of the ECM proteins, although the specific functions of each protein in the ovary remain to be elucidated. Prior investigations have described the matrisome composition in the native human ovarian cortex (Ouni *et al*., 2019,2022) and the decellularized porcine ovary (Henning *et al*., 2019). However, our research represents the first characterization of the matrisome in both native and decellularized bovine ovarian cortex. The total number of matrisome proteins identified in our work, both in the native and dECM ovarian cortex, was greater than that described for the matrisome of the native human ovarian cortex (120 proteins - Ouni *et al*., 2022), and the decellularized porcine ovary (82 proteins - Henning *et al*., 2019). The matrisome proteins are classified into two main categories: core-matrisome proteins and matrisome-associated proteins. Core-matrisome proteins encompass ECM glycoproteins, collagens, and proteoglycans, as previously established (Naba *et al*., 2012, 2016).

Glycoproteins constituted the highest proportion of core-matrisome proteins in the human ovarian cortex (28 glycoproteins - Ouni *et al*., 2019) and porcine dECM (36 glycoproteins - Henning *et al*., 2019), which is consistent with our findings. However, we identified a greater number of glycoproteins in both native (58 glycoproteins) and decellularized (55 glycoproteins) bovine ovarian cortex in comparison with those studies. For instance, tenascin C, which is involved in the process of tissue remodeling and the regulation of cell migration (UniProtKB), specifically supresses estradiol secretion from granulosa cells and androstenedione secretion from theca cells in the ovary (Samir *et al*., 2015). In addition, laminin subunit gamma 3 and matrix Gla protein, which play a role in cell differentiation (UniProtKB). Notably, the most abundant glycoprotein in bovine ovarian cortex is tenascin XB, in contrast to fibrillin-1 in the human ovarian cortex (Ouni *et al*., 2019).

The second most abundant group of proteins in the core-matrisome of the ovarian cortex consists of different types of collagens. While previous studies identified 16 types of collagens in human ovarian cortex matrisome (Ouni *et al*., 2020,2022) and 11 types in decellularized porcine ovary (Henning *et al.*, 2019), we identified 18 different types of collagens in bovine ovarian cortex. Remarkably, we identified three novel collagen types (type IV, alpha 3 collagen (COL4A3), type IV, alpha 6 collagen (COL4A6), and type V, alpha 3 collagen (COL5A3)) within the matrisome that had not been previously reported in other ovarian matrisomes. These collagens unwrap the organizing function of the ECM (UniProtKB). Moreover, COL4A3 also unwraps the function of cell signaling, namely through the collagen-activated tyrosine kinase receptor signaling pathway necessary for transcription, and COL5A3 unwraps the function of cell attachment to the ECM via adhesion molecules (UniProtKB). Furthermore, the most abundant collagen in the bovine ovarian cortex was type VI alpha 3 collagen (COL6A3), consistent with human ovarian cortex (Ouni *et al*., 2019).

Finally, the lowest percentage of proteins identified in the core-matrisome are proteoglycans. Previous studies reported the identification of 8 types of proteoglycans (Ouni *et al*., 2020; Henning *et al*., 2019), whereas we identified 11 different types of proteoglycans. Among these, asporin (ASPN), hyaluronan and proteoglycan link protein 3 (HAPLN3) were novel findings in the ovarian matrisome. ASPN negatively regulates the transforming growth factor beta receptor signaling pathway (UniProtKB) and is implicated in fibrosis regulation (Yan *et al*., 2022), while HAPLN3 is involved in cell adhesion (UniProtKB). Furthermore, the most abundant proteoglycan in the bovine ovarian cortex was heparan sulfate proteoglycan 2, consistent with human ovarian cortex (Ouni *et al*., 2019).

Matrisome-associated proteins are classified as ECM-affiliated proteins, ECM regulators, and secreted factors (Naba *et al*., 2012, 2016), but their precise classification and study are ongoing. Previous studies reported the identification of 47 matrisome-associated proteins in the human ovarian cortex (Ouni *et al*., 2020) and 32 proteins in decellularized porcine ovary (Henning *et al*., 2019). However, our study yielded 68 in the native bovine ovarian cortex and 61 proteins in its decellularized version. Additionally, we discovered novel matrisome-associated proteins that had not been previously described. For example, 72 kDa type IV collagenase is involved in ECM remodeling function and is associated with ovarian cancer metastasis (Planagumà *et al*., 2011; Jia *et al*., 2017). C-type lectin domain containing 11A stimulates female germ line cell proliferation (Li *et al*., 2022), and frizzled-related protein activates primordial follicle granulosa cells (Emmalee

et al., 2022). Similar to the human ovarian cortex (Ouni *et al.*, 2019), annexin A2 was identified as the most abundant ECM-affiliated protein in the bovine ovarian cortex. Moreover, the most abundant proteins in the categories of ECM regulators and secretory factors in the bovine ovarian cortex were serpin family H member 1 and protein S100-A16, respectively, contrasting with osteoglycin and protein S100-A11 in human ovarian cortex.

To the best of our knowledge, this study represents the first comprehensive characterization and comparison of ECM proteins in the native and decellularized bovine ovarian cortex. These findings contribute to a better understanding of the roles played by ECM proteins in folliculogenesis and steroidogenesis in the cow ovary. Furthermore, the results of this research proved that our decellularization method is quite conservative, providing a dECM very similar to the native ECM. Based on these encouraging findings, it can be concluded that the bovine ovarian dECM holds potential for utilization in the development of an ovarian tissue engineering approach for women.

Acknowledgments

We thank EMBRAPA-CENARGEN for donating the bovine ovaries, especially Nayara Ribeiro Kussano and Ligiane de Oliveira Leme.

Funding

The funding for this study was supported by grants from the Coordenação de Aperfeiçoamento de Pessoal de Nível Superior - Brasil (CAPES) (Finance Code 001), Erasmus+ Dimension internationale (convention grant no. DS/VM/CAI45-1011 awarded to C.A.A.) and Southeast Asia – Europe Joint Funding Scheme for Research and Innovation (FNRS PINT, convention grant no. R.8002.21 awarded to C.A.A.).

Conflict of interest

The authors state that they have no known conflicting financial interests or personal relationships that could have influenced the work presented in this paper.

References

Adams, G. P., & Pierson, R. A. (1995). Bovine model for study of ovarian follicular dynamics in humans. Theriogenology, 43(1), 113-120. https://doi.org/10.1016/0093-691X(94)00015-M

Alshaikh, A.B.; Padma, A.M.; Dehlin, M.; Akouri, R.; Song, M.J.; Brännström, M.; Hellström, M. (2019). Decellularization of the mouse ovary: comparison of different scaffold generation protocols for future ovarian bioengineering. Journal of ovarian research, 12(1), 1-9. https://doi.org/10.1186/s13048-019-0531-3

Amorim, C.A.; Shikanov, A. (2016). The artificial ovary: current status and future perspectives. Future oncology, 12(19), 2323-2332. https://doi.org/10.2217/fon-2016-0202

Arhuidese, I., Reifsnyder, T., Islam, T., Karim, O., Nejim, B., Obeid, T., ... & Malas, M. (2017). Bovine carotid artery biologic graft outperforms expanded polytetrafluoroethylene for hemodialysis access. Journal of vascular surgery, 65(3), 775-782. https://doi.org/10.1016/j.jvs.2016.10.080

Bernard, M. P., Chu, M. L., Myers, J. C., Ramirez, F., Eikenberry, E. F., & Prockop, D. J. (1983). Nucleotide sequences of complementary deoxyribonucleic acids for the pro. alpha. 1 chain of human type I procollagen. Statistical evaluation of structures that are conserved during evolution. Biochemistry, 22(22), 5213-5223. https://doi.org/10.1021/BI00291A023

Buckenmeyer, M.J., Sukhwani, M., Iftikhar, A., Nolfi, A.L., Xian, Z., Dadi, S., Case Z.W., Steimer, S.R., D'Amore, A., Orwing, K.E., Brown, B.N. (2020). Bioengineering an in situ ovary (ISO) for fertility preservation. bioRxiv, 2020-01. https://doi.org/10.1101/2020.01.03.893941

Constantinou, C. D., & Jimenez, S. A. (1991). Structure of cDNAs encoding the triple-helical domain of murine α2 (VI) collagen chain and comparison to human and chick homologues. Use of polymerase chain reaction and partially degenerate oligonucleotides for generation of novel cDNA clones. Matrix, 11(1), 1-9. https://doi.org/10.1016/S0934-8832(11)80221-0

Dolmans, M. M., Amorim, C. A. (2019). Fertility preservation: construction and use of artificial ovaries. Reproduction, 158(5), F15-F25. https://doi.org/10.1530/REP-18-0536

Donnez, J., Dolmans, M.M. (2017). Fertility preservation in women. New England Journal of Medicine, 377(17), 1657-1665. https://doi.org/10.1056/NEJMra1614676

Donnez, J., Dolmans, M.M., Pellicer, A., Diaz-Garcia, C., Serrano, M.S., Schmidt, K.T., Ernst, E.E., Luyckx, V., Andersen, C.Y. (2013). Restoration of ovarian activity and pregnancy after transplantation of cryopreserved ovarian tissue: a review of 60 cases of reimplantation. Fertility and sterility, 99(6), 1503-1513. https://doi.org/10.1016/j.fertnstert.2013.03.030

Eivazkhani, F.; Abtahi, N.S.; Tavana, S.; Mirzaeian, L.; Abedi, F.; Ebrahimi, B.; Montazeri, L.; Valojerdi, R.M.R.; Fathi, R. (2019). Evaluating two ovarian decellularization methods in three species. Materials Science and Engineering: C, 102, 670-682. https://doi.org/10.1016/j.msec.2019.04.092

Emmalee A Ford and others, Transcriptomic profiling of neonatal mouse granulosa cells reveals new insights into primordial follicle activation, Biology of Reproduction, 106(3), 503–514, 2022. https://doi.org/10.1093/biolre/ioab193

Gardin, C., Ricci, S., Ferroni, L., Guazzo, R., Sbricoli, L., De Benedictis, G., ... & Zavan, B. (2015). Decellularization and delipidation protocols of bovine bone and pericardium for bone grafting and guided bone regeneration procedures. PloS one, 10(7), e0132344. https://doi.org/10.1371/journal.pone.0132344

Goldner, J. (1938). A modification of the Masson trichrome technique for routine laboratory purposes. The American journal of pathology, 14(2), 237.

Hassanpour, A.; Talaei-Khozani, T.; Kargar-Abarghouei, E.; Razban, V.; Vojdani, Z. (2018). Decellularized human ovarian scaffold based on a sodium lauryl ester sulfate (SLES)-treated protocol, as a natural three-dimensional scaffold for construction of bioengineered ovaries. Stem cell research & therapy, 9(1), 1-13. https://doi.org/10.1186/s13287-018-0971-5

Hayat MA. Stains and Cytochemical Methods. 1st edn. New York, USA: Plenum Press, 1993.

Henning, N. F., LeDuc, R. D., Even, K. A., & Laronda, M. M. (2019). Proteomic analyses of decellularized porcine ovaries identified new matrisome proteins and spatial differences across and within ovarian compartments. Scientific reports, 9(1), 20001. https://doi.org/10.1038/s41598-019-56454-3

Jia, H., Zhang, Q., Liu, F. et al. Prognostic value of MMP-2 for patients with ovarian epithelial carcinoma: a systematic review and meta-analysis. Arch Gynecol Obstet 295, 689–696 (2017). https://doi.org/10.1007/s00404-016-4257-9

Kigel, B., Rabinowicz, N., Varshavsky, A., Kessler, O., & Neufeld, G. (2011). Plexin-A4 promotes tumor progression and tumor angiogenesis by enhancement of VEGF and bFGF

signaling. Blood, The Journal of the American Society of Hematology, 118(15), 4285-4296. https://doi.org/10.1182/blood-2011-03-341388

LeMaitre Vascular Inc., Artegraft® collagen vascular graft, (n.d.). https://www.lemaitre.com/products/artegraft-collagen-vascular-graft (accessed July 09, 2023).

Li, F., Hu, X. & Wu, J. Daidzein Activates Akt Pathway to Promote the Proliferation of Female Germline Stem Cells through Upregulating Clec11a. Stem Cell Rev and Rep 18, 3021–3032 (2022). https://doi.org/10.1007/s12015-022-10394-0

Liu, W.Y., Lin, S.G., Zhuo, R.Y., Xie, Y.Y., Pan, W., Lin, X.F., Shen, F.X. (2017). Xenogeneic decellularized scaffold: a novel platform for ovary regeneration. Tissue Engineering Part C: Methods, 23(2), 61-71. https://doi.org/10.1089/ten.tec.2016.0410

Malhi, P. S., Adams, G. P., & Singh, J. (2005). Bovine model for the study of reproductive aging in women: follicular, luteal, and endocrine characteristics. Biology of reproduction, 73(1), 45-53. https://doi.org/10.1095/biolreprod.104.038745

Maltaris, T., Seufert, R., Fischl, F., Schaffrath, M., Pollow, K., Koelbl, H., Dittrich, R. (2007). The effect of cancer treatment on female fertility and strategies for preserving fertility. European Journal of Obstetrics & Gynecology and Reproductive Biology, 130(2), 148-155. https://doi.org/10.1016/j.ejogrb.2006.08.006

Massaro, M. S., Palek, R., Rosendorf, J., Červenková, L., Liška, V., & Moulisova, V. (2021). Decellularized xenogeneic scaffolds in transplantation and tissue engineering: Immunogenicity versus positive cell stimulation. Materials Science and Engineering: C, 127, 112203. https://doi.org/10.1016/j.msec.2021.112203

Naba, A.; Clauser, K.R.; Ding, H.; Whittaker, C.A.; Carr, S.A.; Hynes, R.O. (2016) The extracellular matrix: Tools and insights for the "omics" era. Matrix Biol, 49,10-24. https://doi.org/10.1016/j.matbio.2015.06.003

Naba, A.; Clauser, K.R.; Hoersch, S.; Liu, H.; Carr, S.A.; Hynes, R.O. (2012). The matrisome: in silico definition and in vivo characterization by proteomics of normal and tumor extracellular matrices. Molecular & Cellular Proteomics, 11(4), M111-014647. https://doi.org/10.1074/mcp.M111.014647

Ouni, E., Nedbal, V., Da Pian, M., Cao, H., Haas, K. T., Peaucelle, A., ... & Vertommen, D. (2022). Proteome-wide and matrisome-specific atlas of the human ovary computes

fertility biomarker candidates and open the way for precision oncofertility. Matrix Biology, 109, 91-120. https://doi.org/10.1016/j.matbio.2022.03.005

Ouni, E., Vertommen, D., Chiti, M. C., Dolmans, M. M., & Amorim, C. A. (2019). A draft map of the human ovarian proteome for tissue engineering and clinical applications. Molecular & Cellular Proteomics, 18, S159-S173. https://doi.org/10.1074/mcp.RA117.000469

Pennarossa, G.; Ghiringhelli, M.; Gandolfi, F.; Brevini, T.A. (2020). Whole-ovary decellularization generates an effective 3D bioscaffold for ovarian bioengineering. Journal of Assisted Reproduction and Genetics, 37(6), 1329-1339. https://doi.org/10.1007/s10815-020-01784-9

Planagumà, J., Liljeström, M., Alameda, F., Bützow, R., Virtanen, I., Reventós, J., & Hukkanen, M. Matrix metalloproteinase-2 and matrix metalloproteinase-9 codistribute with transcription factors RUNX1/AML1 and ETV5/ERM at the invasive front of endometrial and ovarian carcinoma. Human pathology, 42(1), 57-67, (2011). https://doi.org/10.1016/j.humpath.2010.01.025

Qi, Y., & Xu, R. (2018). Roles of PLODs in collagen synthesis and cancer progression. Frontiers in cell and developmental biology, 6, 66. https://doi.org/10.3389/fcell.2018.00066

Rodgers, R. J., Irving-Rodgers, H. F., & Russell, D. L. (2003). Extracellular matrix of the developing ovarian follicle. REPRODUCTION-CAMBRIDGE-, 126(4), 415-424.

Samir, M., Mattar, D. S., & Knight, P. G. Role of Extra Cellular Matrix Glycoprotein Tenascin C (TNC) in Ovarian Steroidogenesis and Tissue Remodelling in the Bovine Ovary. Canadian Journal of Diabetes, 39(6), 538, (2015). https://doi.org/10.1016/j.jcjd.2015.09.047

Sonmezer, M., Oktay, K. (2010). Orthotopic and heterotopic ovarian tissue transplantation. Best Practice & Research Clinical Obstetrics & Gynaecology, 24(1), 113-126. https://doi.org/10.1016/j.bpobgyn.2009.09.002

Tabandeh, M. R., Hosseini, A., Saeb, M., Kafi, M., & Saeb, S. (2010). Changes in the gene expression of adiponectin and adiponectin receptors (AdipoR1 and AdipoR2) in ovarian follicular cells of dairy cow at different stages of development. Theriogenology, 73(5), 659-669. https://doi.org/10.1016/j.theriogenology.2009.11.006

Takamatsu, H., & Kumanogoh, A. (2012). Diverse roles for semaphorin− plexin signaling in the immune system. Trends in immunology, 33(3), 127-135. https://doi.org/10.1016/j.it.2012.01.008

Talaei-Khozani, T., & Yaghoubi, A. (2022). An overview of post transplantation events of decellularized scaffolds. Transplant Immunology, 74, 101640. https://doi.org/10.1016/j.trim.2022.101640

The UniProt Consortium. UniProt: the Universal Protein Knowledgebase in 2023. https://doi.org/10.1093/nar/gkac1052

UniProt: the universal protein knowledgebase in 2023. Nucleic Acids Research, v. 51, n. D1, p. D523-D531, 2023. https://doi.org/10.1093/nar/gkac1052

Woodruff, T. K., & Shea, L. D. (2007). The role of the extracellular matrix in ovarian follicle development. Reproductive sciences, 14, 6-10. https://doi.org/10.1177/1933719107309818

Wu, T., Gao, Y. Y., Tang, X. N., Zhang, J. J., & Wang, S. X. (2022). Construction of artificial ovaries with decellularized porcine scaffold and its elicited immune response after xenotransplantation in mice. Journal of Functional Biomaterials, 13(4), 165. https://doi.org/10.3390/jfb13040165

Wu, T., Huang, K. C., Yan, J. F., Zhang, J. J., & Wang, S. X. (2023). Extracellular matrix-derived scaffolds in constructing artificial ovaries for ovarian failure: a systematic methodological review. Human Reproduction Open, 2023(2), hoad014. https://doi.org/10.1093/hropen/hoad014

Yang, Y., Liu, P., Teng, R., Liu, F., Zhang, C., Lu, X., & Ding, Y. (2022). Integrative bioinformatics analysis of potential therapeutic targets and immune infiltration characteristics in dilated cardiomyopathy. Annals of Translational Medicine, 10(6). https://doi.org/10.21037/atm-22-732

Zegers-Hochschild, F., Adamson, G. D., De Mouzon, J., Ishihara, O., Mansour, R., Nygren, K., ... & Van der Poel, S. (2009). The international committee for monitoring assisted reproductive technology (ICMART) and the world health organization (WHO) revised glossary on ART terminology, 2009. Human reproduction, 24(11), 2683-2687. https://doi.org/10.1093/humrep/dep343

VII. CONCLUSÃO FINAL E PERSPECTIVAS FUTURAS

Neste trabalho, desenvolvemos um protocolo eficaz de descelularização para córtex ovariano bovino. Utilizando uma solução de 0,1% de SDS com 0,01M de NaOH, com um tempo de incubação de 12 horas. Desta forma, conseguimos obter uma dMEC que preserva a morfologia da MEC nativa após a descelularização. Além disso, demonstramos que a dMEC gerada não apresenta toxicidade para células estromais ovarianas humanas, o que reforça sua potencial aplicação como matriz para um OAT. A confirmação da conservação de 93,5% das proteínas da MEC nativa ao aplicar nosso protocolo de descelularização, juntamente com a identificamos 155 proteínas na MEC nativa e 145 proteínas na MEC descelularizada, reforça ainda mais o potencial de nossa dMEC como matriz na área da bioengenheira reprodutiva. Além disso, a classificação dessas proteínas e a identificação de suas funções ratificaram o papel dinâmico das proteínas da MEC ovariana nas diversas funções do ovário, que vão além de sua função de suporte tecidual. Esses resultados contribuem para o avanço do conhecimento na área e podem ter implicações importantes na bioengenheira reprodutiva.

Assim, podemos dizer que o método de descelularização de tecido ovariano aqui apresentado é suave e conservador, podendo ser vantajoso para o desenvolvimento de um OAT. Além disso, este trabalho traz pela primeira vez a descrição do *matrisome* do tecido ovariano bovino, que não havia sido descrito ainda. Esta informação pode contribuir com um melhor entendimento das funções da MEC do ovário e suas funções na foliculogênese e esteroidogênese. Além disso, com base nos resultados obtidos, a dMEC de ovário bovino apresenta potencial para ser utilizada em um OAT para humanos, visto que possui semelhanças na composição proteica.